The spatial distribution and temporal drivers of changing global fire regimes: a coupled socio-ecological modelling approach

Oliver Perkins[1], Matthew Kasoar[2], Apostolos Voulgarakis[2], Tamsin Edwards[1], and James Millington[1]

[1]King's College London
[2]Imperial College London

April 11, 2024

Abstract

In the Anthropocene, humans are the largest drivers of change in vegetation fire regimes. Humans influence fire regimes both directly, by starting, managing and extinguishing fires, and also indirectly by altering fuel composition and connectivity. However, whilst vegetation fire is a coupled socio-ecological process, representation of human influences on fire regimes in global-scale modelling remains limited. This places a fundamental constraint on our ability to understand how human and natural processes combine to create observed patterns of vegetation fire, and how such processes may interact under future scenarios of socioeconomic and environmental change. Here, we respond to this challenge by presenting a novel integration of two global and process-based models. The first is the Wildfire Human Agency Model (WHAM!), which draws on agent-based approaches to represent anthropogenic fire use and management. The second is JULES-INFERNO, a fire-enabled dynamic global vegetation model, which takes a physically-grounded approach to the representation of vegetation-fire dynamics. The WHAM-INFERNO combined model suggests that as much as half of all global burned area is generated by managed anthropogenic fires – typically small fires that are lit and then spread according to land user objectives. Furthermore, we demonstrate that including representation of managed anthropogenic fires in a coupled socio-ecological simulation can improve understanding of the drivers of unmanaged wildfires. Overall, findings presented here have substantial implications for understanding of present-day and future fire regimes, indicating that socio-economic change may be as important as climate change in determining the future trajectory of fire on Earth.

The spatial distribution and temporal drivers of changing global fire regimes: a coupled socio-ecological modelling approach

Oliver Perkins[1,2], Matthew Kasoar[1,3], Apostolos Voulgarakis[1,3,4], Tamsin Edwards[2], and James Millington[1,2]

[1]The Leverhulme Centre for Wildfires, Environment, and Society, Imperial College London, SB7 2BX, UK, [2]Department of Geography, King's College London, WC2B 4BG, UK, [3]Department of Physics, Imperial College London, [4]School of Chemical and Environmental Engineering, Technical University of Crete, Kounoupidiana, 73100, Greece

Corresponding author: Oliver Perkins (oliver.perkins@kcl.ac.uk)

Key Points:

- Representing managed fire in global-scale fire models has represented a substantial research challenge in fire science
- We address this through the offline coupling of a global agent-based model of human fire use with a dynamic global vegetation model
- The coupling improves performance of modelled burned area and allows exploration of drivers of change in global fire regimes

Abstract

In the Anthropocene, humans are the largest drivers of change in vegetation fire regimes. Humans influence fire regimes both directly, by starting, managing and extinguishing fires, and also indirectly by altering fuel composition and connectivity. However, whilst vegetation fire is a coupled socio-ecological process, representation of human influences on fire regimes in global-scale modelling remains limited. This places a fundamental constraint on our ability to understand how human and natural processes combine to create observed patterns of vegetation fire, and how such processes may interact under future scenarios of socioeconomic and environmental change. Here, we respond to this challenge by presenting a novel integration of two global and process-based models. The first is the Wildfire Human Agency Model (WHAM!), which draws on agent-based approaches to represent anthropogenic fire use and management. The second is JULES-INFERNO, a fire-enabled dynamic global vegetation model, which takes a physically-grounded approach to the representation of vegetation-fire dynamics. The WHAM-INFERNO combined model suggests that as much as half of all global burned area is generated by managed anthropogenic fires – typically small fires that are lit and then spread according to land user objectives. Furthermore, we demonstrate that including representation of managed anthropogenic fires in a coupled socio-ecological simulation can improve understanding of the drivers of unmanaged wildfires. Overall, findings presented here have substantial implications for understanding of present-day and future fire regimes, indicating that socio-economic change may be as important as climate change in determining the future trajectory of fire on Earth.

Plain Language Summary

For millennia, humans have used fire as a tool to manage land and they continue to do so across the world today. However, global-scale models which are used to understand how vegetation fire may respond to climate change have not yet robustly accounted for this. So, we built a new model that represents how humans use and manage fire globally and coupled it with a global fire model. We find that improved representation of human impacts on fire significantly improves the model and sheds new light on what is driving change in vegetation fire globally. In particular, our results suggest current global fire models may have underestimated the sensitivity of fire to climate change.

1 Introduction

Vegetation fire is a coupled socio-ecological process, in which humans are the largest driver of change in its global distribution (Andela et al., 2017; Kelley et al., 2019). Perhaps the central example of this is that, whilst the planet has warmed under recent anthropogenic climate change, the area burned globally each year has decreased, particularly in savannas and grasslands (Chen et al., 2023). Drivers of this phenomenon are complex and uncertain (Zubkova et al., 2023), ranging from cropland conversion (Andela et al., 2017) to changes in anthropogenic fire use (Smith et al., 2022), from increased grazing intensity (Archibald & Hempson, 2016) to the CO2 fertilisation effect (Ripley et al., 2022; Stevens et al., 2016). A lack of clarity around the drivers of declining global burned area has made attribution of changes in global fire regimes a significant challenge (Jones et al., 2022). This, in turn, limits understanding of how fire may evolve in the future, including its potential role as a positive feedback to climate change (Lasslop et al., 2019).

At the heart of this uncertainty are the huge diversity of ways in which humans use and manage fire. Human fire use ranges from burning of agricultural residues in intensive land use systems (Kumar et al., 2023) to cultural uses such as religious ceremonies (Smith et al., 2022). Human fire management is similarly diverse, ranging from pro-active indigenous 'patch-burning' methods (Laris, 2002) to industrial fire suppression. As such, fire can broadly be categorised into managed or 'landscape' fires - which are typically small, controlled, and can be beneficial to humans - and unmanaged wildfires, which are larger and burn more intensely (UNEP 2022). Furthermore, human fire use is itself undergoing substantial change, with shifts away from more subsistence-oriented fire uses (Smith et al., 2022) and possibly an overall decline in fire use driven by agricultural intensification (Perkins et al., 2023). Consequently, Shuman et al., (2022) argue that incorporating managed fire into models at all spatial scales is an important step towards equipping fire science for the Anthropocene.

In addition to direct anthropogenic influences on fire, humans also have many indirect influences on fire regimes. For example, multiple authors have argued that anthropogenic fragmentation of vegetated landscapes is a key process shaping the evolution of global fire (Archibald et al., 2012; Driscoll et al., 2021; Harrison et al., 2021). Fragmentation can have opposite effects across ecosystems – with logging and degradation increasing fire in otherwise fire-independent forests, and reduced fuel connectivity decreasing burned area in grassland and savannah ecosystems (Rosan et al., 2022). As such, understanding the drivers of change within global fire regimes requires consideration not only of biophysical factors, but also of both direct and indirect human impacts.

Global-scale fire models have struggled to reproduce the observed decline in global burned area (Hantson et al., 2020). Indeed, in the first intercomparison project of the global fire model community (FireMIP; Rabin et al., 2017), models largely disagreed about both centennial trends, and more recent decadal trends, in global burned area (Teckentrup et al., 2019). Underlying this lack of consensus have been substantial limitations in the representation of human impacts on the fire modules of dynamic global vegetation models (DGVMs; Ford et al., 2021). Typically, these have been restricted to global functions relating population density to numbers of fires in satellite observations (Rabin et al., 2017). This ignores the diversity of human fire use and management, and hence limits the capability of DGVMs to advance understanding of socio-ecological dynamics of present-day fire regimes and how human and biophysical factors may interact in the future (Shuman et al., 2022).

The Wildfire Human Agency Model (WHAM!; Perkins et al., 2023) is the first formal model to represent present-day anthropogenic fire use and management at global scale. Drawing on agent-based approaches, WHAM! is a geospatial behavioural model that captures the underlying land system drivers of anthropogenic fire use and management to simulate human fire use decision-making from the bottom-up (Perkins et al., 2022). As WHAM! only represents human influences on global fire regimes, it was designed to be integrated with fire-enabled DGVMs, such as the JULES-INFERNO model (Mangeon et al., 2016), which capture the biophysical drivers of fire. Here we present the first coupling between WHAM! and JULES-INFERNO, such that biophysical, direct and indirect human drivers of fire regimes are all explicitly represented in an integrated simulation for the first time.

WHAM! takes its empirical basis from the Database of Anthropogenic Fire Impacts (DAFI; Perkins & Millington, 2021). DAFI is the product of a literature meta-analysis of 1809 case studies from 504 academic papers, government and NGO reports (Millington et al., 2022). This dataset addresses a previous barrier to improved representation of anthropogenic fire in DGVMs: the lack of a systematic data set on which to base new parameterisations (Forkel et al., 2019). Alongside development of DAFI, the 5th version of the Global Fire Emissions Database (GFED5; Chen et al., 2023) accounts for smaller fires than previous versions and therefore enables more robust evaluation of global-scale modelling of human fire interactions. Previous iterations of GFED have been based on a combination of MODIS for burned area and VIRS for active fire detection (Giglio et al., 2013). As such, they have not been able to systematically detect anthropogenic fires: DAFI suggests that >50% of anthropogenic fires are smaller than the 21ha threshold above which MODIS can detect (Millington et al., 2022). GFED5 incorporates higher resolution remote sensing (principally from Landsat and Sentinel-2), and hence is much more effective at capturing small fires: global burned area in GFED5 is a 61% increase over GFED4s (Chen et al., 2023). Therefore, with DAFI providing an empirical-basis for bottom-up modelling of human-fire interactions, and GFED5 better able to detect them from space, a comprehensive and empirically-grounded assessment of the role of managed anthropogenic fire in global fire regimes is now possible.

This paper presents the integration of WHAM! with JULES-INFERNO and its application to understand the spatiotemporal drivers of global fire regimes. Section 2 (Methods) focuses on describing the integration of outputs from the two models. Model calibration is described briefly in the main text with further details provided in Supplementary Information A. In Section 3 (Results), we present a brief evaluation of the outputs of the coupled model to establish its credibility, before focusing on understanding how human and biophysical factors combine to produce observed distributions of fire globally. Discussion (section 4) focuses on insights relevant to the question of declining global burned area, and in particular to understanding the relative contribution of direct human influences (starting and suppressing fires), indirect human influences (i.e. landscape fragmentation) and biophysical factors (i.e. climate and vegetation flammability).

2 Methods

Our methods are presented in five sections, which respectively describe the inputs, structure, calibration, evaluation, and analysis of the WHAM-JULES-INFERNO combined model (hereafter WHAM-INFERNO). A schematic overview of the processes represented in WHAM-INFERNO is presented in Figure 1. Calculations of the fire regime at each timestep combine three elements: 1) WHAM! outputs for managed and unmanaged anthropogenic fires and fire suppression; 2) JULES-INFERNO outputs for lightning ignitions, flammability and plant functional types; and 3) a representation of vegetation fragmentation derived from secondary data and WHAM! outputs for logging. These are each detailed further in Section 2.1.

Importantly, two versions of WHAM-INFERNO are presented and assessed: WHAM-INFERNO-JULES (hereafter WI-JULES) and WHAM-INFERNO-Earth Observation (hereafter WI-EO). The difference between these two versions is that in WI-JULES, WHAM! is parameterised using biophysical inputs directly from JULES, whilst in WI-EO, WHAM! takes these inputs from remote sensing. Specifically, inputs for potential evapotranspiration, net primary production and the bare soil fraction are replaced with Earth observation data. The differences between these two versions of WHAM! are described in detail in Perkins et al. (2023; Supplementary Information A).

The primary purpose of the comparison of WI-JULES and WI-EO is to allow interrogation of the robustness of inferences made about the drivers of global fire regimes. For example, if trends are identified in WI-JULES but not in WI-EO, then they may be attributable to underlying model error in JULES' representation of ecosystem dynamics. Similarly, assessing the difference in performance (as measured against GFED5) allows exploration of how far underlying error in the hydrological and vegetation outputs of DGVMs may constrain the capacity of their fire modules to reproduce remotely sensed observations (Hantson et al., 2020).

Code to run and analyse WHAM-INFERNO is written in R version 4.2.2 (R Core Team 2022), using the 'raster' library version 3.6-20 (Hijmans et al., 2023). Code and data to run and analyse outputs of both versions of WHAM-INFERNO are made available on Zenodo (Perkins et al., 2023b).

2.1 Inputs to the coupled model

WHAM-INFERNO takes inputs from WHAM!, JULES-INFERNO and from secondary data sources. Each of these inputs are described in turn below (Sections 2.1.1-2.1.3), and an overview is given in Table 1. WHAM! outputs are annual, whilst as per results in the sixth coupled model intercomparison project (CMIP6), JULES-INFERNO outputs are aggregated monthly means. Therefore, WHAM-INFERNO runs at a monthly timestep, with WHAM! outputs for a given year assumed to be uniformly distributed across calendar months.

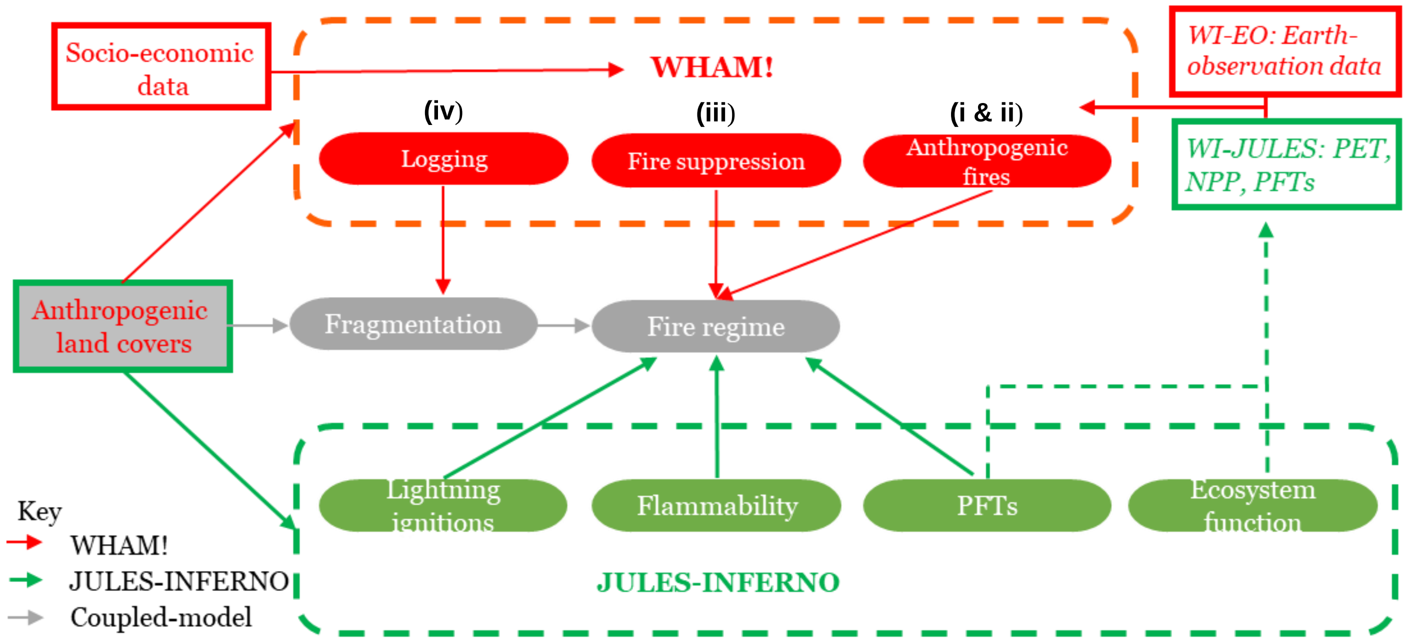

Figure 1: Processes represented in the WHAM-INFERNO combined model. Solid arrows denote dynamic model calculations, whilst dashed lines denote static exchange of information. Socio-economic data and biophysical inputs to WHAM! (Potential Evapotranspiration (PET), Net Primary Production (NPP) and Plant Functional Types (PFTs)) are passed offline. In WHAM-INFERNO-JULES (WI-JULES) these data are taken from JULES outputs, whilst in WHAM-INFERNO-Earth Observation (WI-EO) PET and NPP inputs are taken from remote sensing. Roman numerals (i-iv) correspond to numbers given in section 2.1.1 of the text.

2.1.1 WHAM! inputs to the coupled model

WHAM! inputs to the coupled model comprise i) managed burned area as a fraction of each cell, ii) numbers of unmanaged fires (count km^{-2} yr^{-1}), iii) fire suppression intensity (0-1), and iv) the presence of selective logging as a fraction of the tree cover in each cell (see corresponding numerals in Figure 1). WHAM! inputs used were those presented in Perkins et al., (2023).

2.1.2 JULES-INFERNO inputs to the coupled model

INFERNO (Mangeon et al., 2016) is the fire module of the JULES dynamic global vegetation model. INFERNO calculates burned area from fires with two key components. The first is mean global burned area per fire per Plant Functional Type (PFT), a set of PFT-specific model free parameters. Model parameters for burned area per PFT were as in Burton et al. (2019). The second component of INFERNO burned area calculations is fuel flammability, which INFERNO calculates as a function of leaf carbon and soil carbon pools, temperature, relative humidity, precipitation, and soil moisture (Mangeon et al., 2016). Flammability is therefore important in capturing the impact of both climate and spatial heterogeneity in vegetation on fire regimes. Flammability is calculated per PFT in each model pixel at each timestep. JULES outputs are from the model set-up used in CMIP6 (Wiltshire et al., 2020).

2.1.3 Ancillary inputs to the coupled model from secondary data

In addition to the calculations from the two models, three sets of secondary data were used as inputs: lightning ground strikes, anthropogenic land covers – cropland, pasture, rangeland and urban – and road density. Firstly, as in JULES-INFERNO standalone (Mathison et al., 2023), counts of lightning strikes were sourced from the Lightning Imaging Sensor—Optical Transient Detector (LIS/OTD, Christian et al., 2003). Secondly, as in CMIP6, anthropogenic land cover was taken from the LUH2 dataset (Hurtt et al., 2020). Finally, Haas et al. (2022) demonstrated that road density was effective in capturing vegetation fragmentation effects on fire regimes at global scale; road density data were therefore taken from the GRIP global road database (Meijer et al., 2018).

Table 1: Overview of inputs to the WHAM!-INFERNO combined model. PFT is plant functional type. Data inputs for lightning strikes, road density and anthropogenic land covers were rescaled to the resolution of WHAM!-INFERNO (1.875º x 1.25º). Differing temporal resolutions of inputs were reconciled as noted in Section 2.1.

Coupled model input	**Source**	**Units**	**Temporal resolution**
Managed burned area	WHAM!	Cell fraction (0-1)	Annual
Unmanaged anthropogenic fires	WHAM!	Fires km^{-2}	Annual
Fire suppression	WHAM!	Cell fraction (0-1)	Annual
Selective logging	WHAM!	Cell fraction (0-1)	Annual
Distribution of PFTs	JULES-INFERNO	Cell fraction (0-1)	Monthly
Flammability per PFT	JULES-INFERNO	Dimensionless (0-1)	Monthly
Burned area per fire per PFT	JULES-INFERNO	km^2	Fixed (n/a)
Lightning – ground strikes	Christian et al., (2003)	strikes km^{-2}	Fixed (single daily mean)
Road density	Meijer et al., (2018)	m^2 km^{-2}	Annual
Anthropogenic land cover	Hurtt et al., (2020)	Cell fraction (0-1)	Annual

2.2 WHAM-INFERNO Structure

The coupled WHAM-INFERNO model is a 'prescribed' model coupling (sensu Robinson et al., 2018) such that whilst simulations of global burned area depend on calculations involving outputs of both models, dynamic information transfer is only one way - from WHAM! to INFERNO (see Section 2.2.1). Specifically, for each simulated year, annual burned area from managed fire is taken directly from WHAM!, with $\frac{1}{12}$ assigned to each calendar month. But to calculate unmanaged fire burned area, the original JULES-INFERNO calculations are modified by the number of anthropogenic fires (km^{-2} yr^{-1}) provided by WHAM!. Therefore, description of model coupling here first describes calculation of burned area from unmanaged fires (Section 2.2.1). Then, as burned area from unmanaged fires is also impacted by anthropogenic landscape fragmentation, the representation of such processes is then described in Section 2.2.2. Finally, the calculation of overall burned area combining both managed and unmanaged fire is described in Section 2.2.3.

2.2.1 Unmanaged fire

The calculation of burned area from unmanaged fires is presented in two parts: firstly the calculation of numbers of unmanaged fires, and secondly the calculation of their respective burned area. An overview of this process is given in Figure 2.

2.2.1.1 Number of fires

In the original Mangeon et al. (2016) conception of INFERNO, the numbers of ignitions from lightning strikes are calculated as follows:

$$I_L = 7.7 \times Lightning \times (1 - Suppression) \quad (1)$$

where I_L is the number of ignitions from lightning strikes in a given model timestep, $Lightning$ is the number of lightning strikes and $Suppression$ is a population density-dependent suppression function. The structure of this calculation is retained with two changes: firstly, the suppression function is replaced with an empirically-defined representation of suppression intensity (Section 2.2.2); and secondly the empirically-defined linear scaling parameter (=7.7) from Mangeon et al. (2016) is replaced with a free parameter (λ) to allow re-calibration. A complete set of model free parameters is given in Supplementary Information Table S1.

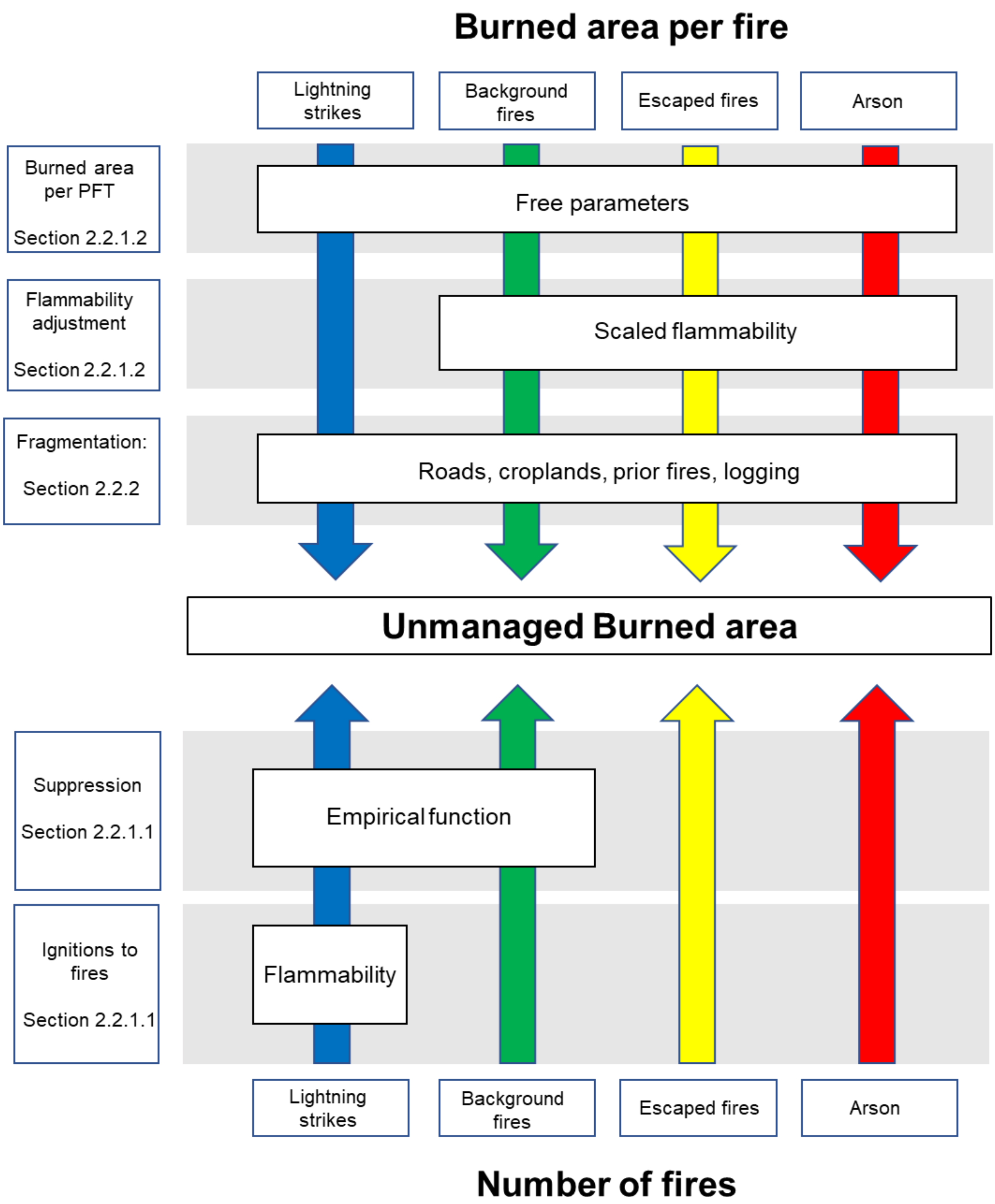

Figure 2: Calculation of burned area from unmanaged fires in the WHAM-INFERNO combined model.

In the WHAM-INFERNO combined model, calculation of lightning fires is integrated with unmanaged anthropogenic fire numbers from WHAM! as follows:

$$Fires_{UM} = Arson + Escaped + (1 - Suppression) * (Background + Lightning) \quad (2)$$

where $Fires_{UM}$ is the annual number of unmanaged fires per grid box per year, $Arson$ and $Escaped$ fire numbers are the number of fires km^{-2} yr^{-1} taken from WHAM! outputs, and $Lightning$ is the number of lightning fires calculated from mean daily ground strikes as in equation (1). Finally, $Background$, is a small globally constant rate used to capture fires that are not arson, lightning or escaped managed fires. The constant rate maintains an aspect of INFERNO, in which a uniform 'ignition' rate is an option.

Fire suppression in the coupled model (Section 2.2.2) is applied to background and lightning fires, but not to arson and escaped fires. This is for ontological reasons, as follows. INFERNO assumes that suppressed *ignitions* have no burned area. However, in DAFI, the database used to develop WHAM!'s calculation of arson and escaped *fires*, numbers of *fires* are recorded, therefore by definition these have burned area > 0. As such, it is illogical to apply modelled suppression to them. By contrast, as the background rate was calculated using a constant, clearly this did not account for the impact of suppression. Similarly, lightning remains calculated based on *ignitions* rather than *fires* and hence could be suppressed before beginning to burn.

2.2.1.2 Burned area per unmanaged fire

After calculation of the numbers of unmanaged fires per pixel ($Fires_{UM}$), these are then converted to burned area. In its original conception, INFERNO calculates the number of fires as:

$$Fires = Ignitions * Flammability \quad (3)$$

In other words, both humans and lightning are conceptualised as producing ignitions, which may or may not become fires based on the flammability of the surrounding vegetation. By contrast, because most human fires are started deliberately, WHAM! does not output numbers of *ignitions*, but numbers of *fires* directly (Figure 2). However, whilst vegetation flammability plays the ontological role of translating ignitions to fires in INFERNO, it also plays an important functional role: capturing geographic variation in the capacity and tendency of the vegetation to sustain unmanaged fire. This is because INFERNO calculates burned area per fire with a simple global mean value per Plant Functional Type. Therefore, simply removing flammability from the calculation and taking numbers of unmanaged fires from WHAM! was not possible.

The solution adopted is to multiply WHAM! unmanaged fires by INFERNO flammability, but to rescale with a free parameter. This leaves a burned area calculation from unmanaged fires of:

$$BA_{UM} = Fires_{UM} * \Phi * \sum_{PFT=1}^{PFT=n} PFT * \ Flammability_{PFT} * BA_{PFT} \ (4)$$

where $BA_{UM}$is the annual burned area from unmanaged fires as a fraction of each model pixel; PFT is the fraction of each model pixel (0-1) occupied by a given PFT; $Flammability_{PFT}$is a PFT-specific dimensionless adjustment (0-1) reflecting spatiotemporal differences in the combustibility of vegetation; BA_{PFT} is the PFT-specific mean burned area per fire from JULES-INFERNO; and Φ is a scaling factor reflecting the differing model ontologies of WHAM! and JULES-INFERNO.

2.2.2 Fragmentation

The impact of landscape fragmentation effects was restricted to unmanaged fires; managed burned area was not altered for fragmentation effects, as these would already be implicitly accounted for in the observations captured in DAFI. Representation of fragmentation is done in three ways. Firstly, as WHAM! accounts for anthropogenic cropland fires, to account for the role of cropland conversion in fragmenting more flammable fuels, burned area per unmanaged fire was set to 0 for cropland PFTs.

Secondly, Haas et al., (2022) demonstrate the importance of road density in reducing both fire sizes and burned area. This finding was implemented in the coupled model by adjusting burned area per fire with a simple negative exponential function:

$$BA_{UM\_frag} = \ BA_{UM} * \left(1 - \frac{\ln(RD)}{\rho}\right) (5)$$

where BA_{UM} and BA_{UM_frag} are annual burned area per pixel (0-1) from unmanaged fire before and after adjustment for fragmentation effects, RD is road density and ρ a free parameter.

By contrast, logging of wet, fire-prone forests can lead to increased fire (both numbers of fires and fire size), as gaps in the canopy lead to drying on the forest floor (Cochrane & Barber, 2009; Lapola et al., 2023). A simple representation of this was implemented by increasing the mean burned area per fire for broadleaf tree PFTs given the presence of the Logging AFT in WHAM! outputs. The values of mean burned area for broadleaf tree PFTs therefore become:

$$BA_{broadleaf} | \ logging = \ BA_{broadleaf} * \ \Lambda(Logging) \ (6)$$

where $BA_{broadleaf}$ is the burned area per fire for broadleaf tree PFTs; $BA_{broadleaf} | \ logging$ is this parameter value when adjusted for logging, $Logging$ is the fraction of tree cover in a cell occupied by WHAM's logging AFT, and Λ a free parameter.

2.2.3 Combining managed and unmanaged fire

JULES-INFERNO typically runs at a timestep of between 30-60 minutes (Clark et al., 2011). This is required for the stability of model equations and has the advantage of capturing temporal fluctuations in vegetation flammability. As such, INFERNO increases the amount of bare soil in a given model pixel when a fire burns, which reduces fuel availability and the amount of area burned from subsequent fires until vegetation resprouts (Burton et al., 2019). However, as it is not meaningful to model human land use decision-making at such short durations (Arneth et al., 2014), managed fire is output at an annual timestep by WHAM!. For these reasons, calculating the combined burned area of managed and unmanaged fires requires an adjustment to account for the effect of preceding fires:

$$BA_{tot} = BA_{Managed} + BA_{UM} * \gamma \quad (7)$$

where $BA_{Managed}$ is burned area from managed fire, BA_{tot} is total burned area and γ a function representing the impact of preceding fires on unmanaged burned area. Managed fire was not adjusted for effects of antecedent fire for several reasons: firstly, because WHAM! has its own internal calculation for including fuel limitations in agent calculations; secondly, because WHAM! outputs are empirically grounded, derived from data that would capture such limitations to a degree. Thirdly, many managed anthropogenic fires are lit to reduce the intensity and spread of unmanaged fire (e.g. prescribed fire or indigenous patch burning mosaics). The γ function was calculated using a linear function after a threshold:

$$\gamma = \begin{Bmatrix} 1 \;\; if\ BA_{UM} \leq \alpha \\ \beta \quad otherwise \end{Bmatrix} \quad (8)$$

where α is a free parameter representing a threshold burned fraction of a cell below which fuel availability is not limiting, whilst β is a further free parameter capturing the rate of decay in burned area once this threshold is reached. This functional form was chosen as it approximates the behaviour observed by Archibald et al. (2012), who explored the impact of fragmentation on burned area in flammable ecosystems.

2.3 WHAM-INFERNO Calibration

The model structure set out in Section 2.2 resulted in 20 free parameters (Supplementary Table S1), which formed the basis of a perturbed parameter ensemble for model calibration. A total of 10,000 perturbed parameter sets were created with a maximin latin hypercube sampling design (Carnell 2022). Using the resulting parameter sets, 10,000 model runs were conducted (i.e. one for each perturbed parameter combination) for both versions of the WHAM-INFERNO ensemble.

The outputs of each run were compared with the recent GFED5 global burned area product (Chen et al., 2023). Firstly, 'implausible' parameter sets were ruled using history matching with the overall magnitude of global burned area in GFED5. Remaining parameter sets were then treated as 'not ruled out yet' (NROY; Rougier & Beven, 2013). Secondly, as well as global burned area, Pearson's correlation (r) was calculated with a square root transformation applied. These two metrics were those used in the FireMIP (Teckentrup et al., 2019), and hence were adopted here to define a pareto-optimal parameter space capturing the trade-offs in maximising performance against each metric. This approach allows, firstly, the evaluation of different model processes in capturing observed fire regimes of the recent past, and secondly overall evaluation of the performance of the WHAM-INFERNO ensemble. The mean outputs of WI-JULES and WI-EO in the pareto parameter space then formed the basis of further analysis. Fuller detail of model calibration is given in Supplementary Information A.

2.4 WHAM-INFERNO Evaluation

WHAM-INFERNO is evaluated in two broad ways, firstly by output corroboration through comparison of model outputs with remotely sensed burned area from GFED5 (as described above) and secondly by model benchmarking against a null or baseline model. The baseline model was an offline version of INFERNO (as presented in Mangeon et al., 2016). As INFERNO was originally calibrated using GFED4 data, in which burned area was 49% lower than the more recent GFED5 burned area product, a process of recalibration required. The re-calibration of this INFERNO offline model (hereafter, 'baseline model') followed broadly the same steps as WHAM-INFERNO combined model: 10,000 parameter sets were used to define a perturbed parameter ensemble, from which both NROY and pareto-optimal parameter spaces were defined using GFED5 burned area. Detailed description of the setup of the baseline model, including how its free parameters differ from WHAM-INFERNO, is described in Supplementary Information A.

2.5 Historical run setup and analysis

As with the WHAM! standalone historical simulations presented in Perkins et al. (2023), WHAM-INFERNO runs span 1990-2014. These two years mark the beginning of the data recorded in the DAFI database of global anthropogenic fire impacts (i.e. 1990; Millington et al., 2022) that was used to parameterise WHAM!, and the end of the CMIP6 historical period (i.e. 2014), respectively. Both models were run at the spatial resolution that JULES-INFERNO adopted in the FireMIP (1.875° x 1.25°). Model outputs are evaluated during the overlapping period in WHAM-INFERNO historical runs and the GFED5 record (2001-2014); GFED5 data were aggregated to the spatial resolution of WHAM-INFERNO.

Analysis of outputs focuses on understanding spatial and temporal variation in the drivers of global fire regimes. Spatial analysis focuses on understanding how managed anthropogenic fire and unmanaged fire combine to produce observed fire regimes across global regions. Similarly, temporal analysis first assessed how far managed fire and unmanaged fire contribute to interannual variability in fire regimes. This was calculated by detrending the global total burned area from GFED5 and WHAM-INFERNO model outputs before calculating the correlation and standard deviation of the residual variabilities.

Then, drivers of longer-term (decadal) change were assessed. Perkins et al. (2023) present analysis of the drivers of change in WHAM! managed fire outputs. Results pointed to land use intensification as a global dampening effect on fire use, whilst conversely land use extensification - particularly for livestock farming - led to increased fire use. Therefore, analysis of temporal trends here focuses on change in unmanaged fire in relation to the human and physical drivers represented in the coupled models. These are annual changes in numbers of unmanaged fires, road density (fragmentation; Haas et al., 2022), vegetation flammability, fire suppression and cropland conversion. The relative influence of these drivers was assessed at a pixel-level firstly by comparing the Kendall's Tau correlations of their interannual changes with interannual change in unmanaged burned area (for each of WI-JULES and WI-EO). Secondly, using these same independent variables, linear models of pixel-level change in unmanaged burned area were fit for both interannual and overall change between 2001-2014. T-values of the independent variables were used to assess the relative strength of their relationships to changes in unmanaged burned area.

3 Results

3.1 Model evaluation

Measured by correlation with the GFED5 record during 2001-2014, both WI-JULES and WI-EO perform significantly better than the baseline model (Z Tests; both $p < 0.001$, $n = 10, 14$). Specifically, the mean correlation of the pareto-optimal parameter space is 0.81 for WI-EO and 0.76 for WI-JULES, compared with 0.58 for the baseline model (Figure 3). This result also compares favourably with INFERNO v1.0 presented in the FireMIP, in which INFERNO had a correlation of 0.70 against GFEDv4 and 0.64 against GFEDv4s (Teckentrup et al., 2019). As such, inclusion of WHAM! seemingly improves INFERNO both in an absolute sense, when compared to GFED5, but also relatively against INFERNO's performance based on the observational data available at the time of its original development.

Furthermore, almost 70% of the baseline model ensemble's runs are ruled out, primarily due to simulating burned area too low to achieve acceptable coherence with the GFED5 record (mean of ruled out runs was 276 Mha vs 802 Mha in GFED5). By contrast, only 182 of WI-EO and 124 of WI-JULES runs are ruled out. In the pareto parameter space, WI-EO has a slight overprediction bias (+11 Mha) and WI-JULES has a slight underprediction bias (-10 Mha), compared to a bias of -52 Mha in the baseline model. Overall, we conclude that the WHAM integration improves the structural capacity of INFERNO to capture the magnitude and distribution of global fire regimes.

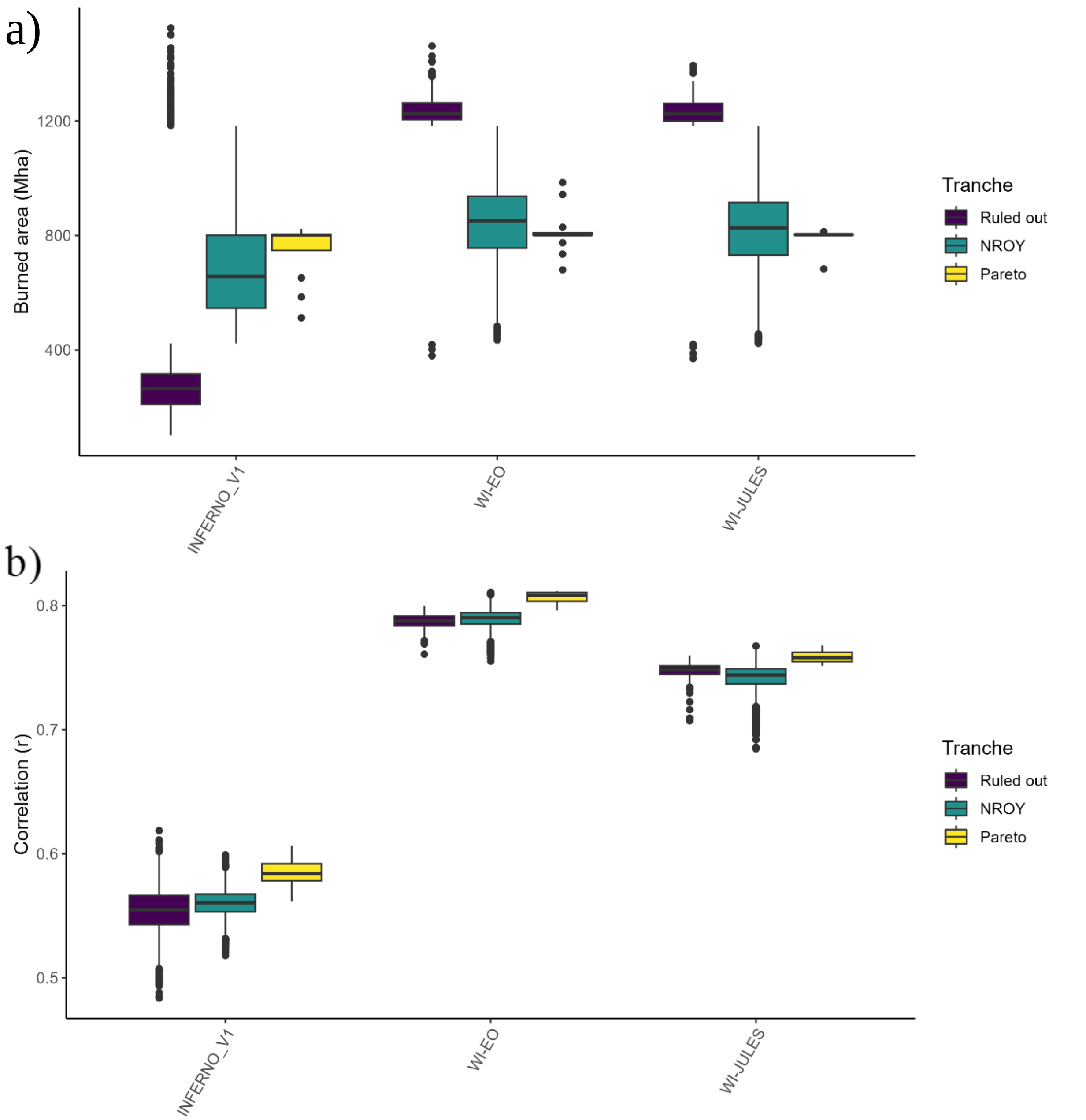

Figure 3: Outputs of WHAM-INFERNO in comparison with a baseline model (INFERNO_V1): a) simulated global burned area and b) Pearson correlation with GFED5. For burned area, the baseline model has many runs ruled out for burned area being too low in comparison with GFED5, whilst in both versions of WHAM-INFERNO a smaller number of runs are ruled out. The two versions of WHAM-INFERNO both produce higher correlations than the baseline model across all three tranches of parameter sets (ruled out, NROY and pareto-optimal). NROY refers to “not ruled out yet”.

3.2 Analysis of WHAM-INFERNO outputs

3.2.1 Spatial Analysis

Across the pareto parameter runs, simulated burned area in both coupled models is split approximately evenly between managed and unmanaged fires. Over the historical period (1990-2014) in WI-JULES a mean of 442 Mha (54%) comes from unmanaged fires and 379 Mha (46%) from managed fires. Similarly, in WI-EO, 405 Mha (47%) comes from unmanaged fires, and 453 Mha (53%) comes from managed fires.

Furthermore, there is substantial heterogeneity in the spatial location of burned area due to managed *versus* unmanaged fires (Figure 4). For example, across 1990-2014 at the level of World Bank regions, in sub-Saharan Africa WI-JULES suggests 65% of mean annual burned area is from unmanaged fires (56% in WHAM-EO; Figure 5). Conversely, in South Asia (which includes India), WI-JULES suggests just 28% of burned area is from unmanaged fires (19% in WI-EO; Figure 5). The predominance of managed fire is driven by large-scale crop-residue burning in the region (Hall et al., 2023; Perkins et al., 2023). Furthermore, there is also regional heterogeneity in the trends in managed and unmanaged fire. For example, in both WI-JULES and WI-EO, managed fire is increasing in South Asia, whilst decreasing in Latin America and the Caribbean (Figure 5).

Perhaps the two most notable differences in sources of burned area between the two models' (WI-JULES and WI-EO) simulations come in Latin America & the Caribbean and sub-Saharan Africa. The difference in Latin America is that WI-JULES simulates higher unmanaged burned area than WI-EO (81 Mha vs 56 Mha) particularly in the Caatinga region of Brazil (Figure 6), which is due to a known anomaly in JULES' hydrological cycle in the region (Perkins et al., 2023). By contrast, in sub-Saharan Africa WI-EO simulates higher unmanaged burned area than WI-JULES (209 Mha vs 132 Mha), attributable to the more homogeneous spatial distribution in WI-EO outputs – particularly in the Guinean Savanna – compared to the comparatively heterogeneous WI-JULES outputs (Figures 4 & 6).

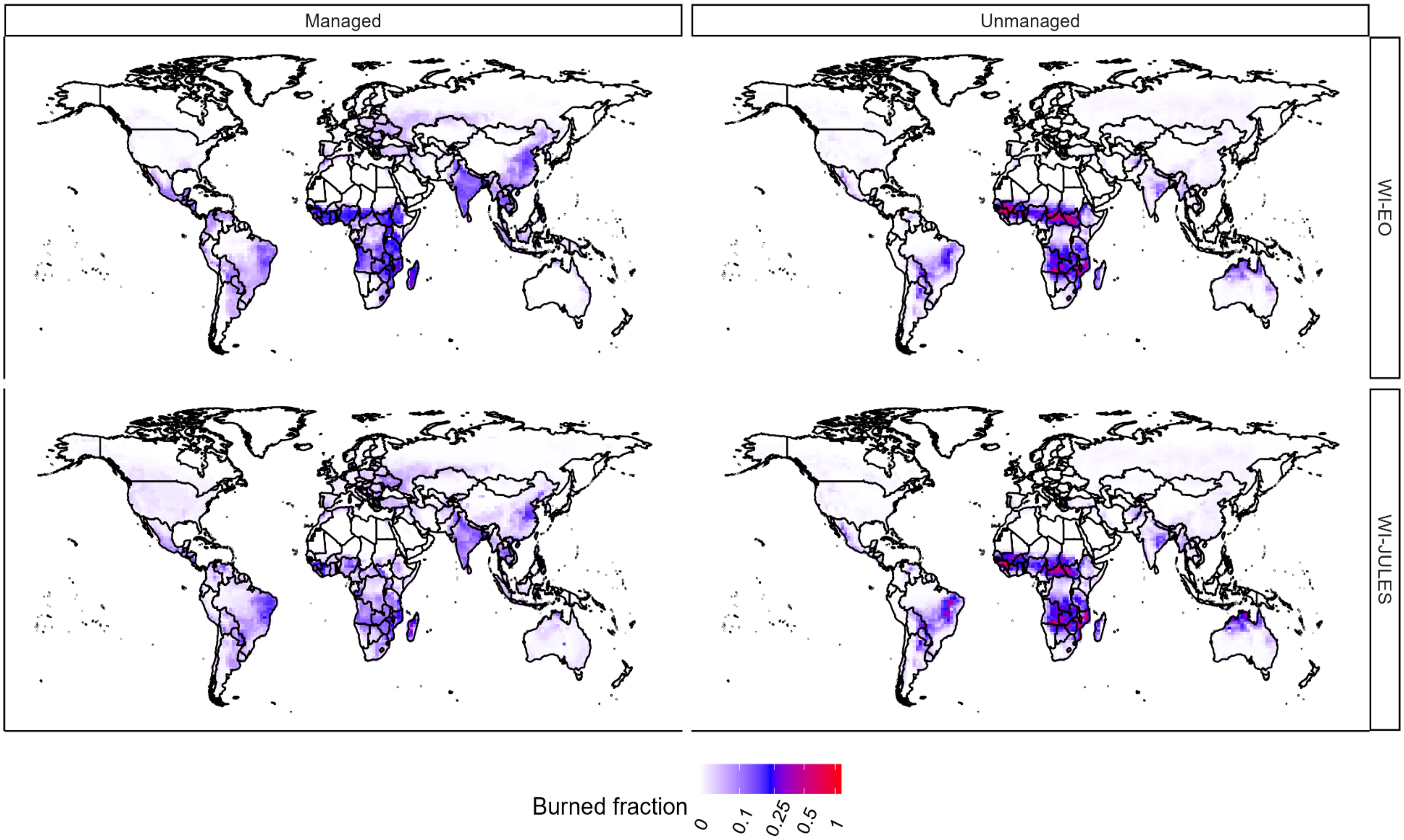

Figure 4: Distribution of managed and unmanaged fire in WHAM-INFERNO-Earth Observation (WI-EO) and WHAM-INFERNO-JULES (WI-JULES) shown as the burned fraction of each pixel. The arithmetic mean of model outputs was taken across the historical model run period (1990-2014). Principle differences between the two versions of WHAM-INFERNO are seen in the managed fire outputs of WI-EO in sub-Saharan Africa, which have a more homogeneous distribution than WI-JULES's more sporadic spatial pattern. Other anomalies between models are seen in the Caatinga region of Brazil and in the Northern Territories of Australia.

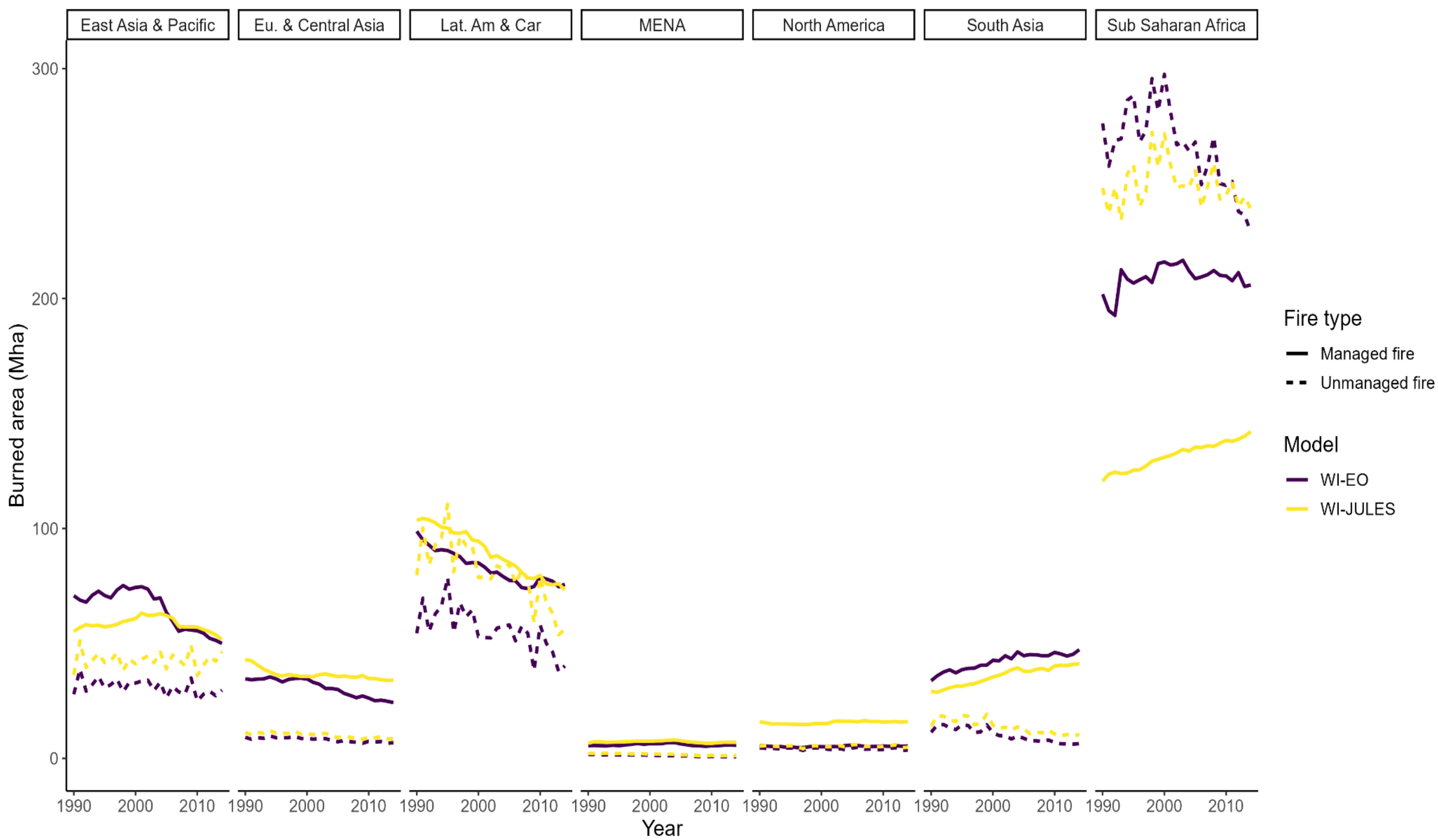

Figure 5: Trends in managed and unmanaged fire across the World Bank global regions. The largest gap between managed and unmanaged fire is seen in sub-Saharan Africa, where unmanaged fire dominates. Conversely, South Asia (including India) is dominated by managed fires, particularly crop residue fires (as shown in Perkins et al., 2023). Key: Eu. & Central Asia = Europe & Central Asia; Lat. Am & Car = Latin America & Caribbean; MENA = Middle East and North Africa.

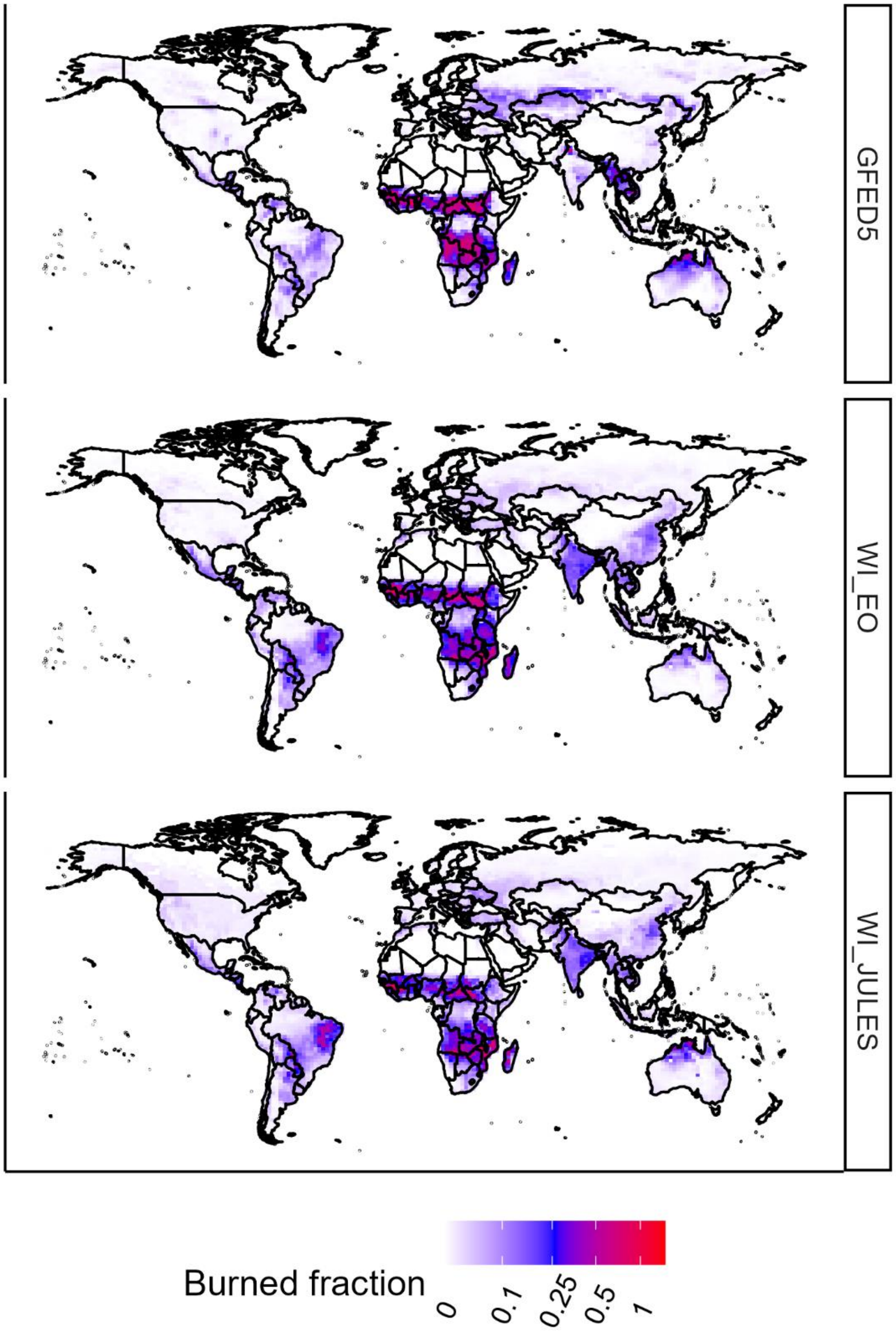

Figure 6: Burned area in GFED5, WI-EO and WI-JULES as a fraction of each pixel. Values shown are the mean of the period (2001-2014). Three clear anomalies between models and GFED5 are present: firstly in the Caatinga region of Brazil, secondly in southern Russia, and thirdly in India. This latter discrepancy is due to differences in burned area from crop residue burning between WHAM! and GFED5 (Perkins et al., 2023).

3.2.2 Temporal analysis

Across the overlapping period with GFED5 (2001-2014), WI-EO global burned area declines by 137 Mha, WI-JULES burned area declines by 52 Mha, and the baseline model declines by 30Mha. This compares with a decline of 193 Mha in GFED5. In WI-EO, this global decline is primarily attributable to the trend in sub-Saharan Africa (Figure 7), where burned area declines by 61 Mha (compared to 112 Mha in GFED5). By contrast, in WI-JULES burned area in sub-Saharan Africa declines by just 9 Mha (Figure 7). This lack of decline in sub-Saharan Africa is in part due to managed fires, which increase by 10 Mha as crop residue burning increases in the region in this model. A similar trend is seen in sub-Saharan African crop-residue burning in WI-EO, but this is offset by a steeper decline in pasture fires (Perkins et al., 2023). Further, WI-JULES seemingly overestimates the rate of declining burned area in Latin America & Caribbean (-42 Mha; GFED5 -18 Mha), whilst WI-EO captures a similar rate of decline to GFED5 (-20 Mha). As such, WI-EO is best able to reproduce the observed decline in burned area, followed by WI-JULES, and then the baseline model. The drivers of this modelled decline are explored in detail below.

Globally, both WI-JULES and WI-EO underestimate the magnitude of interannual variability (IAV) in burned area. The standard deviation of detrended model outputs (i.e. with mean = 0) was 9.5Mha in WI-EO and 9.7Mha in WI-JULES. However, the correlation of the detrended outputs with GFED5 was 0.81 in WI-EO and 0.41 in WI-JULES: indicating that although the magnitude of IAV is underestimated in both models, WI-EO is substantially better at capturing the direction of fluctuations in burned area. IAV in both model is driven by unmanaged fire. Detrended global outputs for unmanaged fire correlate with detrended global burned area in GFED5 (WI-EO: $r = 0.74$, WI-JULES: $r = 0.53$); however there is no meaningful relationship for IAV in GFED5 and detrended outputs for managed fire ($r \leq 0.11$).

Based on the variable with the strongest Kendall's Tau correlation in each pixel, inter-annual change in burned area due to unmanaged fire is most strongly associated with flammability (Figure 8). In WI-JULES, flammability has the highest Tau value across 9,644 Mha (~70% of global land area; Table 2), whilst cropland conversion, which has the strongest relationship over the second largest area, has the highest Tau value across 1,037 Mha (~8% of global land area). A similar trend is seen in WI-EO, where flammability has the highest Tau value across 9,414 Mha and cropland conversion has the highest Tau value across 1,052 Mha.

However, whilst change in burned area is most closely correlated with flammability over the largest area, these areas are seemingly weighted towards model pixels with less overall change in burned area. For both WI-EO and WI-JULES, in linear regression models of interannual variability absolute t-values for flammability are more than twice as large as any other variable (Table 2). By contrast, for the overall change over 2001-2014, t-values are closer between variables, with ignitions having the largest absolute t-values for both models. Similarly, variables with a negative impact on burned area have a larger impact on the overall 2001-2014 change than interannual variation (Table 2). Road density seemingly has the largest impact on declining burned area (t-values: -21.7 & -19.3), followed by cropland conversion (t-values: -16.1 & -19.1) respectively. Fire suppression has only a marginal influence and indeed shows little relationship with the long-term trend in WI-JULES ($t = 0.433$).

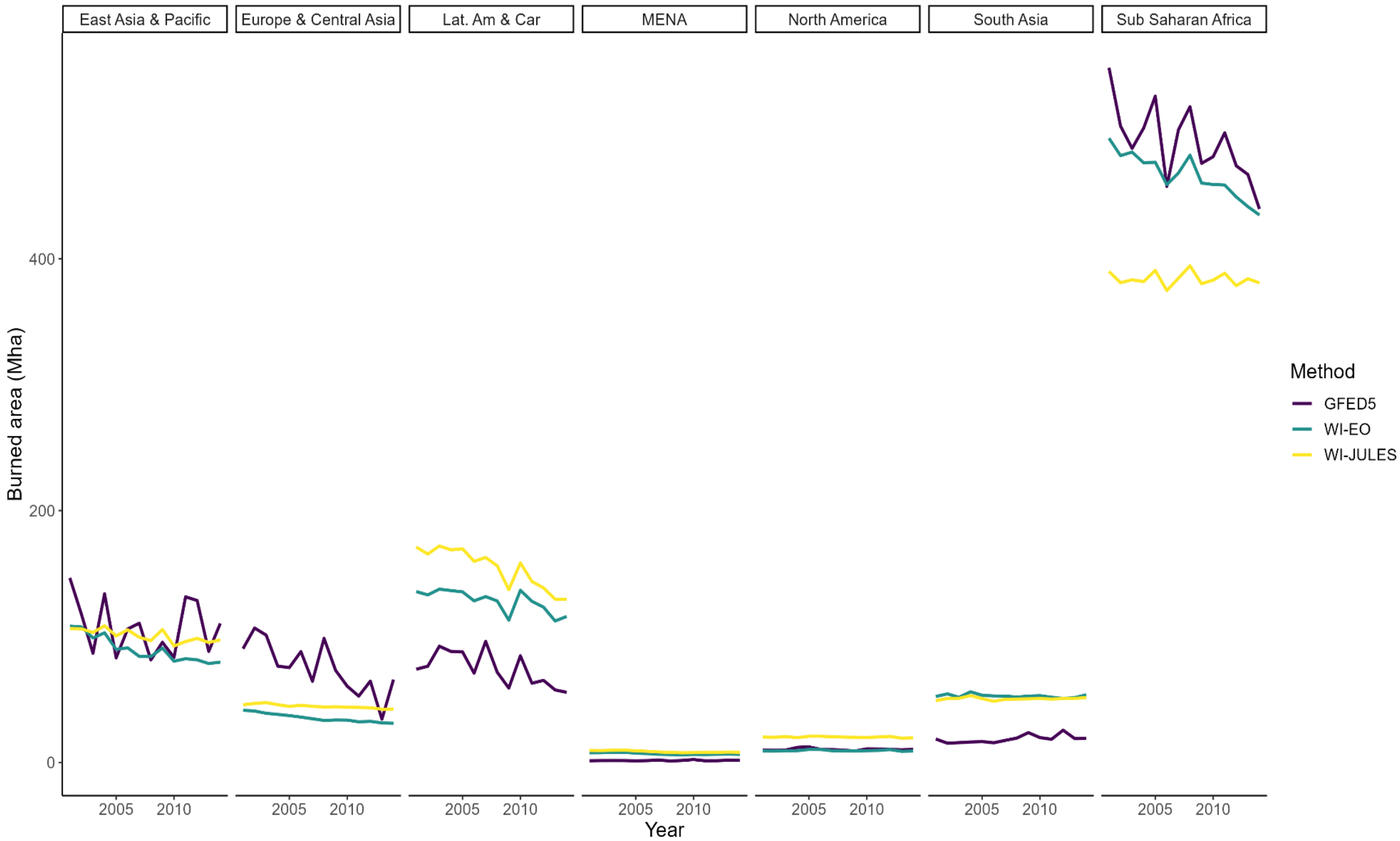

Figure 7: Burned area by World Bank region in GFED5 and the two versions of the WHAM-INFERNO model ensemble (WHAM-EO, WI-JULES). WI-EO is best able to reproduce the observed decline in burned area in sub-Saharan Africa, with WI-JULES showing an essentially static burned area. Conversely, both WI-EO and WI-JULES overestimate burned area in Latin America, though the trend of declining burned area is captured strongly. Both models show generally poor performance in Europe & Central Asia, showing limited discernible trend. Model outputs for WI-EO and WI-JULES are the sum of the managed and unmanaged burned area presented in Figure 5. Key: Lat. Am & Car = Latin America & Caribbean; MENA = Middle East and North Africa.

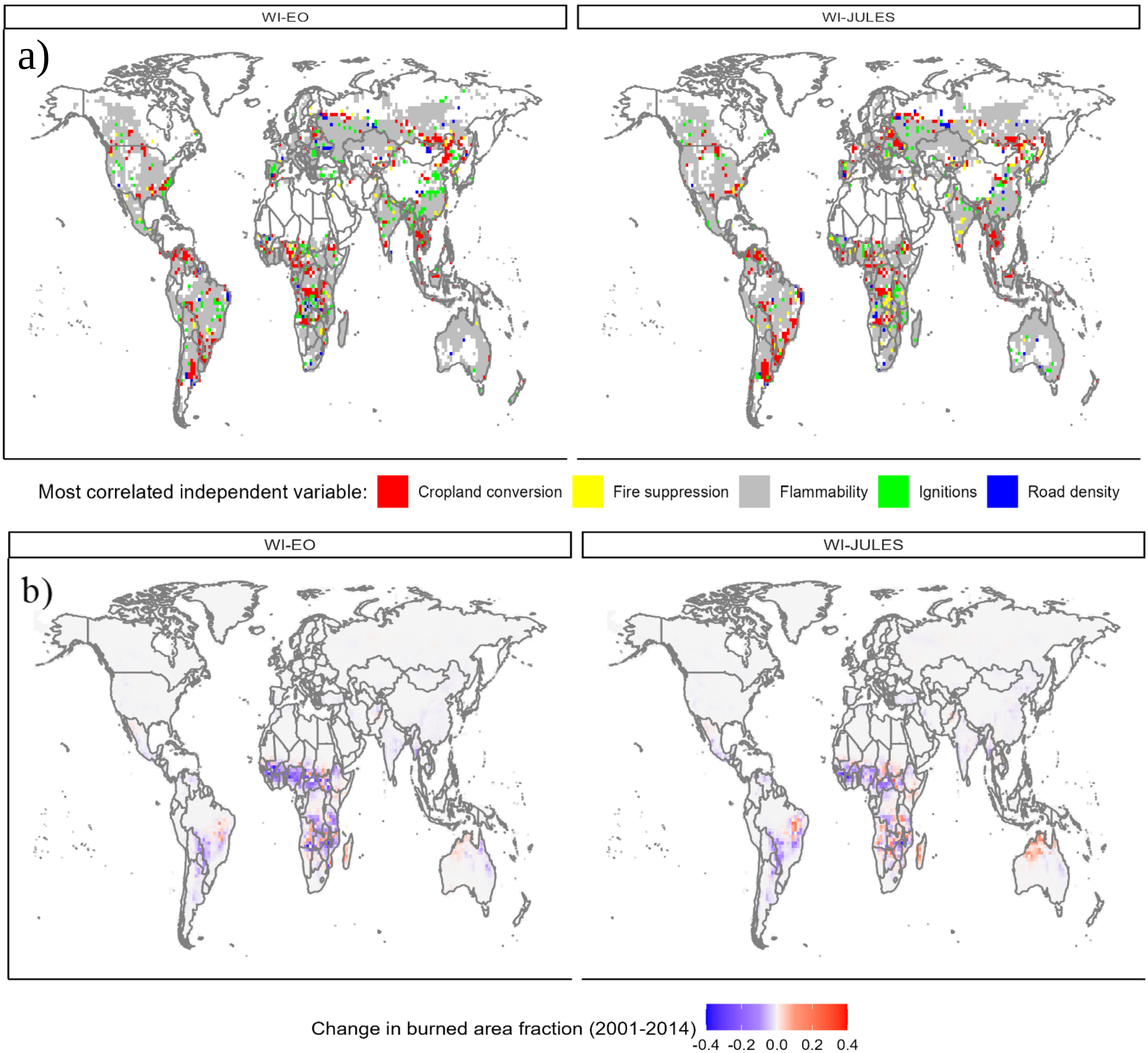

Figure 8: Relationship of changes in unmanaged burned area to independent variables. a) Variable with highest absolute correlation (τ) with change in burned area from unmanaged fire; values were filtered for pixels with at least 0.1% of the land area burned. b) Change in burned area between 2001-2014. Although flammability is most closely correlated with changes in burned area across the largest geographic space, the influence of other factors – particularly cropland conversion – is clustered towards pixels with the largest changes in burned area. A non-linear stretch was applied to the colour scale in b) to show differences between smaller absolute values.

Table 2: Relationship of changes in burned area from unmanaged fires to explanatory variables. Area gives the total land surface over which each variable was most strongly correlated with changing burned area. T-values are from linear models of change in burned area to change in the independent variable; IAV (interannual variation) is for linear models of year-on-year change between 2001-2014, whilst trend denotes overall change during the same period.

	WI-EO (area; Mha)	**WI-EO (t-value; IAV)**	**WI-EO (t-value; trend)**	**WI-JULES (area; Mha)**	**WI-JULES (t-value; IAV)**	**WI-JULES (t-value; trend)**
Cropland conversion	1052	-10.4	-16.1	1037	-13.8	-19.1
Fire suppression	244	-2.78	3.26	377	-1.9	0.43
Flammability	9414	162.3	24.4	9644	267.2	46.0
Ignitions	736	70.61	25.7	522	87.5	46.6
Road density	206	-5.1	-21.7	209	-8.0	-19.3

4 Discussion

This paper has presented the first integration of a global-scale behavioural model of human fire use and management coupled with a dynamic global vegetation model. Discussion focuses on advances made for global understanding of human drivers of vegetation fire regimes through this technical advance, before addressing its limitations and possible future directions for development of WHAM-INFERNO.

4.1 WHAM-INFERNO: Insights for global-human fire interactions

The WHAM-INFERNO model integration reveals both the extent and the diversity of the socio-ecological dynamics of global fire regimes. In pareto model runs of WHAM-INFERNO, managed and unmanaged fire contribute approximately equal amounts of global burned area. Furthermore, the spatiotemporal distribution of anthropogenic managed fire, and its relationship with unmanaged ('wild') fires differs substantially across space. Whilst anthropogenic fire use, primarily for crop residue burning, dominates the South Asian World Bank Region, in sub-Saharan Africa more than half of burned area is from unmanaged fires (Figure 5). Such differences have profound implications for understanding of global fire regimes and illustrates that effective fire management policies and climate adaptation strategies must be based on detailed understanding of how human livelihoods and associated fire use systems contribute to existing fire regimes. At the very least, the large extent of managed anthropogenic fire around the world implied by these results is demonstration of the inadequacy of model approaches seeking to represent direct anthropogenic influence on fire regimes as simple functions of population density (Rabin et al., 2017).

Furthermore, combined global-scale simulations of both managed and unmanaged fire presented here add weight to the finding from Earth observation that small fires have declined less than larger ones (Chen et al., 2023). Managed fire declines by just 35% and 52% of the rate of unmanaged fire in WI-JULES and WI-EO respectively. Data from empirical studies indicates that the two largest sources of burned area from managed human fires – crop residue burning and pasture management – have mean sizes of 5 ha and 34 ha respectively (Millington et al., 2022), whilst in JULES-INFERNO mean burned area per fire for unmanaged fires varies from 170 ha to 320 ha. This result seems to give weight to findings of Smith et al., (2022) and Perkins et al., (2023), that managed fire is changing in line with socio-ecological forces that are distinct from those driving change in unmanaged fire.

In addition, the finding that unmanaged fire is primarily responsible for interannual variability in burned area (Section 3.2.2) is consistent with the findings of Randerson et al., (2012), who find less fluctuation in small fires than those detectable by MODIS (i.e. <21 ha). This is intuitive, as crop residue fires, for example, occur annually according to the logic of cropping systems rather than fluctuations in climate (Millington et al., 2022). However, this opens an intriguing possibility for fire-enabled DGVMs, which have typically struggled with interannual variability whilst also not including representation of managed human fires – the more static part of the regime (Li et al., 2019). In effect, DGVMs may have been *doubly* underestimating the sensitivity of burned area from unmanaged fires to interannual climate variability. This underrepresentation of the sensitivity of unmanaged fires to climate volatility may contribute to the difficulty of attributing changes in global fire regimes to global warming (Jones et al., 2022), although a lack of representation of peat fires may also be a partial explanation (Blackford et al., 2023; Li et al., 2019).

By accounting for the less temporally variable and more spatially homogeneous signal of burned area due to managed fires (Figures 4 & 5), the WHAM-INFERNO integration advances understanding of the drivers of declining global burned area. Whilst interannual variability is primarily driven by changes in vegetation flammability, longer-term change in burned area highlights the important role played by the fragmentation of natural and semi-natural vegetation through road building and cropland conversion (Figure 8). This result coheres strongly with that of Andela et al., (2017) who find that interannual variability is closely linked to precipitation, whilst cropland fraction is strongly associated with declining burned area. Furthermore, WHAM-INFERNO can identify the processes underlying the finding of Andela that cropland has a spatially heterogeneous impact on burned area. For example, increased burned area in croplands in South Asia and Northeastern China is due to large-scale agricultural residue burning, whilst decreased fire in savanna grasslands is due to landscape fragmentation and the subsequent reduced capacity of savanna grasslands to sustain unmanaged fires.

4.2 Model performance and limitations

Both versions of the WHAM-INFERNO ensemble represent a significant improvement in the capacity of INFERNO to reproduce historical global annual burned area over the baseline model (Figure 3), and indeed over the performance of INFERNO against GFED4 presented in FIREMIP (r= 0.70; Mangeon et al., 2016; Teckentrup et al., 2019). This demonstrates the fundamental importance of a process-based approach to understanding and representing human-fire interactions in global modelling. Furthermore, the improvements made in WHAM-INFERNO over the baseline version allow the impact of landscape fragmentation in global burned area to be incorporated and understood (Figures 2 & 8). Indeed, the WHAM-INFERNO integration, and particular WI-EO seems to advance capacity for DGVMs to reproduce the observed decline in global burned area (Hantson et al., 2020).

However, representation of landscape fragmentation, its interaction with different ecosystem types, and other anthropogenic pressures remains incomplete. One way that WHAM-INFERNO represents fragmentation is through the role of roads in reducing fire size (Haas et al., 2022), by applying a road density correction to fire sizes per PFT. Although useful in constraining the model pareto parameter space through restricting burned area in more densely populated areas (Supplementary Information; Figure S1) this single global function is a somewhat simplistic way of capturing such effects, resulting in a substantially larger impact on WHAM-INFERNO burned area outputs than on correlation with GFED5 (Supplementary Information; Figure S2). Hence, the road density parameterisation in WHAM-INFERNO employed to capture fragmentation effects is analogous to representations of anthropogenic 'ignitions' as a global function of population density in previous fire-enabled DGVMs: they are both a first step with outstanding issues to be addressed. By contrast, the representation of selective logging on the flammability of fire-prone tropical forests in WHAM-INFERNO has been more successful. Although having a small impact on global burned area, including this process leads to an improved global correlation between WHAM-INFERNO outputs and GFED5 (Supplementary Information; Figure S2). Representation of logging was derived from WHAM! outputs, hence illustrating the value of process-based representation of anthropogenic impacts on fire regimes, as opposed to the top-down road density parameterisation.

Finally, it is notable that WI-EO performs more strongly than WI-JULES at reproducing the magnitude, spatial distribution and temporal dynamics of burned area found in GFED5. On one hand, this illustrates the benefits of a well-specified parameterisation of managed human fire: by better accounting for this aspect of the observed burned area signal, WI-EO is better able to reproduce the inter-annual variability of unmanaged fire, and its pronounced global decline. Yet the weaker performance of WI-JULES perhaps also illustrates the potential for underlying error in the representation of ecosystems within DGVMs to lead to misleading conclusions being drawn from their fire modules (Hantson et a., 2020). Continued model intercomparison projects and use of model ensembles are likely to remain the most effective means to apply the fire outputs of DGVMs (e.g. Burton et al., 2023). Overall, the large scale of anthropogenic managed fire entails that careful consideration should be given to how future socioeconomic scenarios, and their limitations, inform our projections of how global fire regimes may evolve under a warming climate (Keys et al., 2024).

5 Conclusion

This paper has presented the first integration of a global behavioural model of human fire use and management with a dynamic global vegetation model. Overall, model evaluation highlights the strong benefits of coupled socio-ecological modelling approaches for reproducing the observed spatial and temporal patterns of burned area globally. Furthermore, findings demonstrate the extent and complexity of human-fire interactions. Results imply that managed anthropogenic fire accounts for as much as half of all global burned area, whilst the trends and distribution of, and relationship between, managed and unmanaged fires is highly spatially heterogeneous. Such complexities demonstrate that socio-ecological modelling is vital to advance understanding of present-day and future fire regimes. A key area for future work identified here is in developing more nuanced representation of landscape fragmentation, particularly in grazing lands in sub-Saharan Africa, which remain a central contributor to global burned area.

Acknowledgments

This work was funded by the Leverhulme Centre for Wildfires, Environment and Society through the Leverhulme Trust, grant number RC-2018-023. AV has also been supported by the AXA Research Fund (project 'AXA Chair in Wildfires and Climate') and by the Hellenic Foundation for Research and Innovation (Grant ID 3453). The authors declare no conflicts of interest.

Open Research

Data and code necessary to reproduce the results in this paper, as well as analysis and figures presented are made available on zenodo: https://zenodo.org/doi/10.5281/zenodo.8319445 (Perkins et al., 2023b). Code to run the WHAM-INFERNO ensemble are also made available on GitHub: https://github.com/OliPerkins1987/WHAM_INFERNO. All data and code are mode available under a Creative Commons License.

References

Andela, N., Morton, D. C., Giglio, L., Chen, Y., van der Werf, G. R., Kasibhatla, P. S., et al. (2017). A human-driven decline in global burned area. *Science*, *356*(6345), 1356–1362. https://doi.org/10.1126/science.aal4108

Archibald, S. (2016). Managing the human component of fire regimes: Lessons from Africa. *Philosophical Transactions of the Royal Society B: Biological Sciences*, *371*(1696), 20150346. https://doi.org/10.1098/rstb.2015.0346

Archibald, S., & Hempson, G. P. (2016). Competing consumers: Contrasting the patterns and impacts of fire and mammalian herbivory in Africa. *Philosophical Transactions of the Royal Society B: Biological Sciences*, *371*(1703), 20150309. https://doi.org/10.1098/rstb.2015.0309

Archibald, S., Staver, A. C., & Levin, S. A. (2012). Evolution of human-driven fire regimes in Africa. *Proceedings of the National Academy of Sciences*, *109*(3), 847–852. https://doi.org/10.1073/pnas.1118648109

Arneth, A., Brown, C., & Rounsevell, M. D. A. (2014). Global models of human decision-making for land-based mitigation and adaptation assessment. *Nature Climate Change*, *4*(7), Article 7. https://doi.org/10.1038/nclimate2250

Blackford, K. R., Kasoar, M., Burton, C., Burke, E., Prentice, I. C., & Voulgarakis, A. (2023). INFERNO-peat v1.0.0: A representation of northern high latitude peat fires in the JULES-INFERNO global fire model. *EGUsphere*, 1–31. https://doi.org/10.5194/egusphere-2023-2399

Burton, C., Betts, R., Cardoso, M., Feldpausch, T. R., Harper, A., Jones, C. D., et al. (2019). Representation of fire, land-use change and vegetation dynamics in the Joint UK Land Environment Simulator vn4.9 (JULES). *Geoscientific Model Development*, *12*(1), 179–193. https://doi.org/10.5194/gmd-12-179-2019

Burton, C., Lampe, S., Kelley, D., Thiery, W., Hantson, S., Christidis, N., et al. (2023). Global burned area increasingly explained by climate change, PREPRINT (Version 1) available at Research Square. https://doi.org/10.21203/rs.3.rs-3168150/v1

Carnell, R. (2022). *lhs: Latin Hypercube Samples*. R package version 1.1.6, https://CRAN.R-project.org/package=lhs.

Chen, Y., Hall, J., van Wees, D., Andela, N., Hantson, S., Giglio, L., et al. (2023). Multi-decadal trends and variability in burned area from the 5th version of the Global Fire Emissions Database (GFED5). *Earth System Science Data Discussions*, 1–52. https://doi.org/10.5194/essd-2023-182

Christian, H. J., Blakeslee, R. J., Boccippio, D. J., Boeck, W. L., Buechler, D. E., Driscoll, K. T., et al. (2003). Global frequency and distribution of lightning as observed from space by the Optical Transient Detector. *Journal of Geophysical Research: Atmospheres*, *108*(D1), ACL 4-1-ACL 4-15. https://doi.org/10.1029/2002JD002347

Clark, D. B., Mercado, L. M., Sitch, S., Jones, C. D., Gedney, N., Best, M. J., et al. (2011). The Joint UK Land Environment Simulator (JULES), model description – Part 2: Carbon fluxes and vegetation dynamics. *Geoscientific Model Development*, *4*(3), 701–722. https://doi.org/10.5194/gmd-4-701-2011

Cochrane, M. A., & Barber, C. P. (2009). Climate change, human land use and future fires in the Amazon. *Global Change Biology*, *15*(3), 601–612. https://doi.org/10.1111/j.1365-2486.2008.01786.x

Driscoll, D. A., Armenteras, D., Bennett, A. F., Brotons, L., Clarke, M. F., Doherty, T. S., et al. (2021). How fire interacts with habitat loss and fragmentation. *Biological Reviews*, *96*(3), 976–998. https://doi.org/10.1111/brv.12687

Ford, A. E., Harrison, S. P., Kountouris, Y., Millington, J. D., Mistry, J., Perkins, O., et al. (2021). Modelling human-fire interactions: Combining alternative perspectives and approaches. *Frontiers in Environmental Science*, *9*, 649835.

Forkel, M., Andela, N., Harrison, S. P., Lasslop, G., van Marle, M., Chuvieco, E., et al. (2019). Emergent relationships with respect to burned area in global satellite observations and fire-enabled vegetation models. *Biogeosciences*, *16*(1), 57–76. https://doi.org/10.5194/bg-16-57-2019

Giglio, L., Randerson, J. T., & van der Werf, G. R. (2013). Analysis of daily, monthly, and annual burned area using the fourth-generation global fire emissions database (GFED4). *Journal of Geophysical Research: Biogeosciences*, *118*(1), 317–328. https://doi.org/10.1002/jgrg.20042

Haas, O., Prentice, I. C., & Harrison, S. P. (2022). Global environmental controls on wildfire burnt area, size, and intensity. *Environmental Research Letters*, *17*(6), 065004. https://doi.org/10.1088/1748-9326/ac6a69

Hall, J., Argueta, F., Zubkova, M., Chen, Y., Randerson, J. & Giglio, L. (2024). GloCAB: global cropland burned area from mid-2002 to 2020. *Earth System Science Data*, 16(2), 867-885. https://doi.org/10.5194/essd-16-867-2024

Hantson, S., Kelley, D. I., Arneth, A., Harrison, S. P., Archibald, S., Bachelet, D., et al. (2020). Quantitative assessment of fire and vegetation properties in simulations with fire-enabled vegetation models from the Fire Model Intercomparison Project. *Geoscientific Model Development*, *13*(7), 3299–3318.

Harrison, S. P., Prentice, I. C., Bloomfield, K. J., Dong, N., Forkel, M., Forrest, M., et al. (2021). Understanding and modelling wildfire regimes: An ecological perspective. *Environmental Research Letters*, *16*(12), 125008. https://doi.org/10.1088/1748-9326/ac39be

Hijmans, R. (2023). raster: Geographic Data Analysis and Modeling. R package version 3.6-20. https://CRAN.R-project.org/package=raster

Hurtt, G. C., Chini, L., Sahajpal, R., Frolking, S., Bodirsky, B. L., Calvin, K., et al. (2020). Harmonization of global land use change and management for the period 850–2100 (LUH2) for CMIP6. *Geoscientific Model Development*, *13*(11), 5425–5464. https://doi.org/10.5194/gmd-13-5425-2020

Jones, M. W., Abatzoglou, J. T., Veraverbeke, S., Andela, N., Lasslop, G., Forkel, M., et al. (2022). Global and Regional Trends and Drivers of Fire Under Climate Change. *Reviews of Geophysics*, *60*(3), e2020RG000726. https://doi.org/10.1029/2020RG000726

Kelley, D. I., Bistinas, I., Whitley, R., Burton, C., Marthews, T. R., & Dong, N. (2019). How contemporary bioclimatic and human controls change global fire regimes. *Nature Climate Change*, *9*(9), 690–696. https://doi.org/10.1038/s41558-019-0540-7

Keys, P. W., Badia, L., & Warrier, R. (2024). The Future in Anthropocene Science. *Earth's Future*, *12*(1), e2023EF003820. https://doi.org/10.1029/2023EF003820

Kumar, N., Chaudhary, A., Ahlawat, O. P., Naorem, A., Upadhyay, G., Chhokar, R. S., et al. (2023). Crop residue management challenges, opportunities and way forward for sustainable food-energy security in India: A review. *Soil and Tillage Research*, *228*, 105641. https://doi.org/10.1016/j.still.2023.105641

Lapola, D. M., Pinho, P., Barlow, J., Aragão, L. E. O. C., Berenguer, E., Carmenta, R., et al. (2023). The drivers and impacts of Amazon forest degradation. *Science*, *379*(6630), eabp8622. https://doi.org/10.1126/science.abp8622

Laris, P. (2002). Burning the Seasonal Mosaic: Preventative Burning Strategies in the Wooded Savanna of Southern Mali. *Human Ecology*, *30*(2), 155–186. https://doi.org/10.1023/A:1015685529180

Lasslop, G., Coppola, A., Voulgarakis, A., Yue, C., & Veraverbeke, S. (2019). Influence of Fire on the Carbon Cycle and Climate. *Current Climate Change Reports*, 5, 112-113. https://doi.org/10.1007/s40641-019-00128-9

Li, F., Val Martin, M., Andreae, M. O., Arneth, A., Hantson, S., Kaiser, J. W., et al. (2019). Historical (1700–2012) global multi-model estimates of the fire emissions from the Fire Modeling Intercomparison Project (FireMIP). *Atmospheric Chemistry and Physics*, *19*(19), 12545–12567. https://doi.org/10.5194/acp-19-12545-2019

Mangeon, S., Voulgarakis, A., Gilham, R., Harper, A., Sitch, S., & Folberth, G. (2016). INFERNO: A fire and emissions scheme for the UK Met Office's Unified Model. *Geoscientific Model Development*, *9*(8), 2685–2700. https://doi.org/10.5194/gmd-9-2685-2016

Mathison, C., Burke, E., Hartley, A. J., Kelley, D. I., Burton, C., Robertson, E., et al. (2023). Description and evaluation of the JULES-ES set-up for ISIMIP2b. *Geoscientific Model Development*, *16*(14), 4249–4264. https://doi.org/10.5194/gmd-16-4249-2023

Meijer, J. R., Huijbregts, M. A. J., Schotten, K. C. G. J., & Schipper, A. M. (2018). Global patterns of current and future road infrastructure. *Environmental Research Letters*, *13*(6), 064006. https://doi.org/10.1088/1748-9326/aabd42

Millington, J. D. A., Perkins, O., & Smith, C. (2022). Human Fire Use and Management: A Global Database of Anthropogenic Fire Impacts for Modelling. *Fire*, *5*(4), Article 4. https://doi.org/10.3390/fire5040087

Perkins, O., Kasoar, M., Voulgarakis, A., Smith, C., Mistry, J., & Millington, J. (2023). A global behavioural model of human fire use and management: WHAM! v1.0. *EGUsphere* (accepted for publication in *Geoscientific Model Development*), 1–42. https://doi.org/10.5194/egusphere-2023-2162.

Perkins, O., Kasoar, M., Voulgarakis, A., Edwards, T., & Millington, J. (2023b). [Software] WHAM-INFERNO, code and supporting data. https://zenodo.org/doi/10.5281/zenodo.8319445

Perkins, O., & Millington, J. D. A. (2021). DAFI: A global database of Anthropogenic Fire. *Figshare Https://Doi. Org/10.6084/M9. Figshare. c*, *5290792*.

R Core Team. (2022). R: A language and environment for statistical computing. R Foundation for Statistical Computing, Vienna, Austria. https://www.R-project.org/.

Rabin, S. S., Melton, J. R., Lasslop, G., Bachelet, D., Forrest, M., Hantson, S., et al. (2017). The Fire Modeling Intercomparison Project (FireMIP), phase 1: Experimental and analytical protocols with detailed model descriptions. *Geoscientific Model Development*, *10*(3), 1175–1197. https://doi.org/10.5194/gmd-10-1175-2017

Randerson, J. T., Chen, Y., van der Werf, G. R., Rogers, B. M., & Morton, D. C. (2012). Global burned area and biomass burning emissions from small fires. *Journal of Geophysical Research: Biogeosciences*, *117*(G4). https://doi.org/10.1029/2012JG002128

Ripley, B. S., Raubenheimer, S. L., Perumal, L., Anderson, M., Mostert, E., Kgope, B. S., Midgley, G. F., & Simpson, K. J. (2022). CO2-fertilisation enhances resilience to browsing in the recruitment phase of an encroaching savanna tree. *Functional Ecology*, *36*(12), 3223–3233. https://doi.org/10.1111/1365-2435.14215

Robinson, D. T., Di Vittorio, A., Alexander, P., Arneth, A., Barton, C. M., Brown, D. G., Kettner, A., Lemmen, C., et al. (2018). Modelling feedbacks between human and natural processes in the land system. *Earth System Dynamics*, *9*(2), 895–914. https://doi.org/10.5194/esd-9-895-2018

Rosan, T. M., Sitch, S., Mercado, L. M., Heinrich, V., Friedlingstein, P., & Aragão, L. E. O. C. (2022). Fragmentation-Driven Divergent Trends in Burned Area in Amazonia and Cerrado. *Frontiers in Forests and Global Change*, *5*. https://www.frontiersin.org/articles/10.3389/ffgc.2022.801408

Rougier, J. C., & Beven, K. J. (2013). *Model and data limitations: The sources and implications of epistemic uncertainty* (pp. 40–63). Cambridge University Press. https://doi.org/10.1017/CBO9781139047562.004

Shuman, J. K., Balch, J. K., Barnes, R. T., Higuera, P. E., Roos, C. I., Schwilk, D. W., et al. (2022). Reimagine fire science for the anthropocene. *PNAS Nexus*, *1*(3), pgac115. https://doi.org/10.1093/pnasnexus/pgac115

Smith, C., Perkins, O., & Mistry, J. (2022). Global decline in subsistence-oriented and smallholder fire use. *Nature Sustainability*, *5*(6), Article 6. https://doi.org/10.1038/s41893-022-00867-y

Stevens, N., Erasmus, B. F. N., Archibald, S., & Bond, W. J. (2016). Woody encroachment over 70 years in South African savannahs: Overgrazing, global change or extinction aftershock? *Philosophical Transactions of the Royal Society B: Biological Sciences*, *371*(1703), 20150437. https://doi.org/10.1098/rstb.2015.0437

Teckentrup, L., Harrison, S. P., Hantson, S., Heil, A., Melton, J. R., Forrest, M., et al. (2019). Response of simulated burned area to historical changes in environmental and anthropogenic factors: A comparison of seven fire models. *Biogeosciences*, *16*(19), 3883–3910. https://doi.org/10.5194/bg-16-3883-2019

UNEP - the United Nations Environment Programme (2022). *Spreading like Wildfire: The Rising Threat of Extraordinary Landscape Fires*. http://www.unep.org/resources/report/spreading-wildfire-rising-threat-extraordinary-landscape-fires

Wiltshire, A. J., Duran Rojas, M. C., Edwards, J. M., Gedney, N., Harper, A. B., Hartley, A. J., et al. (2020). JULES-GL7: The Global Land configuration of the Joint UK Land Environment Simulator version 7.0 and 7.2. *Geoscientific Model Development*, *13*(2), 483–505. https://doi.org/10.5194/gmd-13-483-2020

Zubkova, M., Humber, M. L., & Giglio, L. (2023). Is global burned area declining due to cropland expansion? How much do we know based on remotely sensed data? *International Journal of Remote Sensing*, *44*(4), 1132–1150. https://doi.org/10.1080/01431161.2023.2174389

References from the supporting information

Craig, P.S., Goldstein, M., Seheult, A.H., & Smith, J.A. (1997). P*ressure Matching for Hydrocarbon Reservoirs: A Case Study in the Use of Bayes Linear Strategies for Large Computer Experiments*, in: Gatsonis, C., Hodges, J.S., Kass, R.E., McCulloch, R., Rossi, P., Singpurwalla, N.D. (Eds.), *Case Studies in Bayesian Statistics*, Lecture Notes in Statistics. Springer, New York, NY, pp. 37–93. https://doi.org/10.1007/978-1-4612-2290-3_2

Florian, A. (1992). An efficient sampling scheme: Updated Latin Hypercube Sampling. *Probabilistic Engineering Mechanics*, 7, 123–130. https://doi.org/10.1016/0266-8920(92)90015-A

Gupta, H.V., Sorooshian, S., & Yapo, P.O., 1998. Toward improved calibration of hydrologic models: Multiple and noncommensurable measures of information. *Water Resources Research*, 34, 751–763. https://doi.org/10.1029/97WR03495

Kennedy, M., & O'Hagan, A. (2001). Bayesian calibration of computer models, *Journal of the Royal Statistical Society* B, 63:3, 425-464.

Lin, Y., Xu, D., Wang, N., Shi, Z., & Chen, Q. (2020). Road Extraction from Very-High-Resolution Remote Sensing Images via a Nested SE-Deeplab Model. *Remote Sensing*, 12, 2985. https://doi.org/10.3390/rs12182985

Lu, L., Anderson-Cook, C.M., & Robinson, T.J. (2011). Optimization of Designed Experiments Based on Multiple Criteria Utilizing a Pareto Frontier. *Technometrics*, 53, 353–365.

McNeall, D., Williams, J., Booth, B., Betts, R., Challenor, P., Wiltshire, A., & Sexton, D. (2016). The impact of structural error on parameter constraint in a climate model. *Earth System Dynamics*, 7, 917–935. https://doi.org/10.5194/esd-7-917-2016

Pukelsheim, F. (1994). The Three Sigma Rule. *The American Statistician*, 48, 88–91. https://doi.org/10.2307/2684253

Roteta, E., Bastarrika, A., Padilla, M., Storm, T., & Chuvieco, E. (2019). Development of a Sentinel-2 burned area algorithm: Generation of a small fire database for sub-Saharan Africa. *Remote Sensing of Environment*, 222, 1–17. https://doi.org/10.1016/j.rse.2018.12.011

Williamson, D., Goldstein, M., Allison, L., Blaker, A., Challenor, P., Jackson, L., & Yamazaki, K. (2013). History matching for exploring and reducing climate model parameter space using observations and a large perturbed physics ensemble. *Climate Dynamics*, 41, 1703–1729. https://doi.org/10.1007/s00382-013-1896-4

The spatial distribution and temporal drivers of changing global fire regimes: a coupled socio-ecological modelling approach

Oliver Perkins[1,2], Matthew Kasoar[1,3], Apostolos Voulgarakis[1,3,4], Tamsin Edwards[2], and James Millington[1,2]

[1]The Leverhulme Centre for Wildfires, Environment, and Society, Imperial College London, SB7 2BX, UK, [2]Department of Geography, King's College London, WC2B 4BG, UK, [3]Department of Physics, Imperial College London, [4]School of Chemical and Environmental Engineering, Technical University of Crete, Kounoupidiana, 73100, Greece

Corresponding author: Oliver Perkins (oliver.perkins@kcl.ac.uk)

Key Points:

- Representing managed fire in global-scale fire models has represented a substantial research challenge in fire science
- We address this through the offline coupling of a global agent-based model of human fire use with a dynamic global vegetation model
- The coupling improves performance of modelled burned area and allows exploration of drivers of change in global fire regimes

Abstract

In the Anthropocene, humans are the largest drivers of change in vegetation fire regimes. Humans influence fire regimes both directly, by starting, managing and extinguishing fires, and also indirectly by altering fuel composition and connectivity. However, whilst vegetation fire is a coupled socio-ecological process, representation of human influences on fire regimes in global-scale modelling remains limited. This places a fundamental constraint on our ability to understand how human and natural processes combine to create observed patterns of vegetation fire, and how such processes may interact under future scenarios of socioeconomic and environmental change. Here, we respond to this challenge by presenting a novel integration of two global and process-based models. The first is the Wildfire Human Agency Model (WHAM!), which draws on agent-based approaches to represent anthropogenic fire use and management. The second is JULES-INFERNO, a fire-enabled dynamic global vegetation model, which takes a physically-grounded approach to the representation of vegetation-fire dynamics. The WHAM-INFERNO combined model suggests that as much as half of all global burned area is generated by managed anthropogenic fires – typically small fires that are lit and then spread according to land user objectives. Furthermore, we demonstrate that including representation of managed anthropogenic fires in a coupled socio-ecological simulation can improve understanding of the drivers of unmanaged wildfires. Overall, findings presented here have substantial implications for understanding of present-day and future fire regimes, indicating that socio-economic change may be as important as climate change in determining the future trajectory of fire on Earth.

Plain Language Summary

For millennia, humans have used fire as a tool to manage land and they continue to do so across the world today. However, global-scale models which are used to understand how vegetation fire may respond to climate change have not yet robustly accounted for this. So, we built a new model that represents how humans use and manage fire globally and coupled it with a global fire model. We find that improved representation of human impacts on fire significantly improves the model and sheds new light on what is driving change in vegetation fire globally. In particular, our results suggest current global fire models may have underestimated the sensitivity of fire to climate change.

1 Introduction

Vegetation fire is a coupled socio-ecological process, in which humans are the largest driver of change in its global distribution (Andela et al., 2017; Kelley et al., 2019). Perhaps the central example of this is that, whilst the planet has warmed under recent anthropogenic climate change, the area burned globally each year has decreased, particularly in savannas and grasslands (Chen et al., 2023). Drivers of this phenomenon are complex and uncertain (Zubkova et al., 2023), ranging from cropland conversion (Andela et al., 2017) to changes in anthropogenic fire use (Smith et al., 2022), from increased grazing intensity (Archibald & Hempson, 2016) to the CO2 fertilisation effect (Ripley et al., 2022; Stevens et al., 2016). A lack of clarity around the drivers of declining global burned area has made attribution of changes in global fire regimes a significant challenge (Jones et al., 2022). This, in turn, limits understanding of how fire may evolve in the future, including its potential role as a positive feedback to climate change (Lasslop et al., 2019).

At the heart of this uncertainty are the huge diversity of ways in which humans use and manage fire. Human fire use ranges from burning of agricultural residues in intensive land use systems (Kumar et al., 2023) to cultural uses such as religious ceremonies (Smith et al., 2022). Human fire management is similarly diverse, ranging from pro-active indigenous 'patch-burning' methods (Laris, 2002) to industrial fire suppression. As such, fire can broadly be categorised into managed or 'landscape' fires - which are typically small, controlled, and can be beneficial to humans - and unmanaged wildfires, which are larger and burn more intensely (UNEP 2022). Furthermore, human fire use is itself undergoing substantial change, with shifts away from more subsistence-oriented fire uses (Smith et al., 2022) and possibly an overall decline in fire use driven by agricultural intensification (Perkins et al., 2023). Consequently, Shuman et al., (2022) argue that incorporating managed fire into models at all spatial scales is an important step towards equipping fire science for the Anthropocene.

In addition to direct anthropogenic influences on fire, humans also have many indirect influences on fire regimes. For example, multiple authors have argued that anthropogenic fragmentation of vegetated landscapes is a key process shaping the evolution of global fire (Archibald et al., 2012; Driscoll et al., 2021; Harrison et al., 2021). Fragmentation can have opposite effects across ecosystems – with logging and degradation increasing fire in otherwise fire-independent forests, and reduced fuel connectivity decreasing burned area in grassland and savannah ecosystems (Rosan et al., 2022). As such, understanding the drivers of change within global fire regimes requires consideration not only of biophysical factors, but also of both direct and indirect human impacts.

Global-scale fire models have struggled to reproduce the observed decline in global burned area (Hantson et al., 2020). Indeed, in the first intercomparison project of the global fire model community (FireMIP; Rabin et al., 2017), models largely disagreed about both centennial trends, and more recent decadal trends, in global burned area (Teckentrup et al., 2019). Underlying this lack of consensus have been substantial limitations in the representation of human impacts on the fire modules of dynamic global vegetation models (DGVMs; Ford et al., 2021). Typically, these have been restricted to global functions relating population density to numbers of fires in satellite observations (Rabin et al., 2017). This ignores the diversity of human fire use and management, and hence limits the capability of DGVMs to advance understanding of socio-ecological dynamics of present-day fire regimes and how human and biophysical factors may interact in the future (Shuman et al., 2022).

The Wildfire Human Agency Model (WHAM!; Perkins et al., 2023) is the first formal model to represent present-day anthropogenic fire use and management at global scale. Drawing on agent-based approaches, WHAM! is a geospatial behavioural model that captures the underlying land system drivers of anthropogenic fire use and management to simulate human fire use decision-making from the bottom-up (Perkins et al., 2022). As WHAM! only represents human influences on global fire regimes, it was designed to be integrated with fire-enabled DGVMs, such as the JULES-INFERNO model (Mangeon et al., 2016), which capture the biophysical drivers of fire. Here we present the first coupling between WHAM! and JULES-INFERNO, such that biophysical, direct and indirect human drivers of fire regimes are all explicitly represented in an integrated simulation for the first time.

WHAM! takes its empirical basis from the Database of Anthropogenic Fire Impacts (DAFI; Perkins & Millington, 2021). DAFI is the product of a literature meta-analysis of 1809 case studies from 504 academic papers, government and NGO reports (Millington et al., 2022). This dataset addresses a previous barrier to improved representation of anthropogenic fire in DGVMs: the lack of a systematic data set on which to base new parameterisations (Forkel et al., 2019). Alongside development of DAFI, the 5th version of the Global Fire Emissions Database (GFED5; Chen et al., 2023) accounts for smaller fires than previous versions and therefore enables more robust evaluation of global-scale modelling of human fire interactions. Previous iterations of GFED have been based on a combination of MODIS for burned area and VIRS for active fire detection (Giglio et al., 2013). As such, they have not been able to systematically detect anthropogenic fires: DAFI suggests that >50% of anthropogenic fires are smaller than the 21ha threshold above which MODIS can detect (Millington et al., 2022). GFED5 incorporates higher resolution remote sensing (principally from Landsat and Sentinel-2), and hence is much more effective at capturing small fires: global burned area in GFED5 is a 61% increase over GFED4s (Chen et al., 2023). Therefore, with DAFI providing an empirical-basis for bottom-up modelling of human-fire interactions, and GFED5 better able to detect them from space, a comprehensive and empirically-grounded assessment of the role of managed anthropogenic fire in global fire regimes is now possible.

This paper presents the integration of WHAM! with JULES-INFERNO and its application to understand the spatiotemporal drivers of global fire regimes. Section 2 (Methods) focuses on describing the integration of outputs from the two models. Model calibration is described briefly in the main text with further details provided in Supplementary Information A. In Section 3 (Results), we present a brief evaluation of the outputs of the coupled model to establish its credibility, before focusing on understanding how human and biophysical factors combine to produce observed distributions of fire globally. Discussion (section 4) focuses on insights relevant to the question of declining global burned area, and in particular to understanding the relative contribution of direct human influences (starting and suppressing fires), indirect human influences (i.e. landscape fragmentation) and biophysical factors (i.e. climate and vegetation flammability).

2 Methods

Our methods are presented in five sections, which respectively describe the inputs, structure, calibration, evaluation, and analysis of the WHAM-JULES-INFERNO combined model (hereafter WHAM-INFERNO). A schematic overview of the processes represented in WHAM-INFERNO is presented in Figure 1. Calculations of the fire regime at each timestep combine three elements: 1) WHAM! outputs for managed and unmanaged anthropogenic fires and fire suppression; 2) JULES-INFERNO outputs for lightning ignitions, flammability and plant functional types; and 3) a representation of vegetation fragmentation derived from secondary data and WHAM! outputs for logging. These are each detailed further in Section 2.1.

Importantly, two versions of WHAM-INFERNO are presented and assessed: WHAM-INFERNO-JULES (hereafter WI-JULES) and WHAM-INFERNO-Earth Observation (hereafter WI-EO). The difference between these two versions is that in WI-JULES, WHAM! is parameterised using biophysical inputs directly from JULES, whilst in WI-EO, WHAM! takes these inputs from remote sensing. Specifically, inputs for potential evapotranspiration, net primary production and the bare soil fraction are replaced with Earth observation data. The differences between these two versions of WHAM! are described in detail in Perkins et al. (2023; Supplementary Information A).

The primary purpose of the comparison of WI-JULES and WI-EO is to allow interrogation of the robustness of inferences made about the drivers of global fire regimes. For example, if trends are identified in WI-JULES but not in WI-EO, then they may be attributable to underlying model error in JULES' representation of ecosystem dynamics. Similarly, assessing the difference in performance (as measured against GFED5) allows exploration of how far underlying error in the hydrological and vegetation outputs of DGVMs may constrain the capacity of their fire modules to reproduce remotely sensed observations (Hantson et al., 2020).

Code to run and analyse WHAM-INFERNO is written in R version 4.2.2 (R Core Team 2022), using the 'raster' library version 3.6-20 (Hijmans et al., 2023). Code and data to run and analyse outputs of both versions of WHAM-INFERNO are made available on Zenodo (Perkins et al., 2023b).

2.1 Inputs to the coupled model

WHAM-INFERNO takes inputs from WHAM!, JULES-INFERNO and from secondary data sources. Each of these inputs are described in turn below (Sections 2.1.1-2.1.3), and an overview is given in Table 1. WHAM! outputs are annual, whilst as per results in the sixth coupled model intercomparison project (CMIP6), JULES-INFERNO outputs are aggregated monthly means. Therefore, WHAM-INFERNO runs at a monthly timestep, with WHAM! outputs for a given year assumed to be uniformly distributed across calendar months.

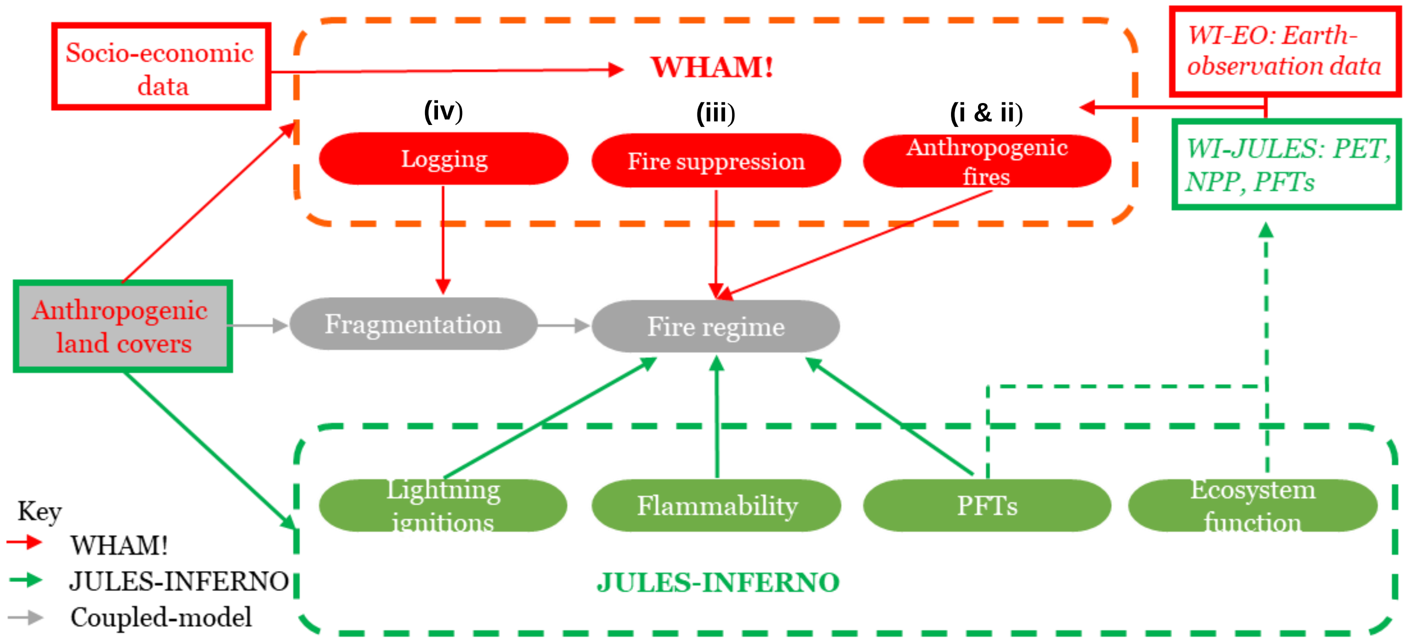

Figure 1: Processes represented in the WHAM-INFERNO combined model. Solid arrows denote dynamic model calculations, whilst dashed lines denote static exchange of information. Socio-economic data and biophysical inputs to WHAM! (Potential Evapotranspiration (PET), Net Primary Production (NPP) and Plant Functional Types (PFTs)) are passed offline. In WHAM-INFERNO-JULES (WI-JULES) these data are taken from JULES outputs, whilst in WHAM-INFERNO-Earth Observation (WI-EO) PET and NPP inputs are taken from remote sensing. Roman numerals (i-iv) correspond to numbers given in section 2.1.1 of the text.

2.1.1 WHAM! inputs to the coupled model

WHAM! inputs to the coupled model comprise i) managed burned area as a fraction of each cell, ii) numbers of unmanaged fires (count km^{-2} yr^{-1}), iii) fire suppression intensity (0-1), and iv) the presence of selective logging as a fraction of the tree cover in each cell (see corresponding numerals in Figure 1). WHAM! inputs used were those presented in Perkins et al., (2023).

2.1.2 JULES-INFERNO inputs to the coupled model

INFERNO (Mangeon et al., 2016) is the fire module of the JULES dynamic global vegetation model. INFERNO calculates burned area from fires with two key components. The first is mean global burned area per fire per Plant Functional Type (PFT), a set of PFT-specific model free parameters. Model parameters for burned area per PFT were as in Burton et al. (2019). The second component of INFERNO burned area calculations is fuel flammability, which INFERNO calculates as a function of leaf carbon and soil carbon pools, temperature, relative humidity, precipitation, and soil moisture (Mangeon et al., 2016). Flammability is therefore important in capturing the impact of both climate and spatial heterogeneity in vegetation on fire regimes. Flammability is calculated per PFT in each model pixel at each timestep. JULES outputs are from the model set-up used in CMIP6 (Wiltshire et al., 2020).

2.1.3 Ancillary inputs to the coupled model from secondary data

In addition to the calculations from the two models, three sets of secondary data were used as inputs: lightning ground strikes, anthropogenic land covers – cropland, pasture, rangeland and urban – and road density. Firstly, as in JULES-INFERNO standalone (Mathison et al., 2023), counts of lightning strikes were sourced from the Lightning Imaging Sensor—Optical Transient Detector (LIS/OTD, Christian et al., 2003). Secondly, as in CMIP6, anthropogenic land cover was taken from the LUH2 dataset (Hurtt et al., 2020). Finally, Haas et al. (2022) demonstrated that road density was effective in capturing vegetation fragmentation effects on fire regimes at global scale; road density data were therefore taken from the GRIP global road database (Meijer et al., 2018).

Table 1: Overview of inputs to the WHAM!-INFERNO combined model. PFT is plant functional type. Data inputs for lightning strikes, road density and anthropogenic land covers were rescaled to the resolution of WHAM!-INFERNO (1.875º x 1.25º). Differing temporal resolutions of inputs were reconciled as noted in Section 2.1.

Coupled model input	**Source**	**Units**	**Temporal resolution**
Managed burned area	WHAM!	Cell fraction (0-1)	Annual
Unmanaged anthropogenic fires	WHAM!	Fires km^{-2}	Annual
Fire suppression	WHAM!	Cell fraction (0-1)	Annual
Selective logging	WHAM!	Cell fraction (0-1)	Annual
Distribution of PFTs	JULES-INFERNO	Cell fraction (0-1)	Monthly
Flammability per PFT	JULES-INFERNO	Dimensionless (0-1)	Monthly
Burned area per fire per PFT	JULES-INFERNO	km^2	Fixed (n/a)
Lightning – ground strikes	Christian et al., (2003)	strikes km^{-2}	Fixed (single daily mean)
Road density	Meijer et al., (2018)	m^2 km^{-2}	Annual
Anthropogenic land cover	Hurtt et al., (2020)	Cell fraction (0-1)	Annual

2.2 WHAM-INFERNO Structure

The coupled WHAM-INFERNO model is a 'prescribed' model coupling (sensu Robinson et al., 2018) such that whilst simulations of global burned area depend on calculations involving outputs of both models, dynamic information transfer is only one way - from WHAM! to INFERNO (see Section 2.2.1). Specifically, for each simulated year, annual burned area from managed fire is taken directly from WHAM!, with $\frac{1}{12}$ assigned to each calendar month. But to calculate unmanaged fire burned area, the original JULES-INFERNO calculations are modified by the number of anthropogenic fires (km^{-2} yr^{-1}) provided by WHAM!. Therefore, description of model coupling here first describes calculation of burned area from unmanaged fires (Section 2.2.1). Then, as burned area from unmanaged fires is also impacted by anthropogenic landscape fragmentation, the representation of such processes is then described in Section 2.2.2. Finally, the calculation of overall burned area combining both managed and unmanaged fire is described in Section 2.2.3.

2.2.1 Unmanaged fire

The calculation of burned area from unmanaged fires is presented in two parts: firstly the calculation of numbers of unmanaged fires, and secondly the calculation of their respective burned area. An overview of this process is given in Figure 2.

2.2.1.1 Number of fires

In the original Mangeon et al. (2016) conception of INFERNO, the numbers of ignitions from lightning strikes are calculated as follows:

$$I_L = 7.7 \times Lightning \times (1 - Suppression) \quad (1)$$

where I_L is the number of ignitions from lightning strikes in a given model timestep, $Lightning$ is the number of lightning strikes and $Suppression$ is a population density-dependent suppression function. The structure of this calculation is retained with two changes: firstly, the suppression function is replaced with an empirically-defined representation of suppression intensity (Section 2.2.2); and secondly the empirically-defined linear scaling parameter (=7.7) from Mangeon et al. (2016) is replaced with a free parameter (λ) to allow re-calibration. A complete set of model free parameters is given in Supplementary Information Table S1.

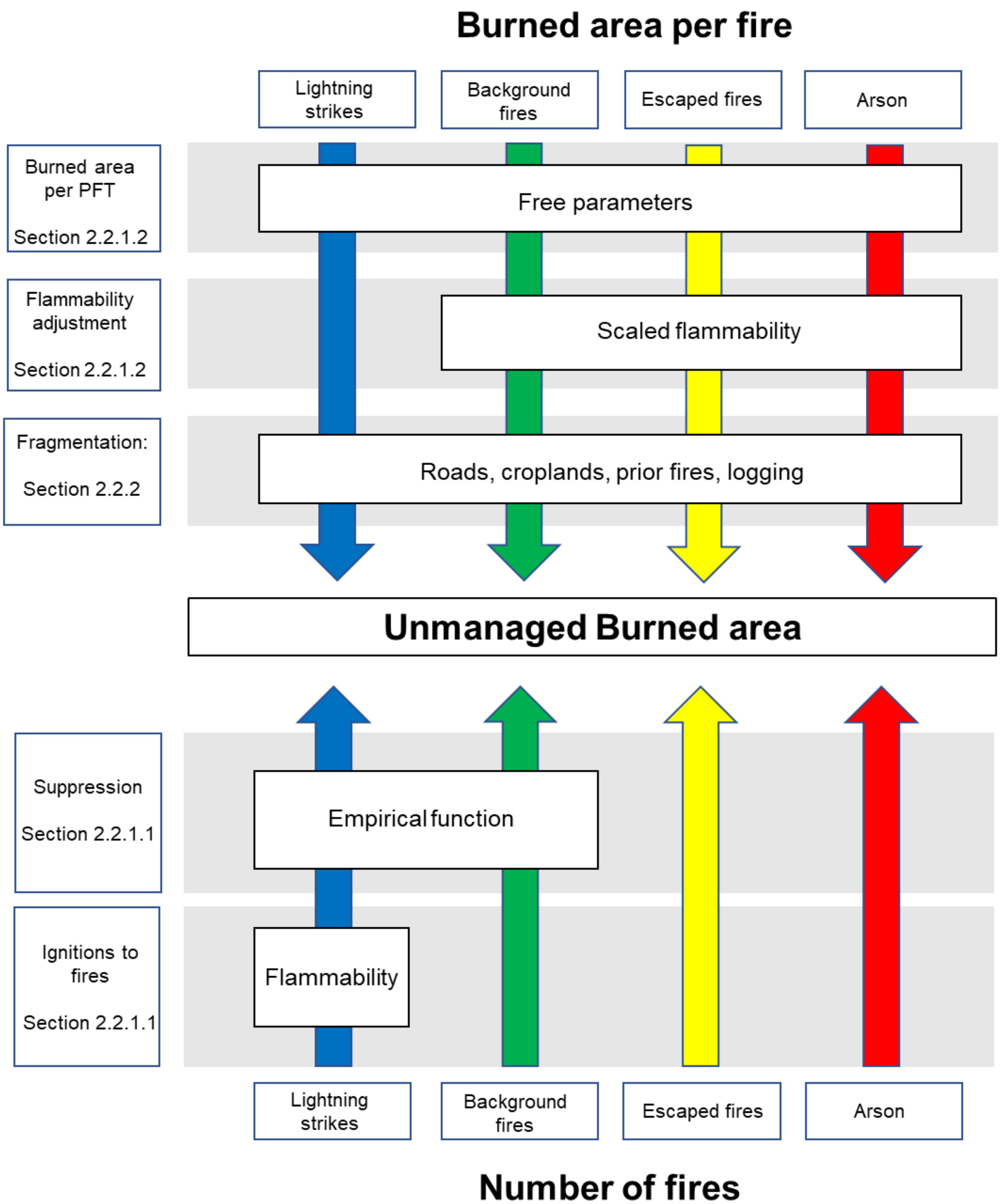

Figure 2: Calculation of burned area from unmanaged fires in the WHAM-INFERNO combined model.

In the WHAM-INFERNO combined model, calculation of lightning fires is integrated with unmanaged anthropogenic fire numbers from WHAM! as follows:

$$Fires_{UM} = Arson + Escaped + (1 - Suppression) * \ (Background + \ Lightning) \ (2)$$

where $Fires_{UM}$ is the annual number of unmanaged fires per grid box per year, $Arson$ and $Escaped$ fire numbers are the number of fires km^{-2} yr^{-1} taken from WHAM! outputs, and $Lightning$ is the number of lightning fires calculated from mean daily ground strikes as in equation (1). Finally, $Background$, is a small globally constant rate used to capture fires that are not arson, lightning or escaped managed fires. The constant rate maintains an aspect of INFERNO, in which a uniform 'ignition' rate is an option.

Fire suppression in the coupled model (Section 2.2.2) is applied to background and lightning fires, but not to arson and escaped fires. This is for ontological reasons, as follows. INFERNO assumes that suppressed *ignitions* have no burned area. However, in DAFI, the database used to develop WHAM!'s calculation of arson and escaped *fires*, numbers of *fires* are recorded, therefore by definition these have burned area > 0. As such, it is illogical to apply modelled suppression to them. By contrast, as the background rate was calculated using a constant, clearly this did not account for the impact of suppression. Similarly, lightning remains calculated based on *ignitions* rather than *fires* and hence could be suppressed before beginning to burn.

2.2.1.2 Burned area per unmanaged fire

After calculation of the numbers of unmanaged fires per pixel ($Fires_{UM}$), these are then converted to burned area. In its original conception, INFERNO calculates the number of fires as:

$$Fires = Ignitions * Flammability \ (3)$$

In other words, both humans and lightning are conceptualised as producing ignitions, which may or may not become fires based on the flammability of the surrounding vegetation. By contrast, because most human fires are started deliberately, WHAM! does not output numbers of *ignitions*, but numbers of *fires* directly (Figure 2). However, whilst vegetation flammability plays the ontological role of translating ignitions to fires in INFERNO, it also plays an important functional role: capturing geographic variation in the capacity and tendency of the vegetation to sustain unmanaged fire. This is because INFERNO calculates burned area per fire with a simple global mean value per Plant Functional Type. Therefore, simply removing flammability from the calculation and taking numbers of unmanaged fires from WHAM! was not possible.

The solution adopted is to multiply WHAM! unmanaged fires by INFERNO flammability, but to rescale with a free parameter. This leaves a burned area calculation from unmanaged fires of:

$$BA_{UM} = Fires_{UM} * \Phi * \sum_{PFT=1}^{PFT=n} PFT * \ Flammability_{PFT} * BA_{PFT} \ (4)$$

where $BA_{UM}$is the annual burned area from unmanaged fires as a fraction of each model pixel; PFT is the fraction of each model pixel (0-1) occupied by a given PFT; $Flammability_{PFT}$is a PFT-specific dimensionless adjustment (0-1) reflecting spatiotemporal differences in the combustibility of vegetation; BA_{PFT} is the PFT-specific mean burned area per fire from JULES-INFERNO; and Φ is a scaling factor reflecting the differing model ontologies of WHAM! and JULES-INFERNO.

2.2.2 Fragmentation

The impact of landscape fragmentation effects was restricted to unmanaged fires; managed burned area was not altered for fragmentation effects, as these would already be implicitly accounted for in the observations captured in DAFI. Representation of fragmentation is done in three ways. Firstly, as WHAM! accounts for anthropogenic cropland fires, to account for the role of cropland conversion in fragmenting more flammable fuels, burned area per unmanaged fire was set to 0 for cropland PFTs.

Secondly, Haas et al., (2022) demonstrate the importance of road density in reducing both fire sizes and burned area. This finding was implemented in the coupled model by adjusting burned area per fire with a simple negative exponential function:

$$BA_{UM\_frag} = \ BA_{UM} * \left(1 - \frac{\ln(RD)}{\rho}\right) \ (5)$$

where BA_{UM} and BA_{UM_frag} are annual burned area per pixel (0-1) from unmanaged fire before and after adjustment for fragmentation effects, RD is road density and ρ a free parameter.

By contrast, logging of wet, fire-prone forests can lead to increased fire (both numbers of fires and fire size), as gaps in the canopy lead to drying on the forest floor (Cochrane & Barber, 2009; Lapola et al., 2023). A simple representation of this was implemented by increasing the mean burned area per fire for broadleaf tree PFTs given the presence of the Logging AFT in WHAM! outputs. The values of mean burned area for broadleaf tree PFTs therefore become:

$$BA_{broadleaf} | \ logging = \ BA_{broadleaf} * \ \Lambda(Logging) \ (6)$$

where $BA_{broadleaf}$ is the burned area per fire for broadleaf tree PFTs; $BA_{broadleaf} | \ logging$ is this parameter value when adjusted for logging, $Logging$ is the fraction of tree cover in a cell occupied by WHAM's logging AFT, and Λ a free parameter.

2.2.3 Combining managed and unmanaged fire

JULES-INFERNO typically runs at a timestep of between 30-60 minutes (Clark et al., 2011). This is required for the stability of model equations and has the advantage of capturing temporal fluctuations in vegetation flammability. As such, INFERNO increases the amount of bare soil in a given model pixel when a fire burns, which reduces fuel availability and the amount of area burned from subsequent fires until vegetation resprouts (Burton et al., 2019). However, as it is not meaningful to model human land use decision-making at such short durations (Arneth et al., 2014), managed fire is output at an annual timestep by WHAM!. For these reasons, calculating the combined burned area of managed and unmanaged fires requires an adjustment to account for the effect of preceding fires:

$$BA_{tot} = BA_{Managed} + BA_{UM} * \gamma \quad (7)$$

where $BA_{Managed}$ is burned area from managed fire, BA_{tot} is total burned area and γ a function representing the impact of preceding fires on unmanaged burned area. Managed fire was not adjusted for effects of antecedent fire for several reasons: firstly, because WHAM! has its own internal calculation for including fuel limitations in agent calculations; secondly, because WHAM! outputs are empirically grounded, derived from data that would capture such limitations to a degree. Thirdly, many managed anthropogenic fires are lit to reduce the intensity and spread of unmanaged fire (e.g. prescribed fire or indigenous patch burning mosaics). The γ function was calculated using a linear function after a threshold:

$$\gamma = \begin{Bmatrix} 1 \;\; if \; BA_{UM} \leq \alpha \\ \beta \quad otherwise \end{Bmatrix} \quad (8)$$

where α is a free parameter representing a threshold burned fraction of a cell below which fuel availability is not limiting, whilst β is a further free parameter capturing the rate of decay in burned area once this threshold is reached. This functional form was chosen as it approximates the behaviour observed by Archibald et al. (2012), who explored the impact of fragmentation on burned area in flammable ecosystems.

2.3 WHAM-INFERNO Calibration

The model structure set out in Section 2.2 resulted in 20 free parameters (Supplementary Table S1), which formed the basis of a perturbed parameter ensemble for model calibration. A total of 10,000 perturbed parameter sets were created with a maximin latin hypercube sampling design (Carnell 2022). Using the resulting parameter sets, 10,000 model runs were conducted (i.e. one for each perturbed parameter combination) for both versions of the WHAM-INFERNO ensemble.

The outputs of each run were compared with the recent GFED5 global burned area product (Chen et al., 2023). Firstly, 'implausible' parameter sets were ruled using history matching with the overall magnitude of global burned area in GFED5. Remaining parameter sets were then treated as 'not ruled out yet' (NROY; Rougier & Beven, 2013). Secondly, as well as global burned area, Pearson's correlation (r) was calculated with a square root transformation applied. These two metrics were those used in the FireMIP (Teckentrup et al., 2019), and hence were adopted here to define a pareto-optimal parameter space capturing the trade-offs in maximising performance against each metric. This approach allows, firstly, the evaluation of different model processes in capturing observed fire regimes of the recent past, and secondly overall evaluation of the performance of the WHAM-INFERNO ensemble. The mean outputs of WI-JULES and WI-EO in the pareto parameter space then formed the basis of further analysis. Fuller detail of model calibration is given in Supplementary Information A.

2.4 WHAM-INFERNO Evaluation

WHAM-INFERNO is evaluated in two broad ways, firstly by output corroboration through comparison of model outputs with remotely sensed burned area from GFED5 (as described above) and secondly by model benchmarking against a null or baseline model. The baseline model was an offline version of INFERNO (as presented in Mangeon et al., 2016). As INFERNO was originally calibrated using GFED4 data, in which burned area was 49% lower than the more recent GFED5 burned area product, a process of recalibration required. The re-calibration of this INFERNO offline model (hereafter, 'baseline model') followed broadly the same steps as WHAM-INFERNO combined model: 10,000 parameter sets were used to define a perturbed parameter ensemble, from which both NROY and pareto-optimal parameter spaces were defined using GFED5 burned area. Detailed description of the setup of the baseline model, including how its free parameters differ from WHAM-INFERNO, is described in Supplementary Information A.

2.5 Historical run setup and analysis

As with the WHAM! standalone historical simulations presented in Perkins et al. (2023), WHAM-INFERNO runs span 1990-2014. These two years mark the beginning of the data recorded in the DAFI database of global anthropogenic fire impacts (i.e. 1990; Millington et al., 2022) that was used to parameterise WHAM!, and the end of the CMIP6 historical period (i.e. 2014), respectively. Both models were run at the spatial resolution that JULES-INFERNO adopted in the FireMIP (1.875° x 1.25°). Model outputs are evaluated during the overlapping period in WHAM-INFERNO historical runs and the GFED5 record (2001-2014); GFED5 data were aggregated to the spatial resolution of WHAM-INFERNO.

Analysis of outputs focuses on understanding spatial and temporal variation in the drivers of global fire regimes. Spatial analysis focuses on understanding how managed anthropogenic fire and unmanaged fire combine to produce observed fire regimes across global regions. Similarly, temporal analysis first assessed how far managed fire and unmanaged fire contribute to interannual variability in fire regimes. This was calculated by detrending the global total burned area from GFED5 and WHAM-INFERNO model outputs before calculating the correlation and standard deviation of the residual variabilities.

Then, drivers of longer-term (decadal) change were assessed. Perkins et al. (2023) present analysis of the drivers of change in WHAM! managed fire outputs. Results pointed to land use intensification as a global dampening effect on fire use, whilst conversely land use extensification - particularly for livestock farming - led to increased fire use. Therefore, analysis of temporal trends here focuses on change in unmanaged fire in relation to the human and physical drivers represented in the coupled models. These are annual changes in numbers of unmanaged fires, road density (fragmentation; Haas et al., 2022), vegetation flammability, fire suppression and cropland conversion. The relative influence of these drivers was assessed at a pixel-level firstly by comparing the Kendall's Tau correlations of their interannual changes with interannual change in unmanaged burned area (for each of WI-JULES and WI-EO). Secondly, using these same independent variables, linear models of pixel-level change in unmanaged burned area were fit for both interannual and overall change between 2001-2014. T-values of the independent variables were used to assess the relative strength of their relationships to changes in unmanaged burned area.

3 Results

3.1 Model evaluation

Measured by correlation with the GFED5 record during 2001-2014, both WI-JULES and WI-EO perform significantly better than the baseline model (Z Tests; both $p < 0.001$, $n = 10, 14$). Specifically, the mean correlation of the pareto-optimal parameter space is 0.81 for WI-EO and 0.76 for WI-JULES, compared with 0.58 for the baseline model (Figure 3). This result also compares favourably with INFERNO v1.0 presented in the FireMIP, in which INFERNO had a correlation of 0.70 against GFEDv4 and 0.64 against GFEDv4s (Teckentrup et al., 2019). As such, inclusion of WHAM! seemingly improves INFERNO both in an absolute sense, when compared to GFED5, but also relatively against INFERNO's performance based on the observational data available at the time of its original development.

Furthermore, almost 70% of the baseline model ensemble's runs are ruled out, primarily due to simulating burned area too low to achieve acceptable coherence with the GFED5 record (mean of ruled out runs was 276 Mha vs 802 Mha in GFED5). By contrast, only 182 of WI-EO and 124 of WI-JULES runs are ruled out. In the pareto parameter space, WI-EO has a slight overprediction bias (+11 Mha) and WI-JULES has a slight underprediction bias (-10 Mha), compared to a bias of -52 Mha in the baseline model. Overall, we conclude that the WHAM integration improves the structural capacity of INFERNO to capture the magnitude and distribution of global fire regimes.

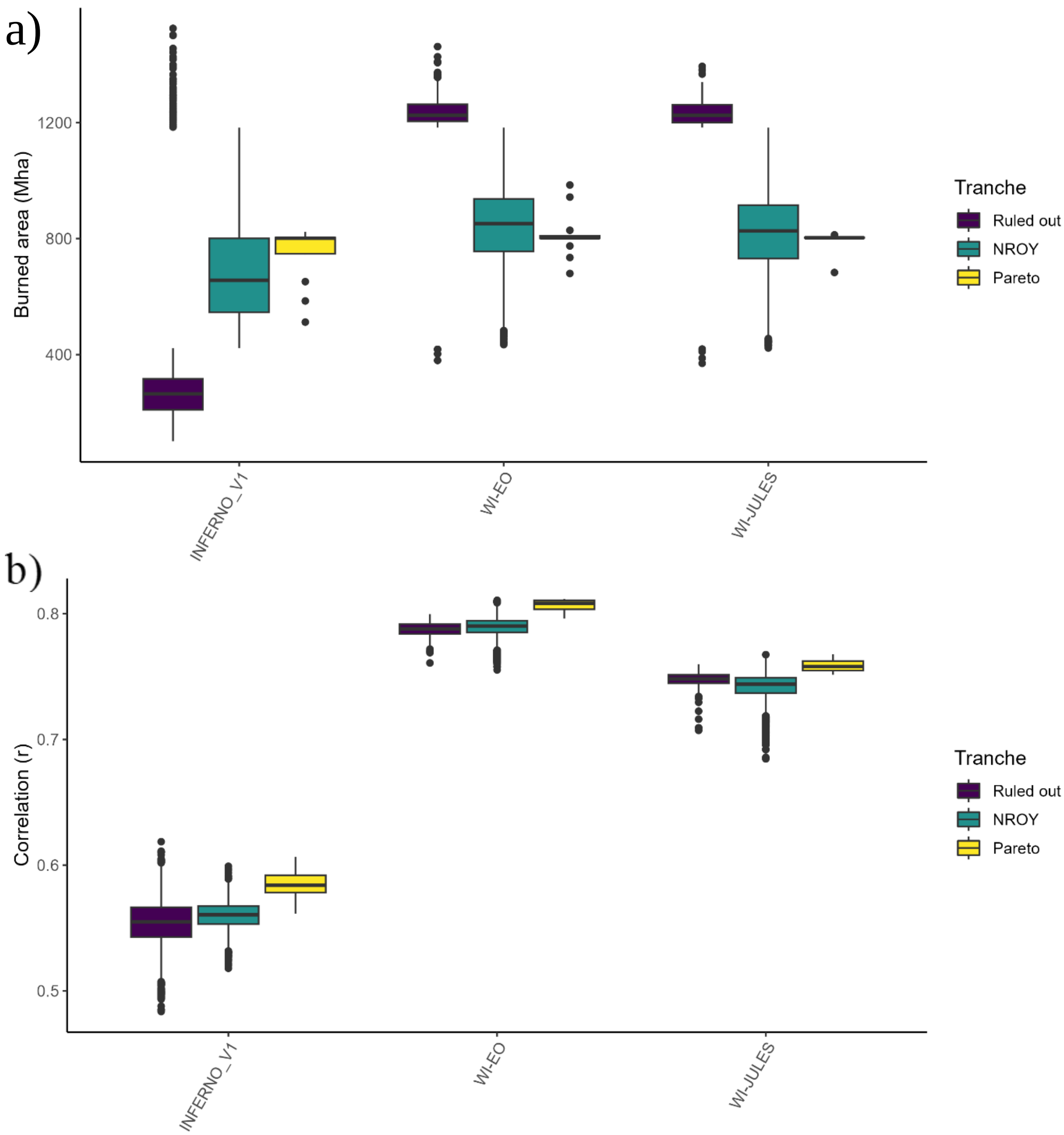

Figure 3: Outputs of WHAM-INFERNO in comparison with a baseline model (INFERNO_V1): a) simulated global burned area and b) Pearson correlation with GFED5. For burned area, the baseline model has many runs ruled out for burned area being too low in comparison with GFED5, whilst in both versions of WHAM-INFERNO a smaller number of runs are ruled out. The two versions of WHAM-INFERNO both produce higher correlations than the baseline model across all three tranches of parameter sets (ruled out, NROY and pareto-optimal). NROY refers to "not ruled out yet".

3.2 Analysis of WHAM-INFERNO outputs

3.2.1 Spatial Analysis

Across the pareto parameter runs, simulated burned area in both coupled models is split approximately evenly between managed and unmanaged fires. Over the historical period (1990-2014) in WI-JULES a mean of 442 Mha (54%) comes from unmanaged fires and 379 Mha (46%) from managed fires. Similarly, in WI-EO, 405 Mha (47%) comes from unmanaged fires, and 453 Mha (53%) comes from managed fires.

Furthermore, there is substantial heterogeneity in the spatial location of burned area due to managed *versus* unmanaged fires (Figure 4). For example, across 1990-2014 at the level of World Bank regions, in sub-Saharan Africa WI-JULES suggests 65% of mean annual burned area is from unmanaged fires (56% in WHAM-EO; Figure 5). Conversely, in South Asia (which includes India), WI-JULES suggests just 28% of burned area is from unmanaged fires (19% in WI-EO; Figure 5). The predominance of managed fire is driven by large-scale crop-residue burning in the region (Hall et al., 2023; Perkins et al., 2023). Furthermore, there is also regional heterogeneity in the trends in managed and unmanaged fire. For example, in both WI-JULES and WI-EO, managed fire is increasing in South Asia, whilst decreasing in Latin America and the Caribbean (Figure 5).

Perhaps the two most notable differences in sources of burned area between the two models' (WI-JULES and WI-EO) simulations come in Latin America & the Caribbean and sub-Saharan Africa. The difference in Latin America is that WI-JULES simulates higher unmanaged burned area than WI-EO (81 Mha vs 56 Mha) particularly in the Caatinga region of Brazil (Figure 6), which is due to a known anomaly in JULES' hydrological cycle in the region (Perkins et al., 2023). By contrast, in sub-Saharan Africa WI-EO simulates higher unmanaged burned area than WI-JULES (209 Mha vs 132 Mha), attributable to the more homogeneous spatial distribution in WI-EO outputs – particularly in the Guinean Savanna – compared to the comparatively heterogeneous WI-JULES outputs (Figures 4 & 6).

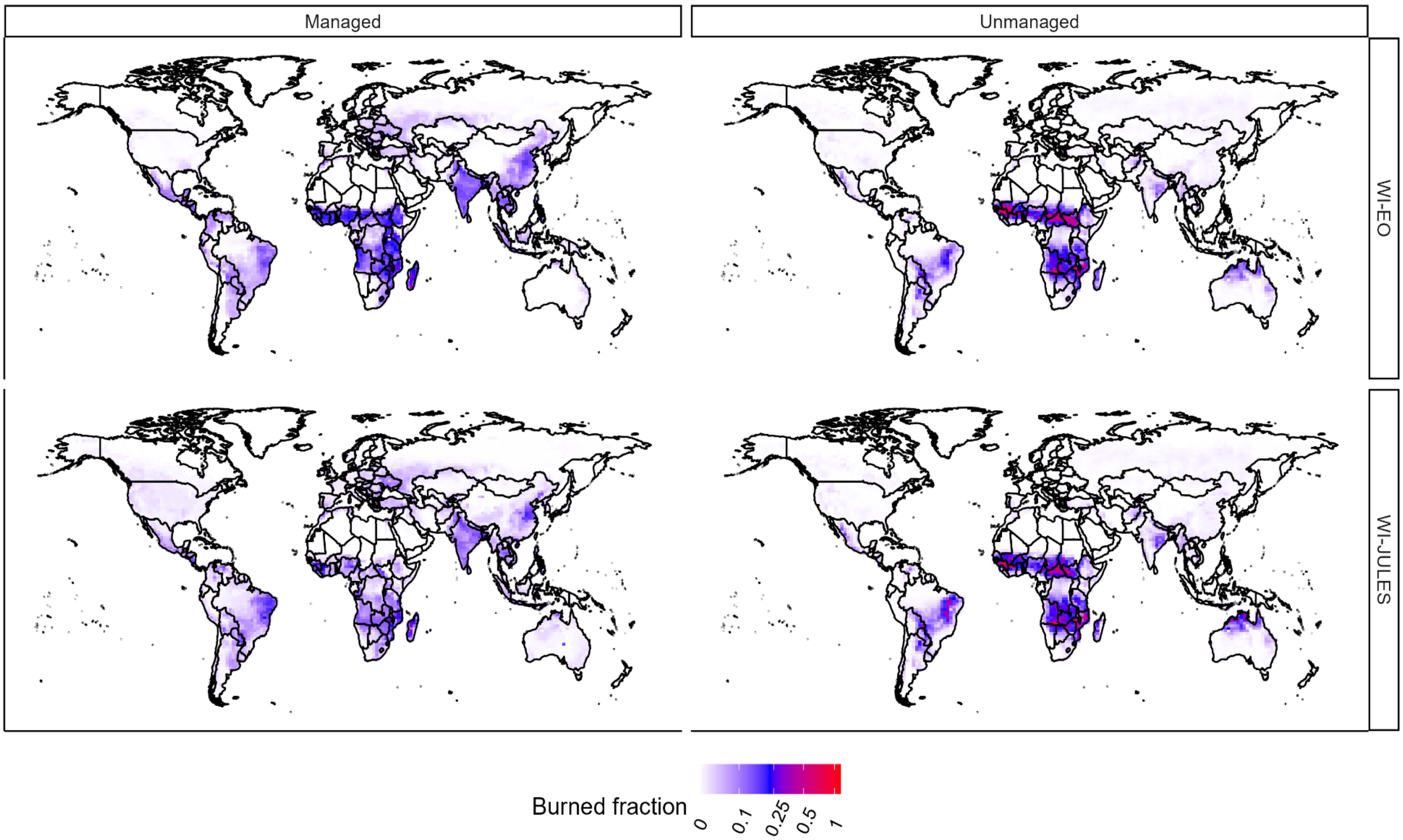

Figure 4: Distribution of managed and unmanaged fire in WHAM-INFERNO-Earth Observation (WI-EO) and WHAM-INFERNO-JULES (WI-JULES) shown as the burned fraction of each pixel. The arithmetic mean of model outputs was taken across the historical model run period (1990-2014). Principle differences between the two versions of WHAM-INFERNO are seen in the managed fire outputs of WI-EO in sub-Saharan Africa, which have a more homogeneous distribution than WI-JULES's more sporadic spatial pattern. Other anomalies between models are seen in the Caatinga region of Brazil and in the Northern Territories of Australia.

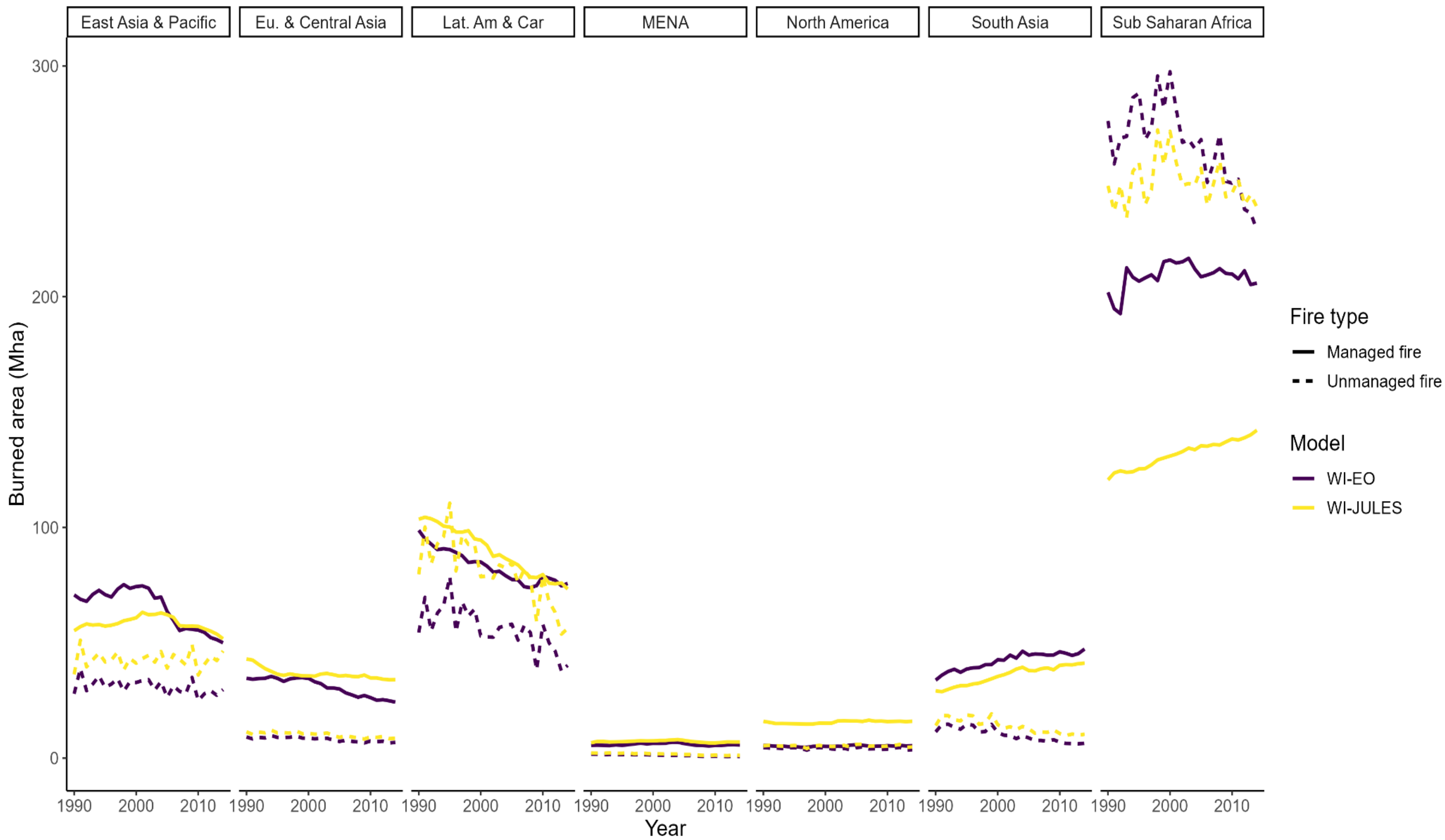

Figure 5: Trends in managed and unmanaged fire across the World Bank global regions. The largest gap between managed and unmanaged fire is seen in sub-Saharan Africa, where unmanaged fire dominates. Conversely, South Asia (including India) is dominated by managed fires, particularly crop residue fires (as shown in Perkins et al., 2023). Key: Eu. & Central Asia = Europe & Central Asia; Lat. Am & Car = Latin America & Caribbean; MENA = Middle East and North Africa.

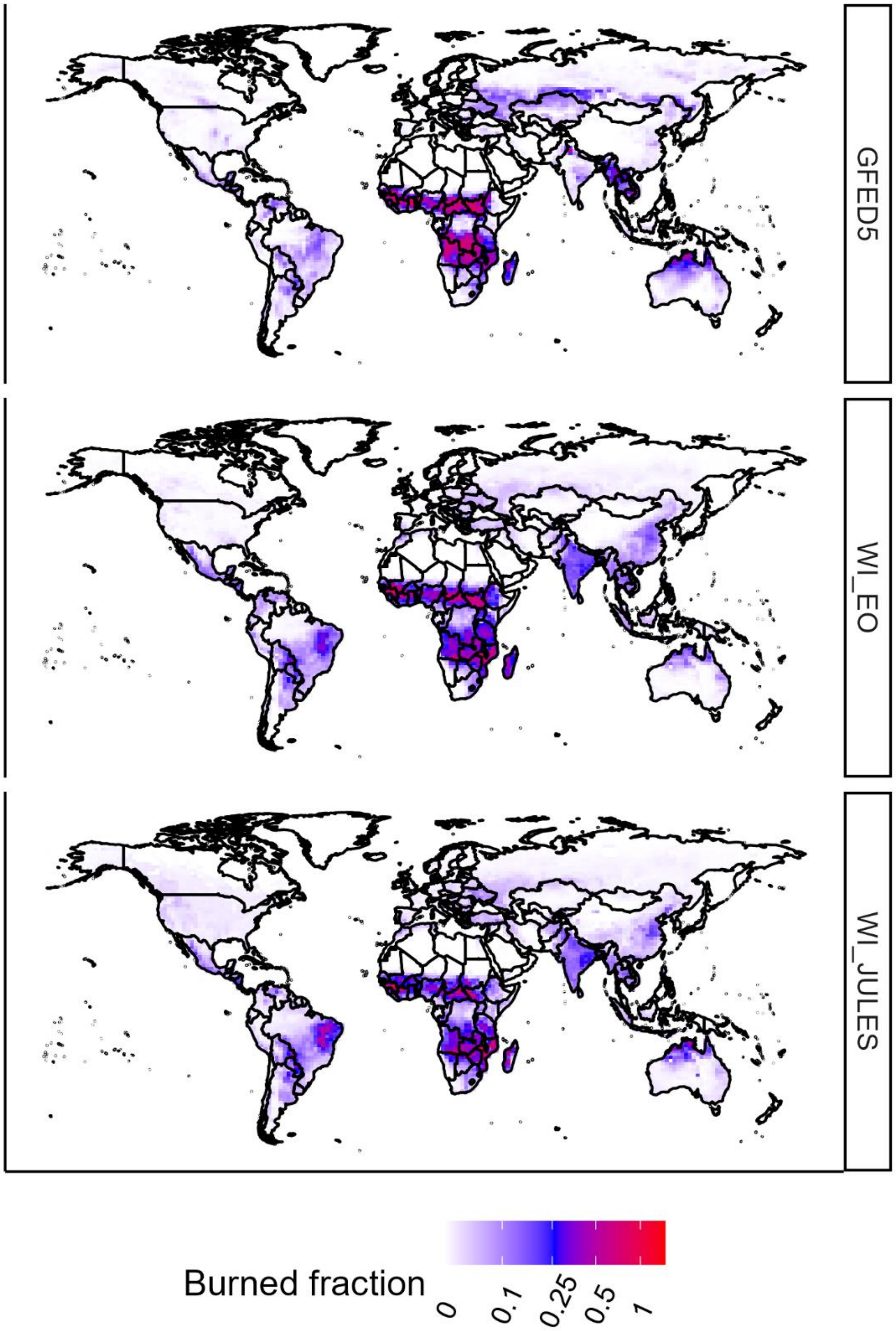

Figure 6: Burned area in GFED5, WI-EO and WI-JULES as a fraction of each pixel. Values shown are the mean of the period (2001-2014). Three clear anomalies between models and GFED5 are present: firstly in the Caatinga region of Brazil, secondly in southern Russia, and thirdly in India. This latter discrepancy is due to differences in burned area from crop residue burning between WHAM! and GFED5 (Perkins et al., 2023).

3.2.2 Temporal analysis

Across the overlapping period with GFED5 (2001-2014), WI-EO global burned area declines by 137 Mha, WI-JULES burned area declines by 52 Mha, and the baseline model declines by 30Mha. This compares with a decline of 193 Mha in GFED5. In WI-EO, this global decline is primarily attributable to the trend in sub-Saharan Africa (Figure 7), where burned area declines by 61 Mha (compared to 112 Mha in GFED5). By contrast, in WI-JULES burned area in sub-Saharan Africa declines by just 9 Mha (Figure 7). This lack of decline in sub-Saharan Africa is in part due to managed fires, which increase by 10 Mha as crop residue burning increases in the region in this model. A similar trend is seen in sub-Saharan African crop-residue burning in WI-EO, but this is offset by a steeper decline in pasture fires (Perkins et al., 2023). Further, WI-JULES seemingly overestimates the rate of declining burned area in Latin America & Caribbean (-42 Mha; GFED5 -18 Mha), whilst WI-EO captures a similar rate of decline to GFED5 (-20 Mha). As such, WI-EO is best able to reproduce the observed decline in burned area, followed by WI-JULES, and then the baseline model. The drivers of this modelled decline are explored in detail below.

Globally, both WI-JULES and WI-EO underestimate the magnitude of interannual variability (IAV) in burned area. The standard deviation of detrended model outputs (i.e. with mean = 0) was 9.5Mha in WI-EO and 9.7Mha in WI-JULES. However, the correlation of the detrended outputs with GFED5 was 0.81 in WI-EO and 0.41 in WI-JULES: indicating that although the magnitude of IAV is underestimated in both models, WI-EO is substantially better at capturing the direction of fluctuations in burned area. IAV in both model is driven by unmanaged fire. Detrended global outputs for unmanaged fire correlate with detrended global burned area in GFED5 (WI-EO: $r = 0.74$, WI-JULES: $r = 0.53$); however there is no meaningful relationship for IAV in GFED5 and detrended outputs for managed fire ($r <= 0.11$).

Based on the variable with the strongest Kendall's Tau correlation in each pixel, inter-annual change in burned area due to unmanaged fire is most strongly associated with flammability (Figure 8). In WI-JULES, flammability has the highest Tau value across 9,644 Mha (~70% of global land area; Table 2), whilst cropland conversion, which has the strongest relationship over the second largest area, has the highest Tau value across 1,037 Mha (~8% of global land area). A similar trend is seen in WI-EO, where flammability has the highest Tau value across 9,414 Mha and cropland conversion has the highest Tau value across 1,052 Mha.

However, whilst change in burned area is most closely correlated with flammability over the largest area, these areas are seemingly weighted towards model pixels with less overall change in burned area. For both WI-EO and WI-JULES, in linear regression models of interannual variability absolute t-values for flammability are more than twice as large as any other variable (Table 2). By contrast, for the overall change over 2001-2014, t-values are closer between variables, with ignitions having the largest absolute t-values for both models. Similarly, variables with a negative impact on burned area have a larger impact on the overall 2001-2014 change than interannual variation (Table 2). Road density seemingly has the largest impact on declining burned area (t-values: -21.7 & -19.3), followed by cropland conversion (t-values: -16.1 & -19.1) respectively. Fire suppression has only a marginal influence and indeed shows little relationship with the long-term trend in WI-JULES ($t = 0.433$).

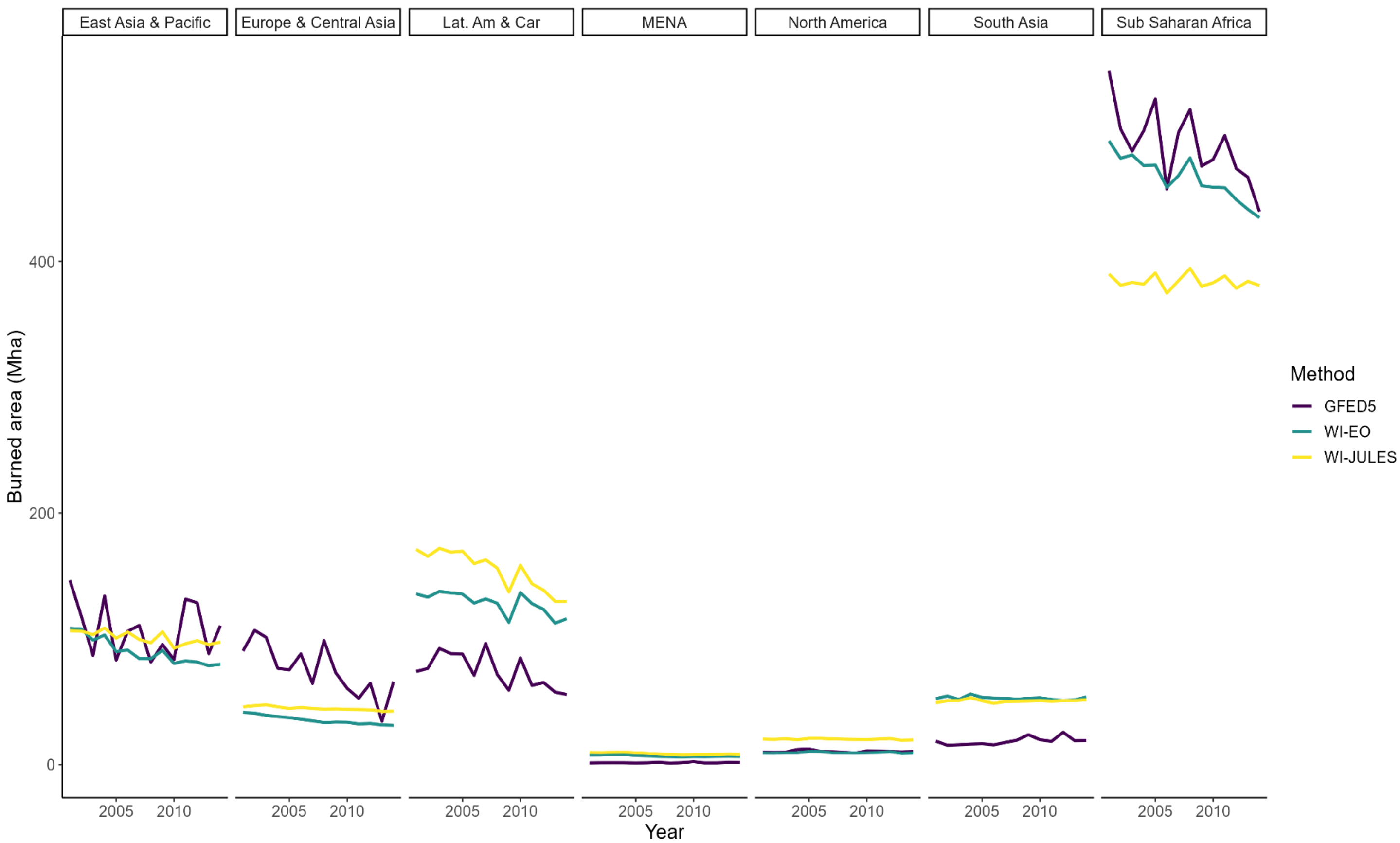

Figure 7: Burned area by World Bank region in GFED5 and the two versions of the WHAM-INFERNO model ensemble (WHAM-EO, WI-JULES). WI-EO is best able to reproduce the observed decline in burned area in sub-Saharan Africa, with WI-JULES showing an essentially static burned area. Conversely, both WI-EO and WI-JULES overestimate burned area in Latin America, though the trend of declining burned area is captured strongly. Both models show generally poor performance in Europe & Central Asia, showing limited discernible trend. Model outputs for WI-EO and WI-JULES are the sum of the managed and unmanaged burned area presented in Figure 5. Key: Lat. Am & Car = Latin America & Caribbean; MENA = Middle East and North Africa.

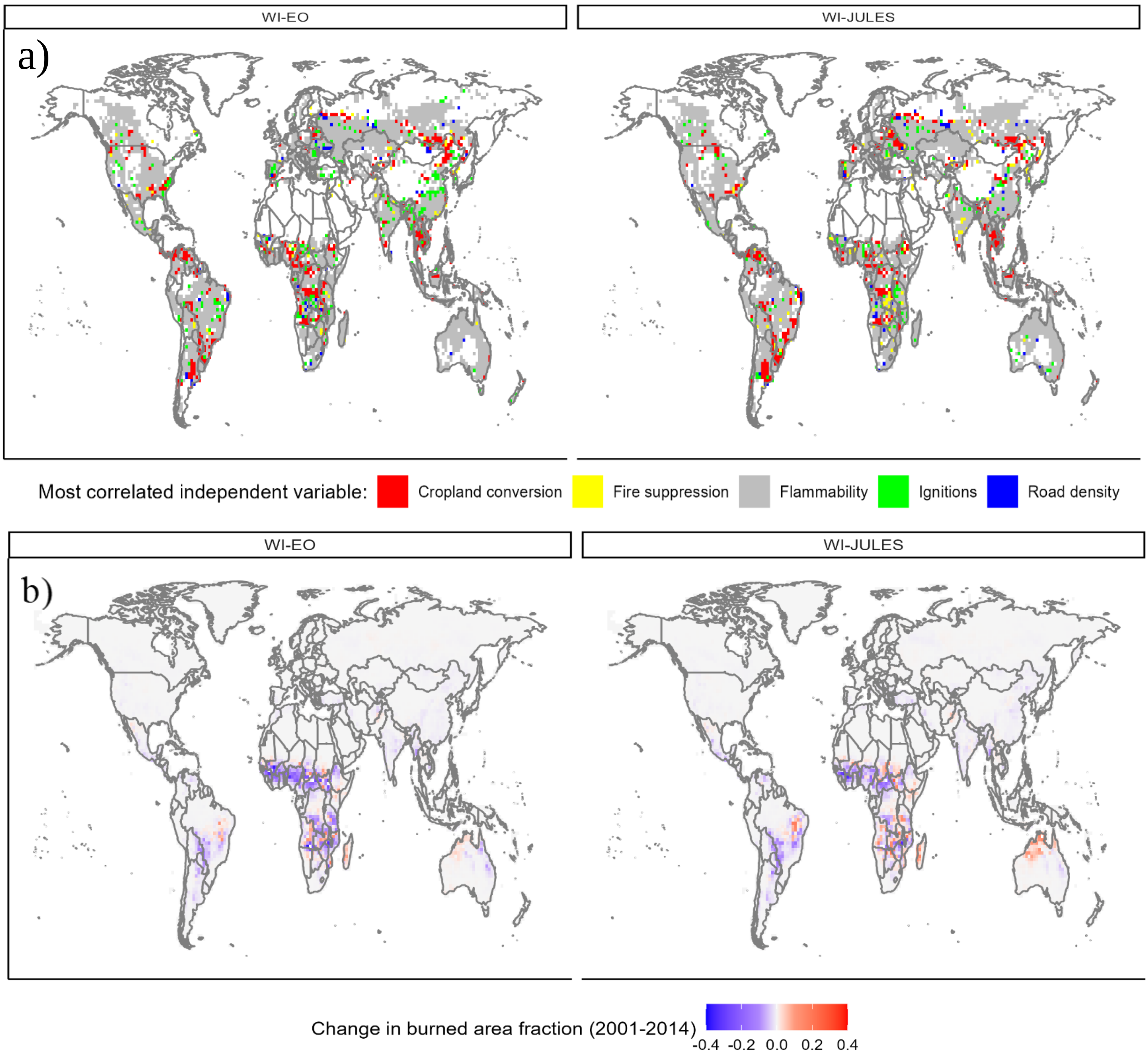

538 **Figure 8**: Relationship of changes in unmanaged burned area to independent variables. a)
539 Variable with highest absolute correlation (τ) with change in burned area from unmanaged fire;
540 values were filtered for pixels with at least 0.1% of the land area burned. b) Change in burned
541 area between 2001-2014. Although flammability is most closely correlated with changes in
542 burned area across the largest geographic space, the influence of other factors – particularly
543 cropland conversion – is clustered towards pixels with the largest changes in burned area. A non-
544 linear stretch was applied to the colour scale in b) to show differences between smaller absolute
545 values.

Table 2: Relationship of changes in burned area from unmanaged fires to explanatory variables. Area gives the total land surface over which each variable was most strongly correlated with changing burned area. T-values are from linear models of change in burned area to change in the independent variable; IAV (interannual variation) is for linear models of year-on-year change between 2001-2014, whilst trend denotes overall change during the same period.

	WI-EO (area; Mha)	**WI-EO (t-value; IAV)**	**WI-EO (t-value; trend)**	**WI-JULES (area; Mha)**	**WI-JULES (t-value; IAV)**	**WI-JULES (t-value; trend)**
Cropland conversion	1052	-10.4	-16.1	1037	-13.8	-19.1
Fire suppression	244	-2.78	3.26	377	-1.9	0.43
Flammability	9414	162.3	24.4	9644	267.2	46.0
Ignitions	736	70.61	25.7	522	87.5	46.6
Road density	206	-5.1	-21.7	209	-8.0	-19.3

4 Discussion

This paper has presented the first integration of a global-scale behavioural model of human fire use and management coupled with a dynamic global vegetation model. Discussion focuses on advances made for global understanding of human drivers of vegetation fire regimes through this technical advance, before addressing its limitations and possible future directions for development of WHAM-INFERNO.

4.1 WHAM-INFERNO: Insights for global-human fire interactions

The WHAM-INFERNO model integration reveals both the extent and the diversity of the socio-ecological dynamics of global fire regimes. In pareto model runs of WHAM-INFERNO, managed and unmanaged fire contribute approximately equal amounts of global burned area. Furthermore, the spatiotemporal distribution of anthropogenic managed fire, and its relationship with unmanaged ('wild') fires differs substantially across space. Whilst anthropogenic fire use, primarily for crop residue burning, dominates the South Asian World Bank Region, in sub-Saharan Africa more than half of burned area is from unmanaged fires (Figure 5). Such differences have profound implications for understanding of global fire regimes and illustrates that effective fire management policies and climate adaptation strategies must be based on detailed understanding of how human livelihoods and associated fire use systems contribute to existing fire regimes. At the very least, the large extent of managed anthropogenic fire around the world implied by these results is demonstration of the inadequacy of model approaches seeking to represent direct anthropogenic influence on fire regimes as simple functions of population density (Rabin et al., 2017).

Furthermore, combined global-scale simulations of both managed and unmanaged fire presented here add weight to the finding from Earth observation that small fires have declined less than larger ones (Chen et al., 2023). Managed fire declines by just 35% and 52% of the rate of unmanaged fire in WI-JULES and WI-EO respectively. Data from empirical studies indicates that the two largest sources of burned area from managed human fires – crop residue burning and pasture management – have mean sizes of 5 ha and 34 ha respectively (Millington et al., 2022), whilst in JULES-INFERNO mean burned area per fire for unmanaged fires varies from 170 ha to 320 ha. This result seems to give weight to findings of Smith et al., (2022) and Perkins et al., (2023), that managed fire is changing in line with socio-ecological forces that are distinct from those driving change in unmanaged fire.

In addition, the finding that unmanaged fire is primarily responsible for interannual variability in burned area (Section 3.2.2) is consistent with the findings of Randerson et al., (2012), who find less fluctuation in small fires than those detectable by MODIS (i.e. <21 ha). This is intuitive, as crop residue fires, for example, occur annually according to the logic of cropping systems rather than fluctuations in climate (Millington et al., 2022). However, this opens an intriguing possibility for fire-enabled DGVMs, which have typically struggled with interannual variability whilst also not including representation of managed human fires – the more static part of the regime (Li et al., 2019). In effect, DGVMs may have been *doubly* underestimating the sensitivity of burned area from unmanaged fires to interannual climate variability. This underrepresentation of the sensitivity of unmanaged fires to climate volatility may contribute to the difficulty of attributing changes in global fire regimes to global warming (Jones et al., 2022), although a lack of representation of peat fires may also be a partial explanation (Blackford et al., 2023; Li et al., 2019).

By accounting for the less temporally variable and more spatially homogeneous signal of burned area due to managed fires (Figures 4 & 5), the WHAM-INFERNO integration advances understanding of the drivers of declining global burned area. Whilst interannual variability is primarily driven by changes in vegetation flammability, longer-term change in burned area highlights the important role played by the fragmentation of natural and semi-natural vegetation through road building and cropland conversion (Figure 8). This result coheres strongly with that of Andela et al., (2017) who find that interannual variability is closely linked to precipitation, whilst cropland fraction is strongly associated with declining burned area. Furthermore, WHAM-INFERNO can identify the processes underlying the finding of Andela that cropland has a spatially heterogeneous impact on burned area. For example, increased burned area in croplands in South Asia and Northeastern China is due to large-scale agricultural residue burning, whilst decreased fire in savanna grasslands is due to landscape fragmentation and the subsequent reduced capacity of savanna grasslands to sustain unmanaged fires.

4.2 Model performance and limitations

Both versions of the WHAM-INFERNO ensemble represent a significant improvement in the capacity of INFERNO to reproduce historical global annual burned area over the baseline model (Figure 3), and indeed over the performance of INFERNO against GFED4 presented in FIREMIP (r= 0.70; Mangeon et al., 2016; Teckentrup et al., 2019). This demonstrates the fundamental importance of a process-based approach to understanding and representing human-fire interactions in global modelling. Furthermore, the improvements made in WHAM-INFERNO over the baseline version allow the impact of landscape fragmentation in global burned area to be incorporated and understood (Figures 2 & 8). Indeed, the WHAM-INFERNO integration, and particular WI-EO seems to advance capacity for DGVMs to reproduce the observed decline in global burned area (Hantson et al., 2020).

However, representation of landscape fragmentation, its interaction with different ecosystem types, and other anthropogenic pressures remains incomplete. One way that WHAM-INFERNO represents fragmentation is through the role of roads in reducing fire size (Haas et al., 2022), by applying a road density correction to fire sizes per PFT. Although useful in constraining the model pareto parameter space through restricting burned area in more densely populated areas (Supplementary Information; Figure S1) this single global function is a somewhat simplistic way of capturing such effects, resulting in a substantially larger impact on WHAM-INFERNO burned area outputs than on correlation with GFED5 (Supplementary Information; Figure S2). Hence, the road density parameterisation in WHAM-INFERNO employed to capture fragmentation effects is analogous to representations of anthropogenic 'ignitions' as a global function of population density in previous fire-enabled DGVMs: they are both a first step with outstanding issues to be addressed. By contrast, the representation of selective logging on the flammability of fire-prone tropical forests in WHAM-INFERNO has been more successful. Although having a small impact on global burned area, including this process leads to an improved global correlation between WHAM-INFERNO outputs and GFED5 (Supplementary Information; Figure S2). Representation of logging was derived from WHAM! outputs, hence illustrating the value of process-based representation of anthropogenic impacts on fire regimes, as opposed to the top-down road density parameterisation.

Finally, it is notable that WI-EO performs more strongly than WI-JULES at reproducing the magnitude, spatial distribution and temporal dynamics of burned area found in GFED5. On one hand, this illustrates the benefits of a well-specified parameterisation of managed human fire: by better accounting for this aspect of the observed burned area signal, WI-EO is better able to reproduce the inter-annual variability of unmanaged fire, and its pronounced global decline. Yet the weaker performance of WI-JULES perhaps also illustrates the potential for underlying error in the representation of ecosystems within DGVMs to lead to misleading conclusions being drawn from their fire modules (Hantson et a., 2020). Continued model intercomparison projects and use of model ensembles are likely to remain the most effective means to apply the fire outputs of DGVMs (e.g. Burton et al., 2023). Overall, the large scale of anthropogenic managed fire entails that careful consideration should be given to how future socioeconomic scenarios, and their limitations, inform our projections of how global fire regimes may evolve under a warming climate (Keys et al., 2024).

5 Conclusion

This paper has presented the first integration of a global behavioural model of human fire use and management with a dynamic global vegetation model. Overall, model evaluation highlights the strong benefits of coupled socio-ecological modelling approaches for reproducing the observed spatial and temporal patterns of burned area globally. Furthermore, findings demonstrate the extent and complexity of human-fire interactions. Results imply that managed anthropogenic fire accounts for as much as half of all global burned area, whilst the trends and distribution of, and relationship between, managed and unmanaged fires is highly spatially heterogeneous. Such complexities demonstrate that socio-ecological modelling is vital to advance understanding of present-day and future fire regimes. A key area for future work identified here is in developing more nuanced representation of landscape fragmentation, particularly in grazing lands in sub-Saharan Africa, which remain a central contributor to global burned area.

Acknowledgments

This work was funded by the Leverhulme Centre for Wildfires, Environment and Society through the Leverhulme Trust, grant number RC-2018-023. AV has also been supported by the AXA Research Fund (project ‘AXA Chair in Wildfires and Climate’) and by the Hellenic Foundation for Research and Innovation (Grant ID 3453). The authors declare no conflicts of interest.

Open Research

Data and code necessary to reproduce the results in this paper, as well as analysis and figures presented are made available on zenodo: https://zenodo.org/doi/10.5281/zenodo.8319445 (Perkins et al., 2023b). Code to run the WHAM-INFERNO ensemble are also made available on GitHub: https://github.com/OliPerkins1987/WHAM_INFERNO. All data and code are mode available under a Creative Commons License.

References

Andela, N., Morton, D. C., Giglio, L., Chen, Y., van der Werf, G. R., Kasibhatla, P. S., et al. (2017). A human-driven decline in global burned area. *Science*, *356*(6345), 1356–1362. https://doi.org/10.1126/science.aal4108

Archibald, S. (2016). Managing the human component of fire regimes: Lessons from Africa. *Philosophical Transactions of the Royal Society B: Biological Sciences*, *371*(1696), 20150346. https://doi.org/10.1098/rstb.2015.0346

Archibald, S., & Hempson, G. P. (2016). Competing consumers: Contrasting the patterns and impacts of fire and mammalian herbivory in Africa. *Philosophical Transactions of the Royal Society B: Biological Sciences*, *371*(1703), 20150309. https://doi.org/10.1098/rstb.2015.0309

Archibald, S., Staver, A. C., & Levin, S. A. (2012). Evolution of human-driven fire regimes in Africa. *Proceedings of the National Academy of Sciences*, *109*(3), 847–852. https://doi.org/10.1073/pnas.1118648109

Arneth, A., Brown, C., & Rounsevell, M. D. A. (2014). Global models of human decision-making for land-based mitigation and adaptation assessment. *Nature Climate Change*, *4*(7), Article 7. https://doi.org/10.1038/nclimate2250

Blackford, K. R., Kasoar, M., Burton, C., Burke, E., Prentice, I. C., & Voulgarakis, A. (2023). INFERNO-peat v1.0.0: A representation of northern high latitude peat fires in the JULES-INFERNO global fire model. *EGUsphere*, 1–31. https://doi.org/10.5194/egusphere-2023-2399

Burton, C., Betts, R., Cardoso, M., Feldpausch, T. R., Harper, A., Jones, C. D., et al. (2019). Representation of fire, land-use change and vegetation dynamics in the Joint UK Land Environment Simulator vn4.9 (JULES). *Geoscientific Model Development*, *12*(1), 179–193. https://doi.org/10.5194/gmd-12-179-2019

Burton, C., Lampe, S., Kelley, D., Thiery, W., Hantson, S., Christidis, N., et al. (2023). Global burned area increasingly explained by climate change, PREPRINT (Version 1) available at Research Square. https://doi.org/10.21203/rs.3.rs-3168150/v1

Carnell, R. (2022). *lhs: Latin Hypercube Samples*. R package version 1.1.6, https://CRAN.R-project.org/package=lhs.

Chen, Y., Hall, J., van Wees, D., Andela, N., Hantson, S., Giglio, L., et al. (2023). Multi-decadal trends and variability in burned area from the 5th version of the Global Fire Emissions Database (GFED5). *Earth System Science Data Discussions*, 1–52. https://doi.org/10.5194/essd-2023-182

Christian, H. J., Blakeslee, R. J., Boccippio, D. J., Boeck, W. L., Buechler, D. E., Driscoll, K. T., et al. (2003). Global frequency and distribution of lightning as observed from space by the Optical Transient Detector. *Journal of Geophysical Research: Atmospheres*, *108*(D1), ACL 4-1-ACL 4-15. https://doi.org/10.1029/2002JD002347

Clark, D. B., Mercado, L. M., Sitch, S., Jones, C. D., Gedney, N., Best, M. J., et al. (2011). The Joint UK Land Environment Simulator (JULES), model description – Part 2: Carbon fluxes and vegetation dynamics. *Geoscientific Model Development*, *4*(3), 701–722. https://doi.org/10.5194/gmd-4-701-2011

Cochrane, M. A., & Barber, C. P. (2009). Climate change, human land use and future fires in the Amazon. *Global Change Biology*, *15*(3), 601–612. https://doi.org/10.1111/j.1365-2486.2008.01786.x

Driscoll, D. A., Armenteras, D., Bennett, A. F., Brotons, L., Clarke, M. F., Doherty, T. S., et al. (2021). How fire interacts with habitat loss and fragmentation. *Biological Reviews*, *96*(3), 976–998. https://doi.org/10.1111/brv.12687

Ford, A. E., Harrison, S. P., Kountouris, Y., Millington, J. D., Mistry, J., Perkins, O., et al. (2021). Modelling human-fire interactions: Combining alternative perspectives and approaches. *Frontiers in Environmental Science*, *9*, 649835.

Forkel, M., Andela, N., Harrison, S. P., Lasslop, G., van Marle, M., Chuvieco, E., et al. (2019). Emergent relationships with respect to burned area in global satellite observations and fire-enabled vegetation models. *Biogeosciences*, *16*(1), 57–76. https://doi.org/10.5194/bg-16-57-2019

Giglio, L., Randerson, J. T., & van der Werf, G. R. (2013). Analysis of daily, monthly, and annual burned area using the fourth-generation global fire emissions database (GFED4). *Journal of Geophysical Research: Biogeosciences*, *118*(1), 317–328. https://doi.org/10.1002/jgrg.20042

Haas, O., Prentice, I. C., & Harrison, S. P. (2022). Global environmental controls on wildfire burnt area, size, and intensity. *Environmental Research Letters*, *17*(6), 065004. https://doi.org/10.1088/1748-9326/ac6a69

Hall, J., Argueta, F., Zubkova, M., Chen, Y., Randerson, J. & Giglio, L. (2024). GloCAB: global cropland burned area from mid-2002 to 2020. *Earth System Science Data*, 16(2), 867-885. https://doi.org/10.5194/essd-16-867-2024

Hantson, S., Kelley, D. I., Arneth, A., Harrison, S. P., Archibald, S., Bachelet, D., et al. (2020). Quantitative assessment of fire and vegetation properties in simulations with fire-enabled vegetation models from the Fire Model Intercomparison Project. *Geoscientific Model Development*, *13*(7), 3299–3318.

Harrison, S. P., Prentice, I. C., Bloomfield, K. J., Dong, N., Forkel, M., Forrest, M., et al. (2021). Understanding and modelling wildfire regimes: An ecological perspective. *Environmental Research Letters*, *16*(12), 125008. https://doi.org/10.1088/1748-9326/ac39be

Hijmans, R. (2023). raster: Geographic Data Analysis and Modeling. R package version 3.6-20. https://CRAN.R-project.org/package=raster

Hurtt, G. C., Chini, L., Sahajpal, R., Frolking, S., Bodirsky, B. L., Calvin, K., et al. (2020). Harmonization of global land use change and management for the period 850–2100 (LUH2) for CMIP6. *Geoscientific Model Development*, *13*(11), 5425–5464. https://doi.org/10.5194/gmd-13-5425-2020

Jones, M. W., Abatzoglou, J. T., Veraverbeke, S., Andela, N., Lasslop, G., Forkel, M., et al. (2022). Global and Regional Trends and Drivers of Fire Under Climate Change. *Reviews of Geophysics*, *60*(3), e2020RG000726. https://doi.org/10.1029/2020RG000726

Kelley, D. I., Bistinas, I., Whitley, R., Burton, C., Marthews, T. R., & Dong, N. (2019). How contemporary bioclimatic and human controls change global fire regimes. *Nature Climate Change*, *9*(9), 690–696. https://doi.org/10.1038/s41558-019-0540-7

Keys, P. W., Badia, L., & Warrier, R. (2024). The Future in Anthropocene Science. *Earth's Future*, *12*(1), e2023EF003820. https://doi.org/10.1029/2023EF003820

Kumar, N., Chaudhary, A., Ahlawat, O. P., Naorem, A., Upadhyay, G., Chhokar, R. S., et al. (2023). Crop residue management challenges, opportunities and way forward for sustainable food-energy security in India: A review. *Soil and Tillage Research*, *228*, 105641. https://doi.org/10.1016/j.still.2023.105641

Lapola, D. M., Pinho, P., Barlow, J., Aragão, L. E. O. C., Berenguer, E., Carmenta, R., et al. (2023). The drivers and impacts of Amazon forest degradation. *Science*, *379*(6630), eabp8622. https://doi.org/10.1126/science.abp8622

Laris, P. (2002). Burning the Seasonal Mosaic: Preventative Burning Strategies in the Wooded Savanna of Southern Mali. *Human Ecology*, *30*(2), 155–186. https://doi.org/10.1023/A:1015685529180

Lasslop, G., Coppola, A., Voulgarakis, A., Yue, C., & Veraverbeke, S. (2019). Influence of Fire on the Carbon Cycle and Climate. *Current Climate Change Reports*, 5, 112-113. https://doi.org/10.1007/s40641-019-00128-9

Li, F., Val Martin, M., Andreae, M. O., Arneth, A., Hantson, S., Kaiser, J. W., et al. (2019). Historical (1700–2012) global multi-model estimates of the fire emissions from the Fire Modeling Intercomparison Project (FireMIP). *Atmospheric Chemistry and Physics*, *19*(19), 12545–12567. https://doi.org/10.5194/acp-19-12545-2019

Mangeon, S., Voulgarakis, A., Gilham, R., Harper, A., Sitch, S., & Folberth, G. (2016). INFERNO: A fire and emissions scheme for the UK Met Office's Unified Model. *Geoscientific Model Development*, *9*(8), 2685–2700. https://doi.org/10.5194/gmd-9-2685-2016

Mathison, C., Burke, E., Hartley, A. J., Kelley, D. I., Burton, C., Robertson, E., et al. (2023). Description and evaluation of the JULES-ES set-up for ISIMIP2b. *Geoscientific Model Development*, *16*(14), 4249–4264. https://doi.org/10.5194/gmd-16-4249-2023

Meijer, J. R., Huijbregts, M. A. J., Schotten, K. C. G. J., & Schipper, A. M. (2018). Global patterns of current and future road infrastructure. *Environmental Research Letters*, *13*(6), 064006. https://doi.org/10.1088/1748-9326/aabd42

Millington, J. D. A., Perkins, O., & Smith, C. (2022). Human Fire Use and Management: A Global Database of Anthropogenic Fire Impacts for Modelling. *Fire*, *5*(4), Article 4. https://doi.org/10.3390/fire5040087

Perkins, O., Kasoar, M., Voulgarakis, A., Smith, C., Mistry, J., & Millington, J. (2023). A global behavioural model of human fire use and management: WHAM! v1.0. *EGUsphere* (accepted for publication in *Geoscientific Model Development*), 1–42. https://doi.org/10.5194/egusphere-2023-2162.

Perkins, O., Kasoar, M., Voulgarakis, A., Edwards, T., & Millington, J. (2023b). [Software] WHAM-INFERNO, code and supporting data. https://zenodo.org/doi/10.5281/zenodo.8319445

Perkins, O., & Millington, J. D. A. (2021). DAFI: A global database of Anthropogenic Fire. *Figshare Https://Doi. Org/10.6084/M9. Figshare. c*, *5290792*.

R Core Team. (2022). R: A language and environment for statistical computing. R Foundation for Statistical Computing, Vienna, Austria. https://www.R-project.org/.

Rabin, S. S., Melton, J. R., Lasslop, G., Bachelet, D., Forrest, M., Hantson, S., et al. (2017). The Fire Modeling Intercomparison Project (FireMIP), phase 1: Experimental and analytical protocols with detailed model descriptions. *Geoscientific Model Development*, *10*(3), 1175–1197. https://doi.org/10.5194/gmd-10-1175-2017

Randerson, J. T., Chen, Y., van der Werf, G. R., Rogers, B. M., & Morton, D. C. (2012). Global burned area and biomass burning emissions from small fires. *Journal of Geophysical Research: Biogeosciences*, *117*(G4). https://doi.org/10.1029/2012JG002128

Ripley, B. S., Raubenheimer, S. L., Perumal, L., Anderson, M., Mostert, E., Kgope, B. S., Midgley, G. F., & Simpson, K. J. (2022). CO2-fertilisation enhances resilience to browsing in the recruitment phase of an encroaching savanna tree. *Functional Ecology*, *36*(12), 3223–3233. https://doi.org/10.1111/1365-2435.14215

Robinson, D. T., Di Vittorio, A., Alexander, P., Arneth, A., Barton, C. M., Brown, D. G., Kettner, A., Lemmen, C., et al. (2018). Modelling feedbacks between human and natural processes in the land system. *Earth System Dynamics*, *9*(2), 895–914. https://doi.org/10.5194/esd-9-895-2018

Rosan, T. M., Sitch, S., Mercado, L. M., Heinrich, V., Friedlingstein, P., & Aragão, L. E. O. C. (2022). Fragmentation-Driven Divergent Trends in Burned Area in Amazonia and Cerrado. *Frontiers in Forests and Global Change*, *5*. https://www.frontiersin.org/articles/10.3389/ffgc.2022.801408

Rougier, J. C., & Beven, K. J. (2013). *Model and data limitations: The sources and implications of epistemic uncertainty* (pp. 40–63). Cambridge University Press. https://doi.org/10.1017/CBO9781139047562.004

Shuman, J. K., Balch, J. K., Barnes, R. T., Higuera, P. E., Roos, C. I., Schwilk, D. W., et al. (2022). Reimagine fire science for the anthropocene. *PNAS Nexus*, *1*(3), pgac115. https://doi.org/10.1093/pnasnexus/pgac115

Smith, C., Perkins, O., & Mistry, J. (2022). Global decline in subsistence-oriented and smallholder fire use. *Nature Sustainability*, *5*(6), Article 6. https://doi.org/10.1038/s41893-022-00867-y

Stevens, N., Erasmus, B. F. N., Archibald, S., & Bond, W. J. (2016). Woody encroachment over 70 years in South African savannahs: Overgrazing, global change or extinction aftershock? *Philosophical Transactions of the Royal Society B: Biological Sciences*, *371*(1703), 20150437. https://doi.org/10.1098/rstb.2015.0437

Teckentrup, L., Harrison, S. P., Hantson, S., Heil, A., Melton, J. R., Forrest, M., et al. (2019). Response of simulated burned area to historical changes in environmental and anthropogenic factors: A comparison of seven fire models. *Biogeosciences*, *16*(19), 3883–3910. https://doi.org/10.5194/bg-16-3883-2019

UNEP - the United Nations Environment Programme (2022). *Spreading like Wildfire: The Rising Threat of Extraordinary Landscape Fires*. http://www.unep.org/resources/report/spreading-wildfire-rising-threat-extraordinary-landscape-fires

Wiltshire, A. J., Duran Rojas, M. C., Edwards, J. M., Gedney, N., Harper, A. B., Hartley, A. J., et al. (2020). JULES-GL7: The Global Land configuration of the Joint UK Land Environment Simulator version 7.0 and 7.2. *Geoscientific Model Development*, *13*(2), 483–505. https://doi.org/10.5194/gmd-13-483-2020

Zubkova, M., Humber, M. L., & Giglio, L. (2023). Is global burned area declining due to cropland expansion? How much do we know based on remotely sensed data? *International Journal of Remote Sensing*, *44*(4), 1132–1150. https://doi.org/10.1080/01431161.2023.2174389

References from the supporting information

Craig, P.S., Goldstein, M., Seheult, A.H., & Smith, J.A. (1997). P*ressure Matching for Hydrocarbon Reservoirs: A Case Study in the Use of Bayes Linear Strategies for Large Computer Experiments*, in: Gatsonis, C., Hodges, J.S., Kass, R.E., McCulloch, R., Rossi, P., Singpurwalla, N.D. (Eds.), *Case Studies in Bayesian Statistics*, Lecture Notes in Statistics. Springer, New York, NY, pp. 37–93. https://doi.org/10.1007/978-1-4612-2290-3_2

Florian, A. (1992). An efficient sampling scheme: Updated Latin Hypercube Sampling. *Probabilistic Engineering Mechanics*, 7, 123–130. https://doi.org/10.1016/0266-8920(92)90015-A

Gupta, H.V., Sorooshian, S., & Yapo, P.O., 1998. Toward improved calibration of hydrologic models: Multiple and noncommensurable measures of information. *Water Resources Research*, 34, 751–763. https://doi.org/10.1029/97WR03495

Kennedy, M., & O'Hagan, A. (2001). Bayesian calibration of computer models, *Journal of the Royal Statistical Society* B, 63:3, 425-464.

Lin, Y., Xu, D., Wang, N., Shi, Z., & Chen, Q. (2020). Road Extraction from Very-High-Resolution Remote Sensing Images via a Nested SE-Deeplab Model. *Remote Sensing*, 12, 2985. https://doi.org/10.3390/rs12182985

Lu, L., Anderson-Cook, C.M., & Robinson, T.J. (2011). Optimization of Designed Experiments Based on Multiple Criteria Utilizing a Pareto Frontier. *Technometrics*, 53, 353–365.

McNeall, D., Williams, J., Booth, B., Betts, R., Challenor, P., Wiltshire, A., & Sexton, D. (2016). The impact of structural error on parameter constraint in a climate model. *Earth System Dynamics*, 7, 917–935. https://doi.org/10.5194/esd-7-917-2016

Pukelsheim, F. (1994). The Three Sigma Rule. *The American Statistician*, 48, 88–91. https://doi.org/10.2307/2684253

Roteta, E., Bastarrika, A., Padilla, M., Storm, T., & Chuvieco, E. (2019). Development of a Sentinel-2 burned area algorithm: Generation of a small fire database for sub-Saharan Africa. *Remote Sensing of Environment*, 222, 1–17. https://doi.org/10.1016/j.rse.2018.12.011

Williamson, D., Goldstein, M., Allison, L., Blaker, A., Challenor, P., Jackson, L., & Yamazaki, K. (2013). History matching for exploring and reducing climate model parameter space using observations and a large perturbed physics ensemble. *Climate Dynamics*, 41, 1703–1729. https://doi.org/10.1007/s00382-013-1896-4

Earth's Future

Supporting Information for

The spatial distribution and temporal drivers of changing global fire regimes: a coupled socio-ecological modelling approach

Oliver Perkins[1,2], Matthew Kasoar[1,3], Apostolos Voulgarakis[1,3,4], Tamsin Edwards[2], and James Millington[1,2]

Corresponding author: Oliver Perkins (oliver.perkins@kcl.ac.uk)

[1The Leverhulme Centre for Wildfires, Environment, and Society, Imperial College London, SB7 2BX, UK, 2Department of Geography, King's College London, WC2B 4BG, UK, 3Department of Physics, Imperial College London, 4School of Chemical and Environmental Engineering, Technical University of Crete, Kounoupidiana, 73100, Greece]

Contents of this file

Introduction

This supplementary information provides further context to the calibration of the WHAM-INFERNO model ensemble presented in the main text. Specifically, it describes the set-up of the perturbed parameter ensembles used to define model free parameters and how these parameter values relate to results presented in the main text. It then briefly describes the setup of a baseline model used to benchmark performance of WHAM-INFERNO, before showing how free parameters vary across parameter spaces.

Text S1.

1. Definition of perturbed parameter ensemble

Four categories of model parameter were included in the perturbed ensemble. These are firstly parameters whose values were defined heuristically in the first version of INFERNO (Mangeon et al., 2016). These comprise the burned area per fire for each plant functional type in the model (seven parameters; Table SI1). Burned area for cropland PFTs was set to 0, as WHAM! represents anthropogenic cropland burning. The second set of parameters included were those that were required to integrate WHAM! with JULES-INFERNO either structurally or ontologically. These are the Φ parameter for accounting for differences in conceptualisation of anthropogenic ignitions (INFERNO) vs anthropogenic fires (WHAM!) and parameters accounting for previous fires within a given calendar year (α, β).

Thirdly, parameters are included for aspects of WHAM! for which no initial external verification was possible, as presented in Perkins et al., (2023). For example, whilst assessment of WHAM! crop residue burning outputs was possible with the new GFED5 crop fires algorithm (Hall et al., 2023), assessment of managed pasture fires and managed vegetation fires (comprising crop field preparation, hunting and gathering, pyrome management and vegetation clearance) was not possible with currently available remote sensing data products or other data sources. As such, two free parameters were added reflecting the unexplored uncertainty in these WHAM outputs. No free parameter was added to the rate of escaped fires (Main text, section 2.2.1) because the rate of escaped fires is implicitly changed with the rate of managed burned area and altering both processes would have led to implausibly high rates of escaped fire in some model parameter sets. Other WHAM! outputs to which free parameters were applied were the rates of background and arson fires, as well as fire suppression.

Fourthly, and finally, free parameters were included in the perturbed parameter ensemble relevant to representations of landscape fragmentations described in the main text. These are a scaling parameter for the impact of road density in reducing fire size (ρ) and for the impact of logging in increasing flammability of tropical forests (Λ).

2. Setup of the perturbed parameter ensembles

2.1 Defining and sampling parameter distributions

Having defined the variables to be included in the perturbed parameter ensembles, probability distributions for their values were defined. Given the large degree of uncertainty surrounding initial values for parameters, these were set as uniform distributions with upper and lower bounds +- 50% of the initial value. Where possible, parameter values were taken from previously defined estimates – as such parameter values for burned area per fire per PFT were taken from Burton et al., (2019). Whilst in the INFERNO baseline model, initial parameter values for anthropogenic and lightning ignitions were those given in Mangeon et al. (2016). Furthermore, WHAM! parameters for fire suppression could be defined on a narrower range than other parameter values, as the impact of limited and moderate fire suppression must ontologically be less than that of intensive fire suppression (see Perkins et al., 2023 for details). Similarly, it was not logically consistent for the role of logging to reduce flammability of tropical forests, and hence values <1 were excluded. Elsewhere, parameters for WHAM! were defined heuristically. For example, the initial value of the road density scaling parameter (ρ) was the global maximum of its own natural logarithm; whilst the initial value of the fire-ignitions scaling parameter (Φ) was defined from the reciprocal of the global mean flammability in JULES-INFERNO.

Having defined sampling distributions for model parameters, a Latin Hypercube sampling strategy was taken using a minmax sampling design (Carnell 2022). Such a sampling design allows for robust exploration of the model parameter space in a computationally efficient way (Florian, 1992). 10,000 parameter sets were defined for WHAM-INFERNO and INFERNO offline, and model runs were conducted for each parameter set.

2.2 Assessing model outputs from the perturbed ensemble

Model outputs were assessed in two ways. Firstly, a process of history matching was conducted to remove implausible parameter sets from consideration. Secondly, a pareto-optimal parameter space was defined, which then became the basis of analysis presented in the main text.

2.2.1 History matching for implausibility assessment

History matching is the process of constraining the parameter space of a model using observations (Craig et al., 1997). A common method of constraining model parameter spaces is to 'rule out' implausible parameter combinations which result in model outputs that are inconsistent with observations (Williamson et al., 2013). Parameter sets that satisfy the implausibility criteria are deemed 'not yet ruled out', whilst in the event an implausibility assessment returns a null parameter space, the model is assessed to be structurally unsuitable (Williamson et al., 2015). Model implausibility, the measure used to rule out parameter sets, is denoted as *I* and is calculated as:

$$I = \left| \frac{y_{mod} - y_{obs}}{\sqrt{(\sigma_{mod}{}^2 + \sigma_{obs}{}^2)}} \right| \qquad (S1)$$

where y_{mod} and y_{obs} are the model outputs and observations respectively; and σ_{mod} and σ_{obs} are the model and observational error, respectively. Applying the I calculation on a pixel-by-pixel basis requires complicated assessment of spatial and temporal autocorrelations, given the non-independence of observations and model outputs (Rougier and Beven, 2013). Furthermore, the goal of implausibility assessment here is not to optimise model parameter values, but rather to provide an initial filtering of parameter space. Therefore, the mean global burned area across 2001-2014 is used as the basis of the implausibility calculation.

As such, observational error can be measured directly and here has a value of 106.72 – the product of the mean annual burned area in the GFED5 product (802.5Mha) and the Dice similarity coefficient of Sentinel-2 burned area observations (0.133). The Dice similarity coefficient (also known as the F1-Score) is used as a measure of true positive detection accuracy in image processing (Lin et al., 2020). The resulting value (106.72Mha) is a conservative estimate of observational error: GFED5, against which model evaluation was conducted, does not use Sentinel-2 burned area directly, but rather scales MODIS burned area observations to Sentinel-2 and Landsat outputs using empirical relationships (Chen et al., 2023). Given this, the GFED5 product does not report observational error directly, and so the underlying Sentinel-2 error is used (Roteta et al., 2019).

Model error, also referred to as structural error, is used to define acceptable divergence from observations, and therefore must be set by the modeller in relation to the domain and research question (Kennedy & O'Hagan 2001; McNeall et al., 2016). Here, we adopt the error in the ensemble of models from the first Fire Model Intercomparison Project (FIREMIP; Teckentrup et al., 2019) – specifically the median disagreement between the mean burned area of the model ensemble and the three remote sensing products used for evaluation – 68.33Mha. The median was chosen to down-weight outlier outputs from the FIREMIP ensemble. The result was a denominator value for (6.9) of 126.72 - i.e. $\sqrt{(68.33^2 + 106.72^2)}$. Adopting a commonly-used and theoretically-robust threshold (Pukelsheim, 1994), parameter sets that produced an I value greater than 3 (equivalent to +-380.2Mha) were taken as implausible, with remaining parameter combinations taken as not ruled out yet (NROY).

2.2.2 Defining a pareto optimal parameter space

From the set of parameters 'not ruled-out yet' by the implausibility assessment (hereafter NROY), the pareto optimal parameter set was defined. Intuitively, pareto optimality refers to a trade-off space between multiple criteria in which one criteria cannot be further increased without reducing performance of another (Gupta et al., 1998). Or, more formally, a parameter space in which alternative sets are all 'non-dominated' against a set of objective functions (Lu et al., 2011). A parameter set $x_1 \in X$ is considered to dominate another parameter set $x_2 \in X$ if for a vector of objective functions $\vec{y}$ of length L:

$$\forall i \in \{1, 2 \dots L\}$$

$$y_i(x_1) \geq \ y_i(x_2) \ \ (S2)$$

Hence in a pareto parameter space, no parameter sets would satisfy the inequality in $(S2)$.

Here, the two criteria chosen for assessing model performance were those used in the recent FIREMIP: global burned area and Pearson's r (Teckentrup et al., 2019). The global burned area metric used was simply the difference in Mha between WHAM!-INFERNO outputs and GFED5 global burned area (802.5Mha). For Pearson's r, as in Teckentrup et al., (2019), a square root transformation was applied to both GFED5 burned area and WHAM!-INFERNO outputs before calculating correlations. Therefore, model outputs for NROY parameter sets outside of the pareto parameter space contained more disagreement with observations (as measured by either global burned area or their pixel-based correlation) than those within the pareto parameter space.

2.2.3 Understanding the pareto optimal parameter space

In order to understand how model parameters were contributing to defining the pareto parameter spaces, Kruskall-Wallis tests were used to assess which parameters differed significantly across NROY and pareto optimal parameter sets. Significant differences were set as those with p-values <0.0025: 0.05 with a Bonferroni correction applied to reflecting multiple testing across 20 parameters. Furthermore, to understand if there were parameters with small impacts on global burned area, but nonetheless meaningful impacts in capturing observed patterns of fire, correlations between parameter values and the correlation of outputs with GFED5 were calculated, and divided by the correlation of parameter values to the amplitude of global burned area:

$$cor\_weighted_i = \frac{cor\_correlation_i}{cor\_BA_i} \quad (S3)$$

where $cor_BA_i$is the correlation coefficient between the values of parameter i and the amplitude of burned area in model outputs; $cor\_correlation_i$ is the correlation coefficient of the values of parameter i and the model correlation with GFED5, and $cor\_weighted_i$ is a measure of how far a given parameter impacts model performance relative to its overall impact on model outputs. This ensured that identification of the role of model parameters in defining the pareto parameter space was not merely an exercise in understanding sensitivity of the model structure, but also which processes may be most pertinent to capturing the distribution of global fire regimes.

2.3 Setup and evaluation of INFERNO baseline model

INFERNO v1.0 (Mangeon et al., 2016) calculates burned area as:

$$BA_{INFERNO} = Ignitions * Suppression * Flammability * \widehat{BA}_{PFT} \quad (S4)$$

Therefore, flammability and burned area per PFT ($\widehat{BA}_{PFT}$) were taken from the same sources as WHAM-INFERNO (Main text; Table 1). As in the WHAM-INFERNO integration, lightning ignitions were calculated following Mangeon et al., (2016) as:

$$I_L = 7.7 \times Lightning \times (1 - Suppression) \quad (S5)$$

where I_L is the number of ignitions from lightning strikes in a given model timestep, $Lightning$ is the number of lightning strikes and $Suppression$ is a population density dependent suppression function. Similarly, as in Mangeon et al., (2016), anthropogenic ignitions and suppression were calculated respectively as:

$$Ignitions_A = (6.8 * PD^{-0.6}) * (0.03 * PD) \quad (S6)$$

$$Supression = 1 - 7.7 * (0.05 + 0.9 * e^{-0.05*PD}) \quad (S7)$$

where $Ignitions_A$ are anthropogenic ignitions, and PD is population density. Two scaling factors {6.8, 7.7} in these equations were first defined by Pechony and Shindell (2009) to calibrate population density with observed fire counts in GFED v4. Therefore, these were replaced by free parameters to enable recalibration with the new GFED5 (Table S2).

As in WHAM-INFERNO, equations in the main text (7) and (8) were used to account for prior fires restricting the connectivity and availability of vegetation. Outputs from the baseline model were analysed in the same way to the WHAM-INFERNO ensemble – firstly by ruling out implausible parameter combinations, and secondly by defining a pareto optimal parameter space. The performance of the baseline model(s) and the two versions of WHAM-INFERNO in this pareto space was then compared.

The parameters in the perturbed ensemble for the baseline version of INFERNO – INFERNO v1.0 recalibrated to GFED5 – were as follows (Table S2). Parameters from the WHAM-INFERNO ensemble that related to uncertain aspects of WHAM! outputs and vegetation fragmentation were removed. These were replaced with two additional parameters, which allowed recalibration of INFERNO fire counts to GFED5 (σ_1, λ, Sup). The original values of these parameters were derived from calibrating lightning strikes and human population density to fire counts observed in GFED v4. As such, with much greater capacity to detect anthropogenic fires in GFED5, these each need recalibration. Further, as WHAM! crop fires did not contribute to the baseline model, burned area parameters per PFT were reintroduced for cropland PFTs.

3. Characteristics of parameter spaces in the perturbed parameter ensembles

Based-on Wilcox tests between pareto and other parameter sets, across the three model setups there are five parameters with significantly different values in the pareto sets (Figure S1). For both WHAM-INFERNO and WHAM-EO, road density shows a strong difference, with pareto parameter sets (mean = 6.00, 6.51) showing lower values than other sets (mean = 9). This has the effect of lowering the threshold at which road density effects apply, and hence increasing its constraint on burned area. Similarly, values for the scaling parameter that corrects for the double counting of flammability effects in the model ensemble are weighted towards the upper end of the parameter range in the perturbed ensemble (Figure S1). Overall, this suggests that increasing the impact of climate (through vegetation flammability) and vegetation fragmentation (through road density) are important in defining the pareto parameter spaces for the two coupled models.

However, when individual parameter correlations with overall WHAM!-GFED5 correlation are calculated and weighted by their respective impact on burned area, a more complex picture emerges (Figure S2). Weighted by impact on overall burned area, for logging, suppression, shrub PFT burned area per fire, and previous fires have the most impact on correlations between WI-JULES, WHAM-EO and GFED5. By contrast, road density and the rate of unmanaged fires, which have a large impact on burned area, have correspondingly less weighted impact on correlations. Therefore, some aspects of the coupled model ensemble have a small impact on overall burned area, but nevertheless pick up meaningful aspects of the burned area record in GFED5.

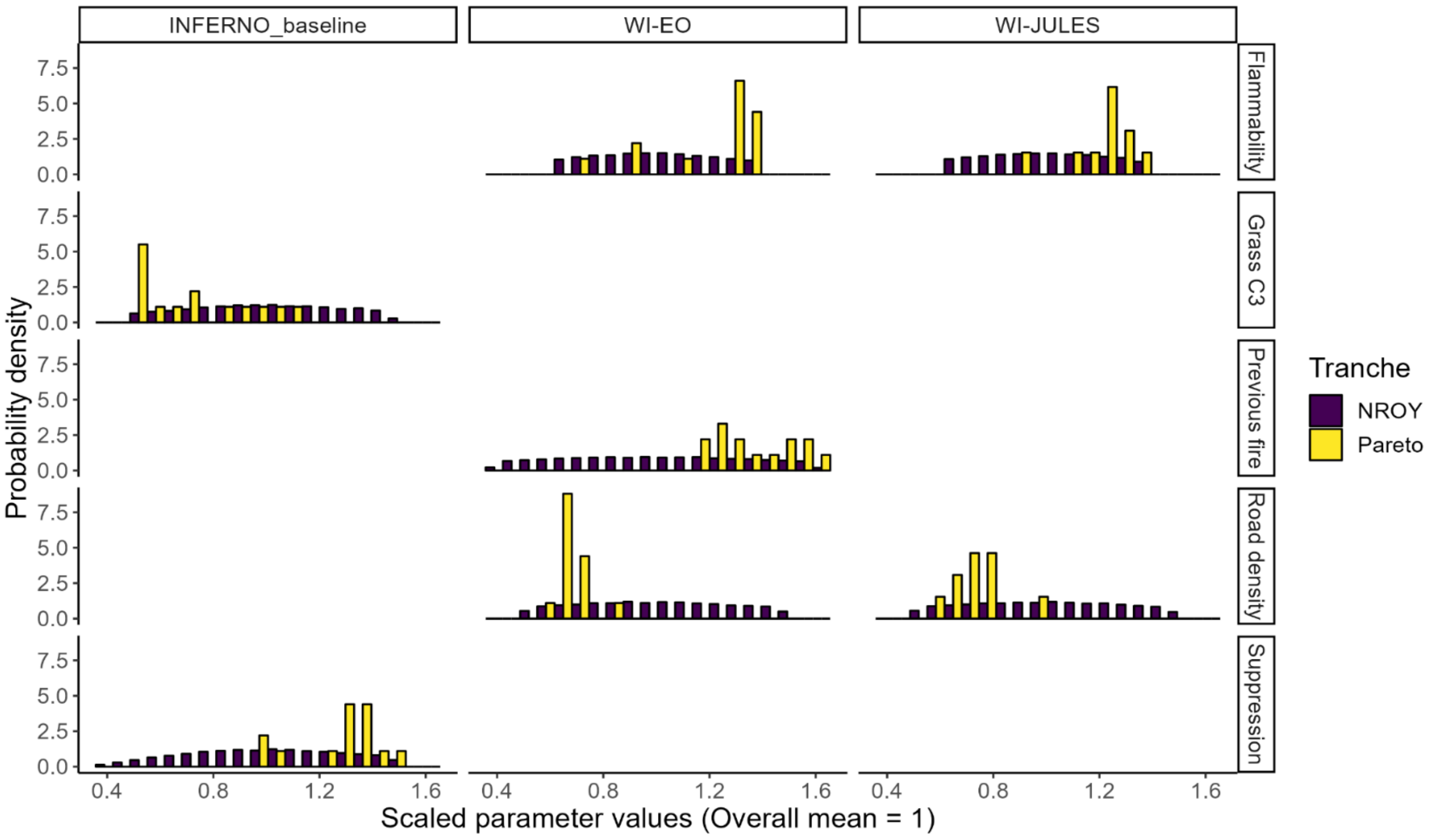

Figure S1: Comparison of parameter distributions across models and parameter tranches. Distributions shown had Wilcox tests with $p<0.05$ (Bonferroni correction applied). Under WHAM coupling, road density is important in constraining the distribution of fire in, but this effect is not captured in the baseline model (INFERNO_baseline).

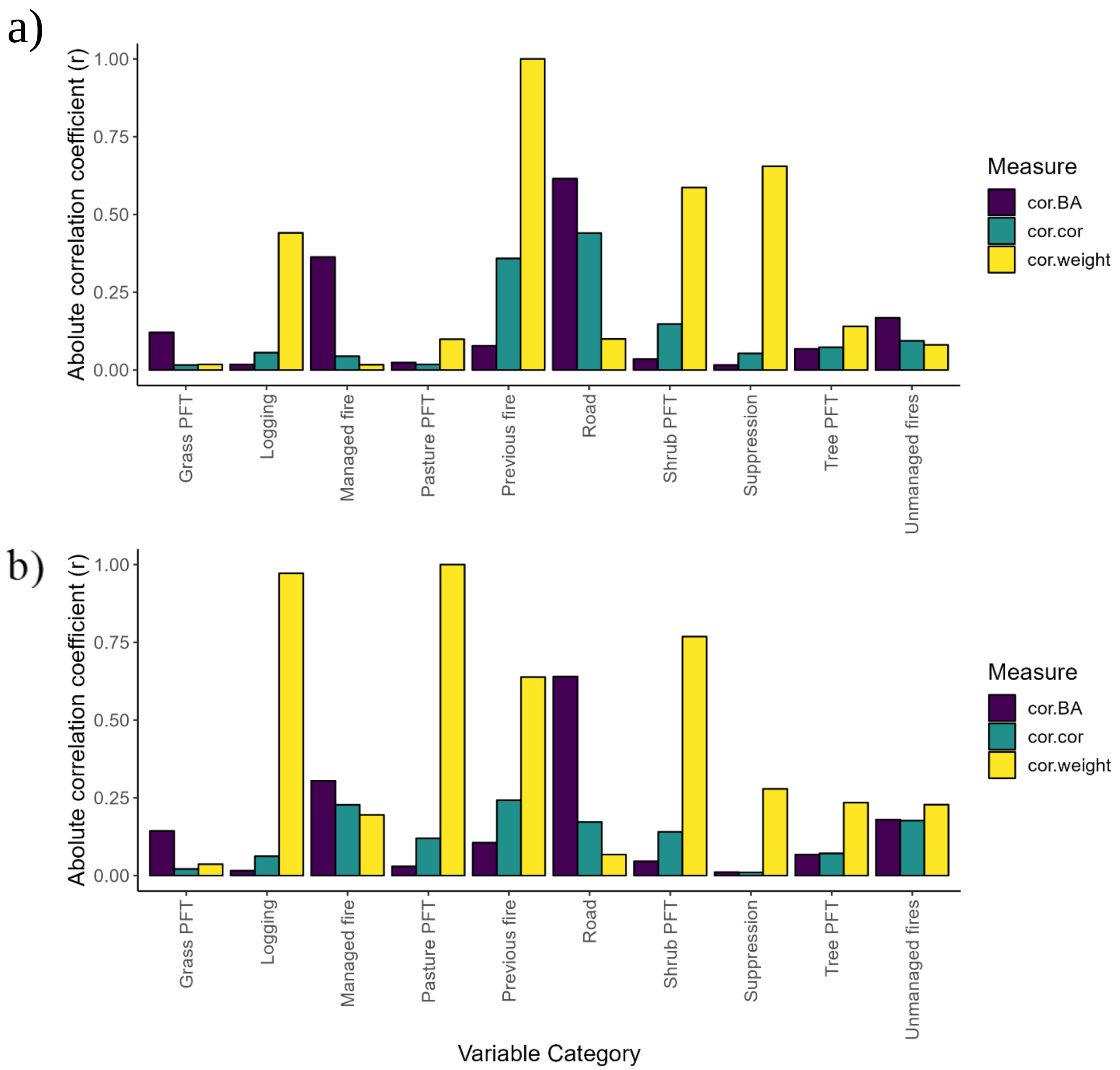

Figure S2: Effect of model parameters on model correlation with GFED5 across NROY & pareto runs for a) WI-EO and b) WI-JULES. Whilst they have limited impact on global burned area parameters for logging, suppression, shrub PFT burned area per fire, and previous fires are effective at capturing the relative spatio-temporal distribution of fire. By contrast, in WI-JULES, pasture PFTs prove useful in capturing the distribution of fire in GFED5, but this effect is not present in WI-EO.

Key: cor.BA – correlation (r) of parameter with global burned area; cor.cor – correlation of parameter values with overall model correlation; cor.weight – correlation of parameter values with overall correlation, weighted by parameter impact on burned area.

Table S1: Model free parameters, their initial, maximum and minimum values in WHAM!-INFERNO calibration. There is no mean burned area for cropland PFTs as it was 0 in all cases, and replaced by outputs from WHAM! Given the substantial uncertainty around parameter values, values were sampled from a uniform distribution around an initial value. Grass and pasture burned area per PFT were given two values for C3 and C4 respectively.

Parameter name	Parameter function	Initial value	Minimum value	Maximum value
TreeBL_BA	Mean global BA for broadleaf trees	1.7	0.85	2.55
TreeNL_BA	Mean global BA for needleleaf trees	1.7	0.85	2.55
Grass_BA	Mean global BA for grass PFTs (C3 & C4)	3.2	1.6	4.8
Shrub_BA	Mean global BA for shrubs	3.2	1.6	4.8
Pasture_BA	Mean global BA for pasture PFTs (C3 & C4)	2.7	1.35	4.05
δ_1	Scaling managed burned area from pasture fires	1	0.5	1.5
δ_2	Scaling managed burned area from vegetation fires	1	0.5	1.5
σ_1	Rate of background ignitions	0.03	0.01	0.05
σ_2	Scaling arson fires	30	15	45
λ	Scaling parameter for lightning strikes	7.7	3.85	11.55
Φ	Harmonising model ontologies of ignitions & fires	650	400	900
Sup_PI	Rate of extinguished fires for the pre-industrial AFR	0	0	0.05
Sup_Trans	Rate of extinguished fires for the transitional AFR	0.05	0	0.1
Sup_Intense	Rate of extinguished fires for the industrial AFR	0.9	0.8	1
ρ	Scaling impact of road density on fire sizes	8.91	4.455	13.4
Λ	Impact of logging on burned area in forests	1.5	1	2.25
α	Threshold for impact of prior fires on fire size	0.2	0.1	0.4
β	Rate of decline in fire size due to prior fires	0.2	0.1	0.4

Table S2: Free parameters in INFERNO v1.0 offline - a baseline model used for evaluation of performance of WHAM!-INFERNO. Parameters' initial, maximum and minimum values in model calibration are shown. The baseline model was run with and without the use of road density in constraining global fire sizes. Given the substantial uncertainty around parameter values, values were sampled from a uniform distribution around an initial value. Cropland, grass and pasture burned area per PFT were given two values for C3 and C4 respectively.

Parameter name	Parameter function	Initial value	Minimum value	Maximum value
TreeBL_BA	Mean global BA for broadleaf trees	1.7	0.85	2.55
TreeNL_BA	Mean global BA for needleleaf trees	1.7	0.85	2.55
Grass_BA	Mean global BA for grass PFTs (C3 & C4)	3.2	1.6	4.8
Shrub_BA	Mean global BA for shrubs	3.2	1.6	4.8
Pasture_BA	Mean global BA for pasture PFTs (C3 & C4)	2.7	1.35	4.05
Cropland_BA	Mean global BA for cropland PFTs (C3 & C4)	3.2	1.6	4.8
σ_1	Scaling parameter for anthropogenic ignitions	1	1.5	0.5
λ	Scaling parameter for lightning strikes	7.7	3.85	11.55
Sup	Suppression scaling parameter	1	0.5	1.5
ρ	Scaling impact of road density on fire sizes	8.91	4.455	13.4
α	Threshold for impact of prior fires on fire size	0.2	0.1	0.4
β	Rate of decline in fire size due to prior fires	0.2	0.1	0.4